Evaluation of WMircrotracker for assessing *C. elegans* stress responses

Hengyi Zhu

Master Thesis
60 credits

Department of Biosciences
The Faculty of Mathematics and Nature Sciences

UNIVERSITY OF OSLO

JUNE 2016

Contents

Acknowledgements

The work presented in this thesis was performed at the Epigen laboratory, Akershus University Hospital, Norway, during the period from December 2014 to March 2016.

First of all, I want to express my sincere gratitude to my main supervisor Hilde Nilsen. Thank you for excellent guidance, patience and encouragement during these period. You have been an incredible motivator and inspiration have always driven me to think, reason and discuss scientifically. You balance personal and scientific aspects perfectly. I would also like to thank my co-supervisor Henok Kassahun for experimental guidance, valuable discussions as well as kind suggestions.

Next I would like to thank all the current and former members of the Nilsen lab for creating a positive working environment. A special thanks goes to Ying, Sergio, Tanima, Anna, Alexandra, and Lene for always helping me with patience and kindness.

Finally, I would like to thank my families and friends for your understanding during hectic periods and always being there when I need you.

Oslo, June 2016

Hengyi Zhu

Abstract

Background: Organisms' lifespan and abilities to withstand stressors tend to be positively correlated. Seen as a mild stressor, DNA repair deficiency can induce compensatory cytoprotective homeostatic responses. In *C. elegans*, a highly significant increase (~30 fold) of the glycerol channel protein gene *aqp-1*, as a part of the compensatory response to the reduced DNA repair capacity, was seen in both *nth-1(-)* and *xpa-1(-)*. In addition, *aqp-1* was found to be downregulated by insulin/IGF-1 signaling (IIS) as the FOXO family member DAF-16 and the heat shock factor HSF-1 was. Hence, it would be interesting to investigate if *aqp-1* is also required as a mediator for the cytoprotective homeostatic response in DNA damage checkpoint deficient strain *atm-1(-)*. Moreover, *sir-2.1* was reported to be partially overlapping with IIS pathway. Therefore, it is fascinating to test whether *sir-2.1* is genetically correlated with *aqp-1* or functions as a factor in compensatory cytoprotective pathway which might be parallel with the cytoprotective homeostatic response pathway that *aqp-1* functions in.

Methods: The model organism *C. elegans*, was used to generate the double mutant strains *aqp-1(-); atm-1(-)* and *aqp-1(-); sir-2.1(-)*. Among them, *aqp-1(-); atm-1(-)* was used to test the function of *aqp*-1 in the DNA checkpoint mutant strain *atm-1(-)*, while *aqp-1(-); sir-2.1(-)* was used to test the hypothetical genetic correlation between *aqp-1* and *sir-2.1*. Strains were assessed with respect to brood size, PQ survival assay, IR sensitivity assay, and heat shock tolerance assay. To increase the efficiency, automatic WMicrotracker measuring system was exploited to the various labor-consuming stress response assay.

Results: The WMicrotracker was proven able for the PQ survival assay, while it can not be applied to heat shock tolerance assay. Additionally, contrary to hypothesis, *aqp-1(-); atm-1(-),* which supposed to be more sensitive than *aqp-1(-)* and *atm-1(-),* showed stronger resistance to PQ, suggesting that *aqp-1* and *atm-1* might have genetic interactions and both function in DNA damage response via a compensatory manner, during which harmful intermediates might be generated. To clarify the genetic connections between *sir-2.1* and *aqp-1*, *aqp-1* and *atm-1* more research is required.

Abbreviations

5hmU	5-hydroxymethyluracil
5-OHU	5-hydrouracil
53BP1	p53-binding protein 1
6-4 PPs	6-4 *photoproducts*
8-oxodA	7,8-dihydro-8oxodeoxyadenine
8-oxodG	7,8-dihydro-8-oxodeoxyguanine
AP	apurinic/apyrimidinic
APAP	acetaminophen
ATM	Ataxia telangiectasia mutated
ATR	Ataxia telangiectasia and Rad3-related
ATRIP	ATR-interaction protein
BAX	Bcl-2-associated X protein
BER	base excision repair
BRCA1	breast cancer type 1
cdA	8,5'-cyclo-2'-deoxyadenosine
cdG	8,5'-cyclo-2'-deoxyguanosine
CDK2	cyclin E- dependent kinase 2
C. elegans	*Caenorhabditis elegans*
CHK1	checkpoint kinase 1
CHK2	checkpoint kinase 2
CPDs	cyclobutyl pyrimidine dimers
CSA	Cockayne syndrome type A
DBE	*daf-16* binding elements
DHT	dihydrothymine
DHU	dyhydrouracil
DNA	deoxyribonucleic acid
DNA-PKcs	DNA-dependent protein kinase catalytic subunit
DR	dietary restriction
DSBs	double strand breaks
dsDNA	double-strand DNA
dTTP	deoxythymidine triphosphate

dUTP	deoxyuridine triphosphate
FapyA	4,6-diamino-5-formamidopyrimidine
FapyG	2,6-diamino-4-hydroxy-5-formamidopyrimidine
GG-NER	global-genome repair
hABH1	human Alk B homolog 1
hHR23B	human rad23b homologous
HJ	Holliday junction
HR	homologous recombination
H_2O_2	hydrogen peroxide
HSPs	heat shock proteins
HU	hydroxy urea
IDLs	insertion-deletion loops
IIS	Insulin/IGF-1 signaling
IR	ionizing radiation
MBD4	methyl-CpG domain protein 4
MGMT	O^6-methylguanine-DNA methyltransferase
MMR	mismatch repair
MPG	methylpurine DNA glycosylase
MRN	Mre11-Rad50-Nbs1
NHEJ	non-homologous end-joining
NEIL1	endonuclease VIII-like 1
NER	nucleotide excision repair
NTHL-1	endonuclease III-like homolog 1
O_2	singlet oxygen
$\cdot O_2^-$	superoxide
OH·	hydroxyl radical
OGG1	8-oxoG DNA glycosylase
PCR	Polymerase chain reaction
PQ	N, N-dimethyl-4, 4-bipyridinium dichloride
PUMA	p53 upregulated modulator of apoptosis
RFC	replication factor C
RNAP II	RNA polymerase II

ROS	reactive oxygen species
RPA	replication protein A
SMUG1	single-strand-selective mono-functional uracil-DNA glycosylase 1
ssDNA	single-strand DNA
TC-NER	transcription-coupled NER
TDG	thymine/uracil DNA glycosylase
TFs	transcription factors
Tg	5,6-dihydrothymine
UDG	uracil-DNA glycosylase
UNG	Uracil *N*-glycosylase
UV	ultraviolet
WT	wild type
XPC	xeroderma pigmentosum complementation group C
XPCC4	x-ray repair cross-complementing protein 4

1. Introduction

Aging is characterized by a progressive loss of physiological integrity, leading to impaired functions and increased vulnerability to death. This progress covers a spectrum of alterations, that molecules, cells, organs and organisms go through over time, from relatively benign anatomical deterioration, to severe functional impairment. This is the primary risk factor for major human pathologies, including cancer, diabetes, cardiovascular disorders, and neurodegenerative diseases (López-Otín, Blasco, Partridge, Serrano, & Kroemer, 2013). The possibility of slowing down aging means to delay the aging related pathologies. Eight candidate hallmarks, which gradually appear due to various kinds of endogenous and environmental stressors, are generally considered to contribute to the aging process and together determine the aging phenotypes. They include: genomic instability, epigenetic alterations, loss of proteostasis, deregulated nutrient sensing, mitochondrial dysfunction, cellular senescence, stem cell exhaustion, and altered intracellular communication. (Kenyon C. J., 2010; Gems & Partridge, 2015; López-Otín, Blasco, Partridge, Serrano, & Kroemer, 2013). This thesis is mainly focus on genomic instability. As many animals with long life span show stronger resistance than wild-type to a variety of stressors, such as heat (Muñoz, 2003), radiation (Murakami & Johnson, 1996), or oxidative damage (Larsen, 1993), it is reasonable to use stress resistance genes to identify novel longevity mutants.

1.1 Environmental and endogenous stimuli induce cellular stress

According to Hans Selye (1973), who is generally considered to be the founder of biological stress concept, stress remains a poorly defined phenomenon despite the fact that it has been extensively studied for the past three decades. Selye defined stress response as “the non-specific response of the body to any demand made upon it”. The term “stressor” was used as the factor/agent that triggers the stress response and refers to endogenous and environmental stimuli (Sandor, Yvette, & Arpad, 2012), such as heat shock, oxidative stress, osmotic stress, nutrient stress, and hypoxia (Enserink, 2015). This study is mainly focused on heat shock, oxidative stress, and the resulting cellular stress.

1.1.1 Heat shock

All living organisms are adapted to live at a certain range of temperature. When the temperature is moderately above the respective ideal temperature, organisms face a challenge for survival (Richter, Haslbeck, & Buchner, 2010) because even a small increase in temperature can cause protein unfolding, entanglement, and aggregation (Richter, Haslbeck, & Buchner, 2010), which trigger heat shock response. This would further influence the intracellular communication and proteostasis, which are the hallmarks of aging. However, unfolded protein is also a result of a variety of other stresses such as, oxidative stress, heavy metals, ethanol, or other toxic substances (Courgeon, Maisonhaute, & Best-Belpomme, 1984). During heat shock, expression of most proteins is inhibited, except for heat shock proteins (HSPs), which are the main players in heat shock response (Schlesinger, 1990). HSPs also accumulate in other stress responses and during aging (Link, Cypser, Johnson, & Johnson, 1999).

1.1.2 Oxidative stress

Different from heat shock stress, which mainly affects protein structures, the oxidative stress exerts a wide range of damage on DNA, lipid, and proteins. The term “oxidative stress” became used more frequently in the 1970s, but its conceptual origins can be traced back to the 1950s to researches on toxic effects of ionizing radiation, free radicals, and the similar toxic effects of molecular oxygen (Hybertson, Gao, Bose, & McCord, 2011). Oxidative stress refers to a disturbance in the balance between the generation of reactive oxygen species (ROS) and the antioxidative defense systems operating for scavenging overproduced ROS (Poljsak, Šuput, & Milisav, 2013). ROS, which are produced by normal metabolism mainly in the mitochondrial, can also be generated from other nonmitochondrial sources such as Fenton’s reaction, microsomal cytochrome P450 enzymes, peroxisomal beta-oxidation, and respiratory burst of phagocytic cells (Gilca, Stoian, Atanasiu, & Virgolici, 2007). In addition, exposure to environmental oxidants, such as ultraviolet (UV), ionizing radiation (IR), metals, reactive nitrogen, sulfur species, and drugs, like acetaminophen (APAP) (Jiang, et al., 2015; Hakim, 1993; Ercal, Gurer-Orhan, & Aykin-Burns, 2001; Rilay,

1994), attribute to increased ROS formation. ROS are comprised of both free radical and nonfree radical oxygen, including molecules such as superoxide ($\cdot O_2^-$), hydrogen peroxide (H_2O_2), hydroxyl radical ($OH\cdot$), and singlet oxygen ($^1O_2$), while $OH\cdot$ is the primary oxidant responsible for macromolecular (Figure 1.1), such as deoxyribonucleic acid (DNA), protein, and lipid damage. DNA damage plays the main role in aging, unlike lipids and proteins which can be replaced totally, DNA can only be repaired.

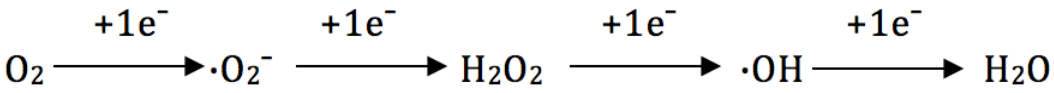

Figure 1.1: Transformation between free radicals. O_2 undergoes a series of reduction reactions and then becomes H_2O. During the process, $\cdot O_2^-$, H_2O_2 and $OH\cdot$ free radicals are generated. Among them, $OH\cdot$ is the most reactive and damaging species.

1.1.3 DNA damage

DNA is the repository of genetic information in living cells, its integrity and stability are essential for survival and growth of organisms. However, DNA is a highly reactive entity and subject to assaults from the environmental and endogenous stressors. If not repaired, it will attribute mutations and associated diseases (Clancy, 2008; Bont & Larebeke, 2004). DNA damage can be divided into endogenous and exogenous DNA damage according to the contributing factor, but the difference between endogenous and exogenous DNA damage is a complex matter. For instance, some exogenous substances, although chemically different from endogenous ones, generate the same DNA adducts (Bont & Larebeke, 2004); the types of damage produced by normal cellular processes are identical or very similar to those caused by some environmental agents (Jackson & Loeb, 2001).

1.1.3.1 Environmental DNA damage

The term environmental DNA damage refers to DNA damage induced by exogenous factors. It includes physical and chemical agents, such as IR, UV, genotoxic chemicals and chemotherapeutic drugs. UV mainly induces the formation of pyrimidine dimers, which can be referred to as intra-strand cross

links. IR, on the other hand, is best known as an inducer of double strand breaks (DSBs). Additionally, both UV and IR contribute to the generation of free radicals, which are the cause of a diversity of DNA adducts. Human beings are also exposed to a wide range of genotoxic chemicals, for instance, originating from processing food and industrial additives. Although the exposure to environmental genotoxins can be limited, the endogenous DNA damage can not be avoided, as they are by-products of normal metabolism.

1.1.3.2 Endogenous DNA damage

The term endogenous DNA damage refers to any type of damage caused by normal cellular processes, which is the main part of DNA damage in human tissues. It occurs at several phases of cell division, including during replication (Bjelland & Seeberg, 2003; Friedberg, et al., 2006). As all cells contain oxygen, ROS become one of the most common causes of endogenous DNA damage (Lindahl & Wood, 1999). In addition, ROS production can also be triggered by exposure to exogenous chemicals (Bont & Larebeke, 2004).
ROS can introduce strand breaks, bases modifications, and apurinic/apyrimidinic (AP) sites in DNA (Lloyd, Carmichael, & Phillips, 1998). The number of oxidative hits per diploid genome per day is estimated to 100,000 in rats and 10,000 in humans (Ames, Shigenaga, & Hagen, 1993; Fraga, Shigenaga, Park, Degan, & Ames, 1990). 7,8-dihydro-8-oxodeoxyguanine (8-oxodG) is the major oxidant products of guanine, which is generated about 100 residues per cell per day, can lead to G:C to T:A mutations (Bjelland & Seeberg, 2003). Other products from purine bases include 7,8-dihydro-8oxodeoxyadenine (8-oxodA), ring-opened 2,6-diamino-4-hydroxy-5-formamidopyrimidine (FapyG) and 4,6-diamino-5-formamidopyrimidine (FapyA) (Hu, et al., 2005). Additionally, the atypical lesions 8,5'-cyclo-2'-deoxyadenosine (cdA) and 8,5'-cyclo-2'-deoxyguanosine (cdG) induce strong blocks to DNA and RNA polymerases (You, Swanson, Dai, Yuan, Wang, & Wang, 2013). The major form of oxidative DNA damage to pyrimidines is 5,6-dihydrothymine (thymine glycol, Tg), which is strongly cytotoxic (Byrne, Cunniffe, O'Neill, & Lomax, 2009). Other potentially harmful pyrimidines contain dihydrothymine (DHT), dihydrouracil

(DHU), 5-hydrouracil (5-OHU), and 5-hydroxymethyluracil (5hmU) (Bjelland & Seeberg, 2003).

1.2 Cellular response to DNA damage

As damage to DNA occurs frequently, sophisticated DDR systems have evolved to keep genetic information intact. The signaling cascades of DDR consist of three main steps, briefly, DNA damage sensors recognize damage, recruit transducers that activate signaling cascades which finally activate effectors to induce cell cycle arrest, senescence or apoptosis. (Errol, Graham, Wolfram, Richard , Roger, & Tom , 2006; Lindahl T., 1993; Stergiou & Hengartner, 2001). According to the type of DNA insult and the stage of cell cycle in which the lesion has occurred, the cell cycle can be arrested at either the G1/S transition, within the S-phase or at the G2/M transition (Zhou & Elledge, 2000). DNA damage accumulated cells may undergo permanent cell cycle arrest or senescence or undergo cell death by apoptosis or autophagy (Zhu, Zhou, Wang, Tai, & Ye, 2014). The current view for eukaryotic cells is that, either stalled/stressed DNA replication forks or all types of DNA damage, converted into ssDNA or DSBs, work together to activate DNA damage response signaling (Maréchal & Zou, 2013) (Figure 1.2).

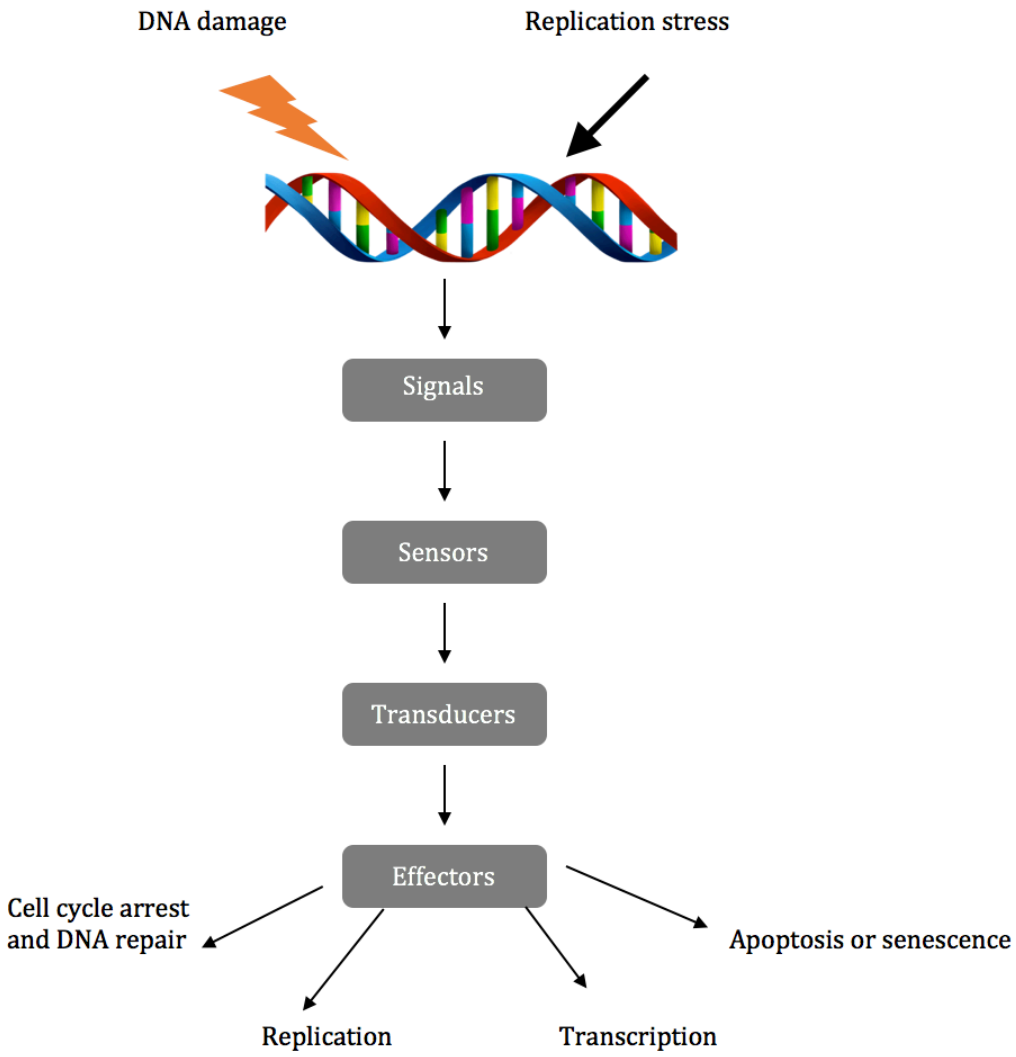

Figure 1.2: A simple schematic representation of DNA damage response signaling pathways. DDR pathway is a signaling pathway consisting of sensors, transducers, and effectors activated upon DNA damage and replication stress. The effectors can lead to cell cycle arrest and DNA repair, DNA replication and transcription blockage. Massive accumulation of unrepaired DNA lesions activates cell death pathways like apoptosis. Adapted and modified from (Maréchal & Zou, 2013).

1.2.1 DNA damage signaling

DNA-dependent protein kinase catalytic subunit (DNA-PKcs), Ataxia telangiectasia mutated (ATM), and Ataxia telangiectasia and Rad3-related (ATR) are the main orchestrators of the DDR (Figure 1.3) (Bartek & Lukas, DNA damage checkpoints: from initiation to recovery or adaptation, 2007). In the G1 phase, Ku70-Ku80 heterodimer can recruit DNA-PKcs to DSBs and activate the non-homologous end-joining (NHEJ) pathway. In the S-G2 phase, DSBs bound to

the Mre11-Rad50-Nbs1 (MRN) complex, breast cancer type 1 (BRCA1), and p53-binding protein 1 (53BP1) phosphorylates and activates ATM (van den Boch, Bree, & Lowndes, 2003). ATM can further phosphorylate Nbs1 and histone H2AX and lead to phosphorylation of the downstream cellular targets p53 and serine/threonine protein kinases checkpoint kinase 2 (CHK2) (Burma, Chen, Murphy, Kurimasa, & Chen, 2001; Kitagawa, Bakkenist, McKinnon, & Kastan, 2004). DNA replication block and replication protein A (RPA) coated ssDNA filaments, activate ATR via the ATR-interaction protein (ATRIP) (Zou & Elledge, 2003; Falck, Coates, & Jackson, 2005; Lee & Paull, 2005). Once ATM or ATR is recruited to the site of damage, they activate effectors to modulate the cell-cycle by CHK2 phosphorylation (Matsuoka, Huang, & Elledge, 1998) and check point kinase 1(CHK1) (Zhao & Piwnica-Worms, 2001) respectively. Although it was shown that both ATM and ATR are required for CHK1 activation in response to IR in human cells (Jazayeri, et al., 2006). Additionally, ATR activation is regulated by ATM in a cell-cycle dependent manner in response to DSBs (Jazayeri, et al., 2006). CHK2 may be activated in response to DSBs throughout the cell cycle, whereas CHK1 is largely restricted to the S and G2 phase (Bartek & Lukas, 2003). There is a two-wave model for activation of G1 to S phase arrest, one is CHK1/CHK2 based and the other is p53 based. CHK1/CHK2 are activated by phosphorylation, and once CHK1/CHK2 are activated the Cdc25A phosphatase is phosphorylated and degraded by proteasomal degradation after ubiquitination. The decrease, or absence of Cdc25A, inhibits the activity of the cyclin E-dependent kinase 2 (CDK2) complex which is required for cell-cycle progression from the G1 to S phase. Based on the other model, p53 is known to induce p21 that inhibits, arresting the cells at the late G1 to S phase (Costanzo, et al., 2000). The intra-S-phase checkpoint is also controlled by ATM-CHK2-Cdc25A-CDK2-Cdc45 signaling upon DSBs (Falck, Mailand, Syljuåsen, Bartek, & Lukas, 2001). Unrepaired DNA damage may leave the cell destined to undergo programmed cell death or senescence induced by p53 (Polyak, Xia, Zweier, Kinzler, & Vogelstein, 1997). In addition, p53 transcriptionally regulates the CDK inhibitor p21 and the proapoptotic protein Bcl-2-associated X protein (BAX) and p53 upregulated modulator of apoptosis (PUMA). Further, it has also been shown that members of the p38 mitogen-activated protein kinase protein

(p38MAPK) are activated by phosphorylation to induce senescence upon genotoxic stress which further activates p53. This pathway is independent of the classical DDR (Freund, Patil, & Campisi, 2011). Thanks to the DNA damaging signaling, most of the cells with DNA damage stopped at a certain phase of the cell cycle, and gained time for DNA repair, otherwise; apoptosis.

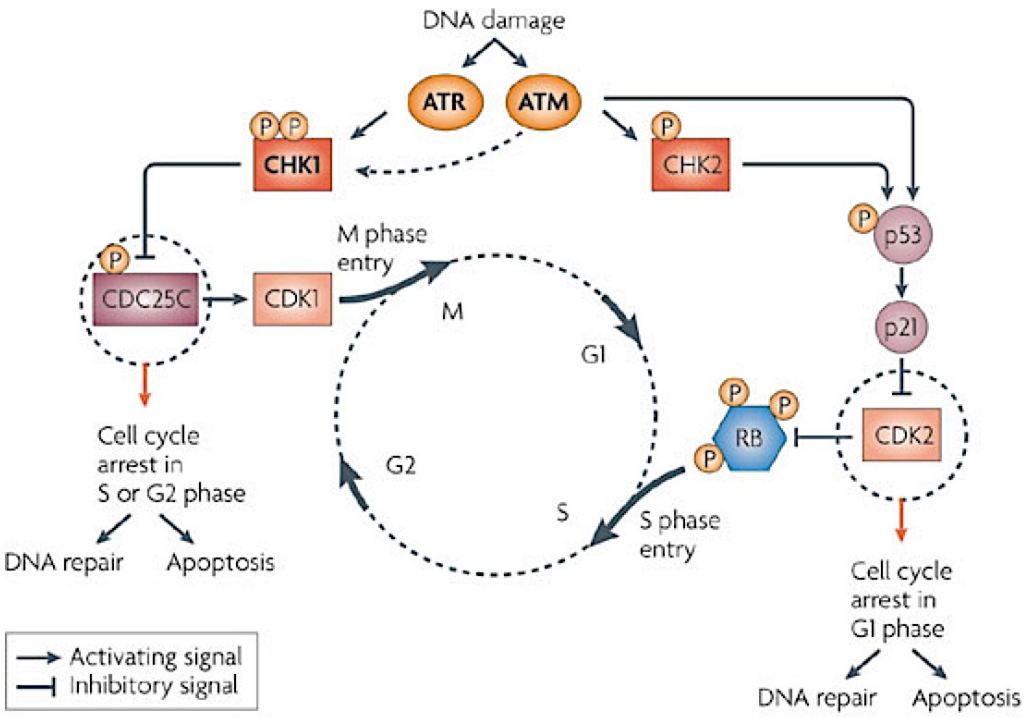

Figure 1.3: DNA damage signaling. ATM and ATR are DNA damage sensor proteins that can induce cell cycle arrest, DDR or apoptosis, depending on the extent of the DNA lesions. the ATM-CHK2 pathway predominantly regulates the G1 checkpoint, whereas the ATR-CHK1 pathway mainly regulates the S and G2 checkpoints, although there is crosstalk between these pathways. Taken from (Lapenna & Giordano, 2009).

1.2.2 DNA repair

Organisms have evolved several highly conserved DNA repair pathways to maintain the integrity and stability of DNA (Friedberg, Walker, & Siede, 1995). However, there are two fundamental mechanism of DNA repair: reversal and excision.

1.2.2.1 Direct reversal (DR)

Direct reversal is the simplest, most efficient, and most accurate repair mechanism, which repairs the lesion without removing the nucleotide (Friedberg, et al., 2006). Direct demethylation is used to repair O^6-methylguanine, O^4-methythymine, *1*-methyadenine, and *3*-methylcytosine. The mammalian O^6-methylguanine-DNA methyltransferase (MGMT) selectively removes the methyl group from O^6-methylguanine and O^4-methythemine (Christmann, Verbeek, Roos, & Kaina, 2011). MGMT uses a cysteine as a methyl recipient and it is a suicide enzyme (Fan, Liu, Cao, Wen, Chen, & Jiang, 2013). The *Escherichia coli (E. coli)* Alk B protein is a dioxygenase that, in the presence of α-ketogluterate as a cosubstrate and Fe (II) as a cofactor, catalyzes the reversal of N^1-methyladenine and N^3-methycytosine lesions by an oxidative demethylation mechanism. Three human homologs of Alk B were found: human Alk B homolog 1 (hABH1), hABH2, and hABH3 (Shankaracharya, Das, & Vidyarthi, 2011). AlkB and hABH3 prefer single-stranded nucleic acids, while hABH2 acts more efficiently on double-stranded DNA (Aas, et al., 2003).

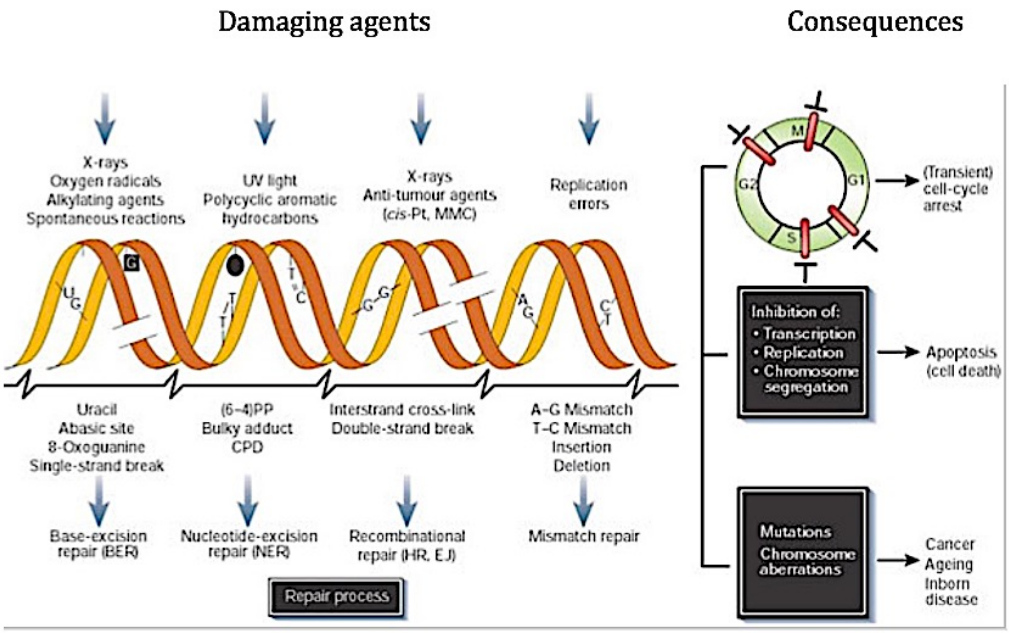

Figure 1.4: DNA repair pathways and possible consequences. DNA damaging agents result in lesions in DNA, which are repaired by relevant DNA repair pathway. Acute effects of DNA damage lead to transient cell cycle arrest in the G1, S, G2, and M phases and on DNA metabolism.

Accumulated DNA damage activates cell death pathway, for example, apoptosis. Failure in cell cycle and cell death contributes to mutation, which is the hallmark of cancer. Adapted from (Hoeijmakers, 2001).

Repair pathways that excise the damaged bases or nucleotides are: nucleotide excision repair (NER), homologous recombination (HR), non-homologous end joining (NHEJ), base excision repair (BER), and mismatch repair (MMR) (Figure 1.4). Although the pathways have distinct functions towards specific DNA lesions, there is considerable crosstalk between them.

1.2.2.2 Nucleotide excision repair

Lesions repaired by NER are characterized by being DNA helix distorting and disrupt transcription as well as DNA replication (Friedberg, et al., 2006). For example, cyclobutyl pyrimidine dimers (CPDs) and (6-4) photoproduct (6-4 PP), and bulky chemical adducts (Li, et al., 2010). The general procedure of NER is: firstly, the lesion is recognized and verified; secondly, both sides of the damage are incised; thirdly, excision of the oligonucleotide fragment; fourthly, the gap is filled by DNA polymerase and finally ligated by ligases (de Boer & Hoeijmakers, 2000). There are two modes of NER, transcription-coupled NER (TC-NER) and global-genome repair (GG-NER). GG-NER repair lesions that occur through the whole genome, while TC-NER specifically removes lesion that block RNA polymerase (Laat, Jaspers, & Hoeijmakers, 1999). The processes differ in the damage recognition step. The damage recognition is done by the complex of xeroderma pigmentosum complementation group C (XPC) and the human rad23b homologue (hHR23B) in GG-NER (Sugasawa, et al., 1998), whereas the stalled RNA polymerase II (RNAP II) itself is the recognition signal for TC-NER (Anindya, et al., 2010). These complexes attract the XPB/XPD helicase subunit of TF II H, single-strand banding RPA, and XPA, and facilitate the formation of preincision complex. RNAP II is then displaced by a complex consisting of cockayne syndrome type A (CSA), CSB, TH II F, and XPG, where as the XPC complex is displaced by XPA (Sugasawa, et al., 1998). After damage recognition and local unwinding, an oligonucleotide of 24-32 nucleotides containing the lesion is excised by the endonuclease activity of XPG at the 3' end of the open

complex and at the 5' end by the XPF/ERCC1 complex. The specificity of XPF/ERCC1 is coordinated by RPA, but the specificity of XPG is not clear. The last step is gap filling by repair DNA polymerase δ and ε, and ligated by DNA ligase I (Fanning, Klimovich, & Nager, 2006).

1.2.2.3 Double strand break repair

Highly deleterious double strand breaks (DSBs) are mainly repaired by HR or NHEJ pathways in eukaryotic cells (Jackson S. P., 2002). However, in higher eukaryotes, NHEJ plays a predominant role for DSBs repair because the cells spend most of their life cycle in the G0 or G1 phases of the cell cycle (Chapter 1.2.1). During the late S/G2 phase of the cell cycle, when sister chromatids are close together and available for exchange, HR and NHEJ compete for repair (Allen, Halbrook, & Nickoloff, 2003).

DSBs repaired by HR results in faithful repair of the DNA lesion but requires the homologous sequence, a sister chromatid as a template. HR is initiated by the MRN complex. The 5' end of the DSB is resected by the 5'-3' exonuclease activity of the MRN complex which gives a 3'-OH overhang (Chapman, Taylor, & Boulton, 2012). More extensive resection involves the 5'-3' exonuclease activity of exonuclease 1 (EXO1) and bloom syndrome protein (BLM) helicase to generate the 3'-ssDNA overhang (Nimonkar, et al., 2011). To stabilize the structure and prevent secondary structure formation, the ss-DNA overhangs are coated by RPA. Subsequently, RPA is replaced by RAD51 with the help of mediator proteins like BRCA2 and the RAD51 paralogs. The RAD51 coated, nucleoprotein filament is referred as the presynaptic filament. This presynaptic filament captures the duplex sister chromatid and searches for homology (Krejci, Altmannova, Spirek, & Zhao, 2012). If sequence of sufficient homology is found, the presynaptic filament invades the sister chromatid and forms the D-loop structure. Replicative DNA polymerases extends from the 3'-end of the invading past the original DSB site. Then the second DSB end is captured by annealing to the extended D loop, forming two crossed-strands or Holliday junction (HJ). Resolution of the HJ by resolvases like SLX1/SLX4 leads to error free repair (Fekairi, et al., 2009).

In contrast to the error free HR pathway, NHEJ involves loss of a few nucleotides from the two broken ends to make them ligatable, which makes NHEJ an error

prone pathway. Key enzymes required for NHEJ are the Ku heterodimer, DNA-PKcs, X-ray repair cross-complementing protein 4 (XPCC4), and DNA ligase IV. The Ku heterodimer is a DNA binding protein consisting of 70 and 86 kDa subunits. Ku binds to the DSB ends and, increase the binding affinity of DNA-PKcs to DSBs (Lieber, 2010). The bound DNA-PKcs then phosphorylates and forms a complex with the Artemis endonuclease, which trims both the 5'- and 3'-ends at DSBs. The gaps are filled by DNA pol μ and λ. Finally, the ligation is performed by XRCC-DNA ligase IV complex (Francis, et al., 2014). This pathway functions throughout the cell cycle to repair DSBs, and it is also crucial for normal physical process such as, class switch recombination and V(D)J recombination (Soulas-Sprauel, et al., 2007).

1.2.2.4 Base excision repair

Base excision repair is thought to be the major repair pathway protecting cells against single-base DNA damage in form of small chemical modifications, which do not cause large helix distortion (Jacobs & Schär, 2012). This pathway was discovered by Tomas Lindahl in 1974. BER is mainly used to repair oxidative bases, uracil in DNA, alkylated bases and single-strand breaks (Lindahl T. , 1993). The first step of BER involves recognition, typically excision of modified bases by DNA damage specific DNA glycosylases. A general mechanism of all DNA glycosylases includes a nucleophilic attack at the the 2'-deoxyribose of the modified nucleoside, resulting in incision of the *N*-glycosylic bond (Kim & Wilson, 2012). The DNA glycosylases are either mono-functional or bi-functional. Mono-functional DNA glycosylases have only one catalytic activity. They remove the base leaving an intact AP site in DNA (Krokan, Standal, & Slupphaug, 1997). The mono-functional glycosylases use nucleophiles from the medium, like activated water molecules, to attack the *N*-glycosylic bond (Krokan, Standal, & Slupphaug, 1997). Bi-functional DNA glycosylases, have both glycosylase and AP lysate activity that cleaves DNA at 3'-side of the AP site. Instead of activated water molecule, an internal amine nucleophile cleaves the DNA strand at the AP site by β- or β, δ-elimination generation a strand break with a 3'-phospho α, β-unsaturated aldehyde (3'dRP) and a 5'-phosphate (5'-P) ends (Fromme & Verdine, 2003).

There are 11 DNA glycosylases, with molecular weights ranging from 20 to 50kDa, monomeric proteins that can work without cofactors known in mammals. The mono-functional DNA glycosylases are uracil-DNA glycosylase (UDG) like Uracil *N*-glycosylase (UNG), the mismatch specific thymine/uracil DNA glycosylase (TDG), single-strand-selective mono-functional uracil-DNA glycosylase 1 (SMUG1), and methylpurine DNA glycosylase (MPG). UNG and TDG have narrow substrate specificities, whereas MPG can excise a large array of substrates that have a weak *N*-glycosylic bond as a common feature (Krokan & Bjørås, 2013). The bi-functional DNA glycosylases are 8-oxoG DNA glycosylase (OGG1), endonuclease III-like homolog 1 (NTHL-1), methyl-CpG domain protein 4 (MBD4) and three endonuclease-VIII-like enzymes (NEIL1,2 and 3). A conserved helix-hairpin-helix motif and an invariant Asp residue are found in the active site of both mono and bi-functional DNA glycosylase. (Jacobs & Schär, 2012). DNA glycosylases have a common-lesion processing step that involves flipping of the damaged nucleotide out from the double-strand DNA. The lesion is then bound to the active site of the DNA glycosylase (Hegde, Hazra, & Mitra, 2008).

1.2.2.5 Mismatch repair

The MMR is a highly conserved DNA repair pathway, which repairs mismatched or misaligned bases and insertion-deletion loops (IDLs) during DNA replication or recombination (Li G.-M. , 2008). Enzymes involved in MMR were first identified in *E. coli*, and the genes were named as "Mut", because of hypermutator phenotypes were seen in the mutants (Meyers, et al., 2003). Mismatches are recognized by the MutS complex, which contains a highly conserved C-terminal ATPase domains (Manelyte, Urbanke, Giron-Monzon, & Friedhoff, 2006). In eukaryotes, as a heterodimer, MutS functions as the "mismatch recognition" protein. The eukaryotic MutSα is a heterodimer of MSH2 and MSH6, whereas MutSβ consists of MSH2 and MSH3. MutSα recognizes single base-base mismatches and IDLs of 1-2 nucleotides, while MutSβ recognizes larger IDLs (Clark, Cook, Tran, Gordenin, Resmick, & Kunkel, 1999). After efficient recognition of the mismatch, it is important to discriminate between the parental and the newly synthesized DNA strand. This is quite efficiently achieved

in *E. coli*, as the semi-methylated dGATC sites act as signals for strand discrimination. In eukaryotes, a proposed model for strand discrimination is the molecular-switch model or sliding clamp model. In this model MutS binds to mismatched DNA when in an ADP-bound state. This binding induces a conformation change that allows phosphorylation of ADP to ATP. This promotes a second conformation change and allows the MutS to form a bi-directional sliding clamp. It is the binding of ATP and not ATP hydrolysis that stimulates formation of the ternary complex with MutL heterodimer. The MutLα complex, which is a heterodimer of MHL1 and PMS2, is recruited to the MutSα complex. The MutS/MutL complex undergoes an ATP-driven conformation change, that releases the ternary complex from the mismatch to search for a nick. It is believed that 5' or 3' nick is the strand discrimination signal (Li G.-M. , 2008). After mismatch recognition and strand discrimination, the next step involves repair and synthesis. Human exonuclease-1 (hEXO-1) is recruited, when the ternary clamp encounters a 5' nick, displacing replication factor C (RFC) (Sertic, et al., 2011). The hEXO-1 chews the DNA strand in the 5' to 3' direction beyond the mismatch. When the ternary complex encounters a 3' nick, the MutLα endonuclease makes an incision 5' to the mismatch in a PCNA and RFC-dependent manner. This nick is used for loading hEXO-1 for degradation in the 5' to 3' direction between the MutL-generated break and the original 3' nick. The other proteins involved in MMR are RPA, RFC, PCNA and DNA pol δ and pol ε. The single-strand gap generated during excision is stabilized by RPA. RPA is phosphorylated after recruitment of DNA pol δ. Unphosphorylated RPA stimulates mismatch provoked DNA excision. But the phosphorylated RPA facilitates MMR-associated DNA synthesis more efficiently than the unphosphorylated state. Human MutLα was reported to regulate termination of the mismatch-provoked excision. Finally, the gap is filled by DNA pol δ which is recruited to the 3'-terminus by PCNA and ligated by DNA ligase I (Ortega, Li, Lee, Tong, Gu, & Li, 2015).

1.3 *C.elegans* as a model system

Though *Caenorhanditis elegans (C. elegans)* is often mischaracterized as a soil nematode, it can most easily be isolated from rotting vegetable matter, which is a sufficient supply of their bacterial food source (Barrière & Félix, 2014).

Pioneered by Sydney Brenner as a model organism in the 1960s, the free-living nematode *C. elegans* started to be used to study a variety of biological process, for example, aging. *C. elegans*, 1 mm long in adult, exists as two sexes: self-fertilizing hermaphrodites (XX) and males (XO). The reasons for why *C. elegans* became a popular model system are: firstly, it can be easily maintained in laboratory, either in NGM agar plates or in liquid cultures with bacteria as food source; secondly, *C. elegans* has a short life cycle of 3 days at 25°C, which contains embryonic stage, 4 larval stages, and adulthood (Figure 1.5); thirdly, the adult hermaphrodite produces about 300 offspring by self-fertilization during a 4-day reproductive period; in addition, the normal life span of *C. elegans* is 2-3 weeks under laboratory conditions. It is known that there are 959 somatic cells in adult hermaphrodites. The nervous system contains 302 neurons, whereas adult gonad has about 2000 germ cells, which is the only proliferative tissue. Lastly, *C. elegans* was the first multicellular animal whose whole genome was completely sequenced. It has been showed that *C. elegans* has about 20,000 genes, of which about 40% of genes have recognizable homologs in humans (Panowski & Dillin, 2009; Hashmi, Tawa, & Lustigman, 2001).

Reverse genetics by RNA interference (RNAi) is a robust technique in *C. elegans* (Ni & Lee, 2010), by which genes are silenced by double-strand RNA that is introduced through feeding, soaking, or injection. Since *C. elegans* is transparent, it can be easily studied by microscopy and cell cycle arrest and apoptosis can be followed in living worms using DIC microscopy. Since the discovery of single gene mutations that double its lifespan, the nematode *C. elegans* has provided remarkable insights into the biology of aging (Amrit, Ratnappan, Keith, & Ghazi, 2014; Kenyon, Chang, Gensch, Rudner, & Tabtiang, 1993).

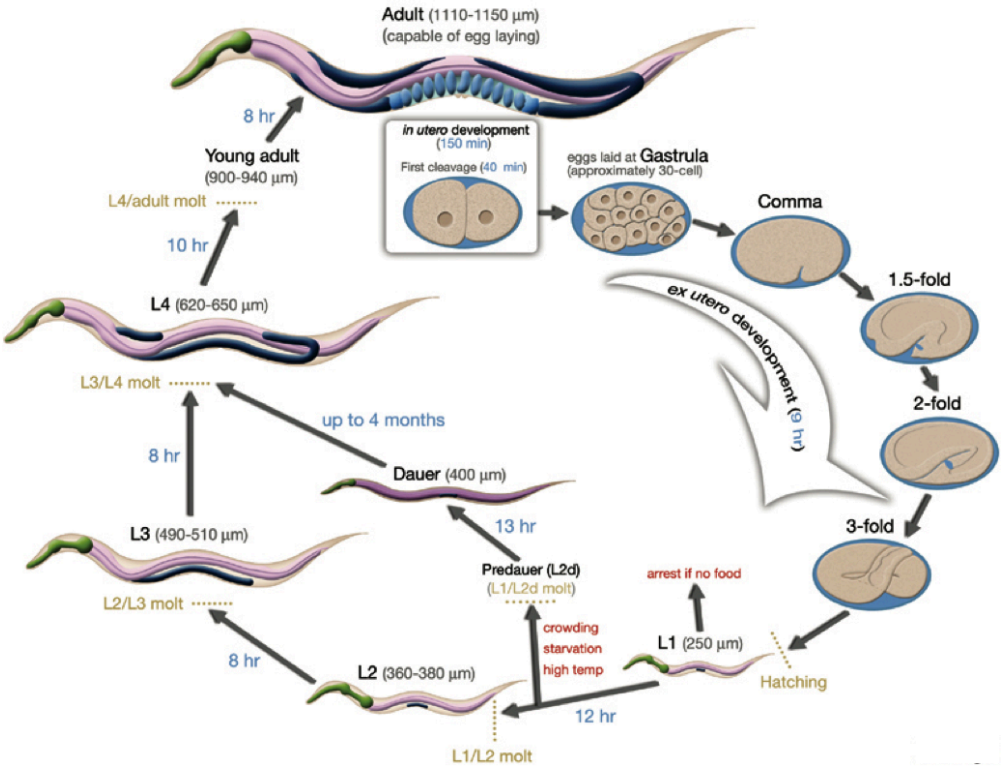

Figure 1.5: Life cycle of *C. elegans*. *C. elegans* has a short life cycle of 3 days at 25°C, which contains embryonic stage, 4 larval stages, and adulthood. The figure uses a hermaphrodite as an example to illustrate the life cycle. The numbers in blue along the arrow show the duration of each stage. Under certain conditions, for example, food-limited condition, *C. elegans* enters dauer stage. When the condition is suitable again, *C. elegans* backs to the normal life cycle. Taken from (http://www.wormatlas.org).

1.3.1 Stress response pathways in *C. elegans*

Carried out by a stress response system, hormesis is a phenomenon by which a mild stress provides an organism with increased resistance to a subsequent and more extreme stressor (Minois, 2000). Exposure to mild stress has been shown to somehow slow down the aging process (Tissenbaum & Guarente, 2001; Khazaeli, Tatar, Pletcher, & Curtsinger, 1997; Shama, Lai, Antoniazzi, Jiang, & Jazwinski, 1998). *C. elegans* has an elaborate stress response system, which is of high evolutionary conservation, involves antioxidant enzymes and transcription factors that orchestrate a large set of stress-response pathways (Lant & Storey, 2010). These pathways involve the heat-shock response pathway, insulin/IGF-1 signaling(IIS) pathway, target of rapamycin (TOR) pathway, AMPK

(AMP-activated protein kinase) pathway, as well as sirtuin pathways. (López-Otín, Blasco, Partridge, Serrano, & Kroemer, 2013),

1.3.1.1 DAF-16-mediated IIS pathway

The *C. elegans* IIS pathway connects nutrient levels to metabolism, growth, development, longevity, and stress response. The FOXO transcription factor, DAF-16 (an ortholog to mammalian FOXO-family) is the major downstream effector of DAF-2, which is the sole insulin/IGF-1-like receptor (Tater, Bartke, & Antebi, 2003). DAF-16 functions as a transcriptional regulator in the IIS pathway to defend, for example, heat shock and oxidative stress, and to induce the developmental arrest and DNA repair. The DAF-16-mediated signaling pathway is initiated by binding of an insulin/insulin-like ligand to the DAF-2 receptor, the activated DAF-2 activates a phosphorylation cascade that involves in phosphorylation of the *C. elegans* AGE-1(ortholog to the human phosphoinositide-3-kinase (PI-3Ks)). AGE-1 in turn triggers a signaling cascade to activate several downstream serine/threonine kinases including AKT-1, AKT-2(homologous to the human Akt/PKB kinase) and serum- and glucocorticoid inducible kinase 1 (SGK-1) (homologous to human SGK). These kinases have been reported to form a multimeric protein complex that function to regulate DAF-16 negatively (Murphy C. T., 2013). Hence, active DAF-2 signaling leads to phosphorylation and nuclear exclusion of DAF-16 which accumulates in the cytosol. Mutations in the DAF-2 signaling pathway or stress induction result in reduction of AKT-1/2 and SGK-1 mediated phosphorylation of DAF-16, thereby permitting the translocation of DAF-16 from cytoplasm to nucleus. As a consequence, non-phosphorylated DAF-16 modulates the transcription of various target genes (Paradis & Ruvkun, 1998).

DAF-16 target genes regulate a wide range of stress-response genes such as molecular chaperones, superoxide dismutases, metabolic genes, antimicrobial, hormone signaling, and regulators of the cell cycle (Landis & Murphy, 2010; Murphy, et al., 2003). Activation of DAF-16 upon IIS suppression is associated with extended lifespan and increased stress resistance. Several DAF-16 target genes have been identified after searching for genes with daf-16 binding

elements (DBE). The optimal DNA-binding sequence for DAF-16 contains the core sequence 5'-TTGTTTAC-3'. One of these *daf-16*-downstream genes, *aqp-1*, downregulated by glucose, which encodes an aquaporin glycerol channel (Obsil & Obsilova, 2011). Interestingly, according to Kenyon, adding 2% glucose to the medium shortened the lifespan of *C. elegans* by inhibiting the activities of life span extending transcription factors that are also inhibited by insulin signaling: the FOXO family member DAF-16 and the heat shock factor HSF-1. This effect also involves the downregulation of an aquaporin glycerol channel, aqp-1. This suggests that changes in glycerol metabolism may underlie the life span-shortening effect of glucose and that aqp-1 may act cell nonautonomously as a feedback regulator in the IIS pathway (Lee, Murphy, & Kenyon, 2009).

SKN-1 and DAF-16 share several features; they have overlapping expression patterns and both undergo cytoplasmic and nuclear translocation to induce stress-responsive genes. Thus, it has been suggested that these transcriptional factors share regulatory control. In an attempt to address this question, a recent work revealed that, similar to DAF-16, SKN-1 is negatively regulated by the IIS pathway. Tullet, and his colleagues, showed that the translocation of SKN-1 to the nucleus is controlled by the IIS pathways as AKT-1/2 and SGK-1 directly phosphorylate multiple sites of SKN-1 in response to DAf-2 receptor activation. Activation of target genes by SKN-1 upon IIS suppression, increased stress tolerance and longevity. Interestingly, although these finding suggest that the transcriptional network regulated by SKN-1 is modulated by IIS, DAF-16 is not required for these events. SKN-1 contributes the phenotypes associated with reduced IIS in parallel to DAF-16 (Tullet, et al., 2008).

Another pathway converging on DAF-16 involves a member of the JNK family. JNK-1, the *C. elegans* homolog of mammalian JNK, is thought to regulate lifespan in parallel to the IIS pathway, by regulating the subcellular location of DAF-16. Whereas phosphorylation of DAF-16 by AKT-1 and SGK-1 kinases constrains it to the cytoplasm, phosphorylation of DAF-16 by JNK-1 leads to nuclear translocation. Consistent with this observation, *jnk-1* mutants have shorter lifespan, and mutants overexpressing JNK-1 exhibit extended lifespan in a

manner independent of IIS but dependent on *daf-16* (Zhou, Pincus, & Slack, 2011).

The protein deacetylase SIR-2.1, the homologous to yeast *SIR2* in *C. elegans*, with co-factor Nicotinamide adenine dinucleotide (NAD^+), involves the activation of stress signaling via the mitochondrial unfolded protein response (UPR^{mt}) and the nuclear translocation and activation of DAF-16 (Mouchiroud, et al., 2013). In addition, according to Tissenbaum and Guarente, a *sir-2.1* duplication extended lifespan by up to 50% via a *daf-16*-dependent manner. (Tissenbaum & Guarente, 2001). When *C. elegans* is treated with the small molecule resveratrol, however, life span is extended via a fully *sir-2.1*-dependent manner, without the involvement of *daf-16* (Viswanathan, Kim, Berdichevsky, & Guarente, 2005). Briefly, *sir-2.1* influence DDR and aging in both the *daf-16*-dependent and the *daf-16*-independent manners.

1.3.1.2 The HSF-1/Heat-shock pathway

One signature event in cellular stress responses is the induction of HSPs. HSPs function as molecular chaperones, playing a variety of roles including assisting protein folding, targeting damaged proteins for degradation, and other responses associated with the protection of cells from damage. The induction of the heat-shock response is mediated by heat-shock transcription factors (HSFs). The *C. elegans* HSF-1 is orthologs to mammalian heat shock factor 1 (HSF1), which forms homotrimeric complexes in response to stress and thereby acquire DNA-binding activity to the heat-shock elements (HSE) located in the promoters of *hsp* genes such as *hsp-16*, thereby mediating transcriptional activation. The high level of HSP-16 is often used as surrogate phenotype for stress resistance (Stringham, Dixon, Jones, & Candido, 1992). Downstream target genes for HSF-1 are, among others, chaperones and small heat shock proteins that also are controlled by DAF-16 (Morley & Morimoto, 2004).

1.3.1.3 DNA damage response in *C. elegans*

Table 1.1: Orthologous DDR proteins in *C. elegans* and mammalian cells. This table is adapted and modified from (Stergiou & Hengartner, 2001).

Protein function	*C. elegans*	Mammals
Sensors		
RFC1-like	HPR-17	RAD17
PCNA-like	HPR-9	RAD9
	HUS-1	HUS1
	MRT-2	RAD1
BRCT-containing DSB repair	HSR-9	BRCA1
	MRE-11	MRE11
	RAD-50	RAD50
		NBS1
Transducers		
PI3-kinases	ATM-1	ATM
	ATL-3	ATR
Effector kinases	CHK-1	CHK1
	CHK-2	CHK2
Downstream effectors	CEP-1	p53

DDR signaling is well conserved from mammals to *C. elegans* (Table 1.1), and has been well studied in the *C. elegans* germ line in response to UV and IR (Gartner, MacQueen, & Villeneuve, 2004). DNA damage in the germ line leads to cell-cycle arrest and apoptosis. Cell-cycle arrest can be observed in the distal and mitotic region of the germ line, whereas apoptosis occurs in the pachytene region in response to the genotoxic stress. The DDR sensor 9-1-1 complex, composed of HUS-1, MRT-2 and HPR-9, is required for genomic stability and induction of apoptosis to IR. Similar to mammals, the DDR transducers, ATL-1 and ATM-1 are required for checkpoint activation in response to IR and UV (Stergiou & Hengartner, 2001). Stalled replication folk activates ATL-1 only. ATL-1 is required for checkpoint responses towards stalled replication fork, which is recruited by RPA-1 filament, functions upstream of CLK-2. Also, ATL-1 is recruited by DSBs in a MRE-11 and RPA-1 dependent manner. CHK-1 is considered as the main effector kinase at downstream of ATL-1 and ATM-1, by being phosphorylated at Ser345 in response to hydroxy urea (HU), IR, and UV. Uracil misincorporation leads to formation of single- and double-strand breaks activating DDR. Interestingly, there is a genetic interaction between the DDR checkpoint CLK-2 and UNG-1 in respone to processing of uracil misincorporation in DNA (Dengg, Garcia-Muse, Gill, Ashcroft, Boulton, & Nilsen, 2006).

The embryonic cell cycle lacks the G1 and G2 phases. At the 28-cell stage, the G2 phase appears, whereas the timing of the introduction of the G1 phase is still not clear. However, CHK-1 is required for the S to M checkpoint during early embrogenesis. The ATL-1/CHK-1 pathway is active and controls the embryonic

cell cycle from the first division. RNAi of CHK-1 gives sterile progeny, abolishes cell-cycle arrest and apoptosis after IR in the germ line. Inhibition of CHK-1 delays early embryonic cell cycle progression in response to DNA damage, suggesting that CHK-1 is important for both embryogenesis and DDR in *C. elegans.* Interestingly, CHK-1 has no known function in somatic cell divisions. Recently, it has been reported that the embryonic cell cycle depends on CLK-2. The *clk-2* mutants acquire elevated levels of spontaneous mutation suggesting that *clk-2* mutant accuire elevated level of DNA damage, which triggers the ATL-1/CHK-1 checkpoint, demonstrating that CLK-2 and ATL-1 in *C. elegans* are antagonistic. They also reported that the cell cycle delay in *clk-2* mutants depends on CEP-1. CHK-2, on the other hand, doesn't contribute to IR-induced checkpoint response. Instead, CHK-2 is required to meiotic chromosome pairing and to mediate UV triggered germ cell apoptosis.

2. Aims of the study

There is mounting evidence suggesting DNA repair deficiency as a mild stressor that induces a favorable cytoprotective homeostatic response.

Transcriptional signatures of *nth-1(-)* shows that the loss of NTH-1(the only BER initiation enzyme in *C. elegans*), is accompanied by activation of stress-response pathways, for example SLK-2 and SKN-1, which are the two major stress-responsive transcription factors in *C. elegans,* and downregulation of IIS (Fensgård, Kassahun, Bombik, Rognes, Lindvall, & Nilsen, 2010; Arczewska, et al., 2013). In addition, a highly significant increase (~30 fold) of the aquaporin, *aqp-1*, was seen in the *nth-1(-)* and *xpa-1(-)* and is a part of the compensatory response to reduced DNA repair capacity (Arczewska, et al., 2013; Fensgård, Kassahun, Bombik, Rognes, Lindvall, & Nilsen, 2010). *aqp-1* was also shown to be involved in lifespan determination as *aqp-1(-)* strain has a shortened lifespan (Lee, Murphy, & Kenyon, 2009). Unpublished data from the Nilsen lab suggests that AQP-1 might be a mediator of the cytoprotective homeostatic response in DNA repair mutants as the *aqp-1(-); xpa-1(-)* is hypersensitive to heat stress but not UV. (Kassahun and Nilsen, unpublished).

Moreover, the Bohr and Nilsen groups described that the defection in the NER pathway (specifically XPA mutants) leads to over-activation of the DNA damage sensor poly (ADP-ribose) polymerase 1 (PARP1) (Fang, et al., 2014). As PARP1 is a major consumer of NAD+, PARP1 over-activation leads to NAD+-depletion and progressive mitochondrial dysfunction, partly, because NAD^+ is a rate-limiting co-substrate for SIRT1, a nuclear protein that can regulate mitochondrial biogenesis (Fang et al., 2016).

The overall aims of this study are to identify genes that orchestrate the cell non-autonomous cytoprotective homeostatic response to DNA repair deficiency and to exploit the WMicrotracker automatic measuring system to various labor-consuming stress response assay, such as, heat shock tolerance assay and paraquat (PQ) survival assay.

Specific aims include:

1) Evaluate WMicrotracker system for automatic measuring of stress sensitivity;
2) Generate *aqp-1(-); atm-1(-)* double mutant;

3) Test and verify whether *aqp-1* functions as the mediator of non-autonomous cytoprotective homeostatic response in DNA repair deficient strain *atm-1(-)*;
4) Generate *aqp-1(-); sir-2.1(-)* double mutant, to test if *aqp-1* and *sir-2.1* both function in non-autonomous cytoprotective homeostatic response in a mutual compensatory manner.

3. Materials and Methods

3.1 Maintenance of *C. elegans*

3.1.1 Strains and constructs

E.coli strain OP50 were used as food for *C. elegans*. *C. elegans* were cultured at 20°C on solid nematode growth medium (NGM) agar plates using standard procedure (Brenner, 1974). All experiments were performed at 20°C unless otherwise stated. Reference strain Bristol N2, *aqp-1 (tm2309) II*, *sir-2.1 (ok434) IV* were obtained from the *Caenorhabditis* Genetics Center (CGC) (University of Minnesota, St paul, MN, USA), and *atm-1 (gk186) I* was kindly provided by the Clare Hall Labs of Francis crick institute. All mutants are expected to be loss-of-function mutants (Supplementary figure S1). *apq-1 (tm2309) II*; *atm-1 (gk186) I* and *aqp-1 (tm2309) II*; *sir-2.1 (ok434) IV* double mutant strains were generated during the study (Table 1.1).

Table 1.1: Strains and associated genotypes

Strains	Genotypes
N2	wild type (WT)
RB2570	*aqp-1 (tm2309) II*
VC381	*atm-1 (gk186) I*
VC199	*sir-2.1 (ok434) IV*
RB2570 x VC381	*aqp-1 (tm2309) II; atm-1 (gk186) I*
RB2570 x VC199	*aqp-1 (tm2309) II; sir-2.1 (ok434) IV*

3.1.2 Freezing and recovery of *C. elegans*

C. elegans can be frozen and stored indefinitely in liquid nitrogen (−196°C) (Brenner, 1974) . *C. elegans* was stored at -80°C freezer for this study. A successful freezing mainly depends on using animals at the correct developmental stage, the addition of glycerol to the freezing media, as well as a gradual cooling down to -80°C. Freshly starved L1-L2 stage larvae can survive freezing best, while the well-fed animals, adults, eggs, dauers do not survive well. In this study, freshly starved plates with a main population of worms at L1-L2 stage were washed off by M9 buffer (Appendix 8.1), added with an equal amount of freezing solution, containing 30% glycerol (Appendix 8.1). The resulting worm

suspensions were mixed briefly, which contain 15% glycerol, and then 1mL of mixtures were transferred to 1.8ml cryogenic tubes and immediately inserted into a cell-freezing container for achieving 1°C decrease in temperature per minute. A test thaw was performed for each strains after 24-hour storage at -80°C. Thawing was done quickly by holding the cryogenic tubes in hand until suspension thawed. 800µl supernatant was discarded, 200µl leftover was transferred to an unseeded plate and incubated at 20°C for 2 hours before being assessed for survival and basic morphology.

3.1.3 Synchronization of *C. elegans*

Preparing a large synchronized population of *C. elegans* is recommended for use in high throughput assays in order to eliminate variation in results due to developmental differences (Sulston, 1983). Two basic methods were adopted for synchronization of worms.

Worms can be synchronized by alkaline hypochlorite solution (bleaching solution) (Appendix 8.1). The principle of the method lies in the fact that worms are sensitive to bleaching solution, while egg shells protect embryo from it. Bleaching method is also recommended when plates are contaminated. Gravid adults were recovered by washing plates with M9 buffer in 15 ml tubes, which then were centrifuged at 1500rpm at room temperature for 1 minute. The supernatants were discarded which may contain bacteria. 1.5 mL bleaching solution was added to each 3.5ml leftover and the mixture was agitated for no more than six minutes, the reaction then stopped by adding M9 buffer to fill the tubes. The mixtures were quickly centrifuged at 1500 rpm for 1 minute and supernatants were discarded. The pellets were washed for 2 more times by filling the tube with M9 buffer. After three times of washing, 2ml of M9 buffer was added to each tube, samples then were resuspended and transferred to 3.5cm plates and kept on the shaker in 20°C over night. After treatment with bleaching solution, embryos are incubated in liquid media without food, which allows hatching but prevents further development. The L1 worms were transferred to newly OP50-seeded NGM plates the next day.

For certain mutant strains, bleaching method can be quite stressful on the embryos, as evidenced by hatching rates below 99%. This is likely due to the

time required to remove the bleach after ''popping'', which also leads to variability between trials. In addition, the stress of a bleach preparation has the potential to cause a hormetic response in worms that will increase their resistance to heat stress (Zevian & Yanowitz, 2014). Egg-laying method was adopted to eliminate the possible influence of bleaching solution to larvae. Briefly, 30-50 gravid worms for each strain were transferred to new OP50-seeded plates respectively, which were then kept in 20°C incubator. Gravid worms were removed after 1.5-2 hours. Eggs left on these plates were synchronized.

3.2 Generation of double mutant *C. elegans*

C. elegans was chosen as an experimental organism partly because its genetic system advantages (Brenner, 1974). Genetic analysis is an especially powerful approach for investigating complex biological pathways. One gene, once thoroughly characterized, can become the starting point for further exploration. With a strain bearing a mutation in the gene, functional interactions between genes or gene products can be examined by generating double mutant strain through simple crosses with previously characterized mutants.

3.2.1 Genetic cross

Genetic cross was performed to generate double mutants. In the study, *aqp-1 (tm2309) II; atm-1 (gk186) I* and *aqp-1 (tm2309) II; sir-2.1 (ok434) IV* were generated. The generation of the *aqp-1 (tm2309) II; atm-1 (gk186) I* double mutant is used as an example to explain the genetic crossing process.
One *atm-1(-)* L4 virgin hermaphrodite was mated with 5 *aqp-1(-)* males on a new 3.5cm OP50-seeded NGM plates. Since L4 hermaphrodite had not reached reproductive stage, all the resultant offspring were from sexual reproduction. Hence, approximately 50% incidence of males in F1 generation, which is much higher than the self-fertilized, was used to confirm successful mating. 4-5 L4 hermaphrodites from F1 generation were then single on 3.5cm OP50 seeded NGM plates separately and allowed self-fertilize. Worms from F2 generation were then singled onto 32 3.5cm NGM OP50 seeded plates, after 20 eggs were laid, the F2 gravid hermaphrodites were genotyped.

3.2.2 Males generation

As males were required and the low frequency (approximately 0.2%) of males in different strain, heat shock and mating were applied to generate males for mating. The principle of heat shock method lies in the fact that, during meiosis, heat shock results in higher percentage of X-chromosome nondisjunction which contributes a higher incidence of male progeny (Anderson, Morran, & Phillips, 2010). Young adult *aqp-1(-)* hermaphrodites were incubated at 20°C after 4-hour 32°C heat shock treatment, males were collected from the F1 generation. Otherwise, males can be generated by keeping 5-6 males and 1-2 hermaphrodites of the same mutant on one 3.5cm OP50-seeded NGM plate, males were collected from the next generation.

3.2.3 Single-worm lysis

The gravid F2 hermaphrodites, which were single to new 3.5cm OP50-seeded NGM plates, after the they laid approximately 10-20 eggs (for the sake of keeping the possible double mutant strains), were then lysed in order to generate genomic DNA for genotyping. Single worm, from different strains were picked and placed into PCR tube containing 10µl lysis buffer (Appendix 8.1) separately. The single worm lysis was then performed in Eppendorf Mastercycler ep Gradient S at 60°C for 60 minutes followed by incubation at 95°C for 20 minutes to inactivate proteinase K, which was used to digest protein and release genome (Figure3.1). Lysates were stored at -80°C freezer overnight (lysates kept in -80°C freezer was somehow more efficient than the ones were used directly after the single worm lysis). 2µl of worm lysates were required for the Polymerase chain reaction (PCR) genotyping system.

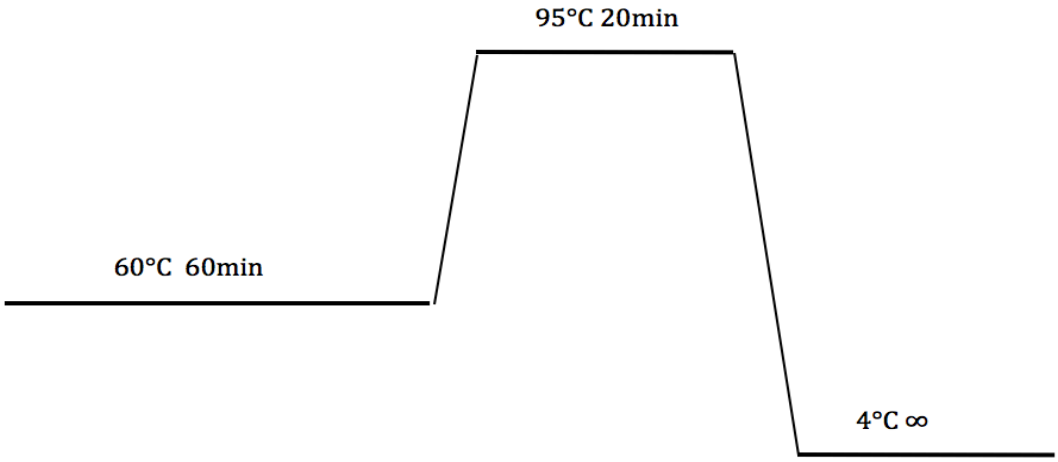

Figure 3.1: Single worm lysis program. The single worm lysis was performed in Eppendorf Mastercycler ep Gradient S at 60°C for 60 minutes followed by incubation at 95°C for 20 minutes to inactivate proteinase K, the samples then kept in the -80°C freezer.

3.2.4 PCR genotyping

To detect and confirm the genotypes of double mutant in F2 generation, PCR was applied to amplify the selected fragment, normally the fragment with mutant, so that difference would appear between the wild type and the one with mutant by gel electrophoresis. In this study, the fragments of *aqp-1*, *atm-1*, and *sir-2.1* genes were amplified. PCR was carried out by following the protocol optimized from AccuPrime™ Pfx SuperMix protocol (Supplementary figure S2) (Thermo Fisher Scientific). The PCR system contained 22.5µL AccuPrime™ Pfx SuperMix, 1µL of 10µM each primer (Invitrogen) and 2µl single lysates. The PCR mixes were subjected to denaturation at 94°C for 2 minutes, followed by 35 to 40 cycles of 94°C for 30 seconds to 2 minutes, annealing at 55.5°C to 59°C for 30 seconds, according to the Tm of primers and the size of the target fragments. Normally, the genotyping PCR condition was optimized by starting to test the annealing temperature 5-10°C lower than the primer Tm. In this study, as the protocol for *aqp-1* and *atm-1* were optimized already in previous study, therefore, only the condition for *sir-2.1* need to be optimize.

Major modification to improve PCR performance was directed towards factors affecting annealing. The annealing temperature is of critical importance in

designing parameters for specific amplification of desire bands. Thus, multiplex gradient PCR was applied to find the optimum annealing temperature for *sir-2.1*, 11 identical PCR reaction mixtures were prepared and run in Eppendorf Mastercycler ep Gradient S which has a program for gradient function. Primers, binding site sequences, and expected bands are showed below (Table 3.1), (Figure 3.2). For *atm-1*, there were two pairs of different enzymes were used, because the first enzyme was suspected to be invalid. Therefore, a new pair of primer was designed by using Primer 5.

Table 3.1: Primers used in this study (Invitrogen).

Primers	**Sequences**			
aqp-1 (tm2309) *II*				
*Aqp-1*_del_L	5'-AAGACAACTGAATGGATTGG-3'			
*Aqp-1*_del_R	5'-AGATGACCACCTGAAAGATG-3'			
*Aqp-1*_Contr_L	5'-GTTCTCGCATACTTCCTCTG-3'			
*Aqp-1*_Contr_R	5'-GCTTGAAGCAATTTTTGTTG-3'			
Expected bands	N2	381bp and 125bp	*aqp-1*	381bp
atm-1 (gk186) *I*				
Forward I	5'-AACCCCAAAGGGTATTACGG-3'			
Reverse I	5'-GTGTGCAAAACGTGATACGG-3'			
Expected bands	N2	820bp	*atm-1*	272bp
Forward II	5'-CCCAAAGGGTATTACGGAACT-3'			
Reverse II	5'-GTTTTCAAGAAGCCTTTCACCT-3'			
Expected bands	N2	874bp	*atm-1*	326bp
sir-2.1 (ok434) *IV*				
Forward	5'-GTCATCTAGCGATTGTGCTCTAG-3'			
Reverse	5'-CGTACCATCTGTATCACATCG-3'			
Expected bands	N2	1083bp	*sir-2.1*	315bp

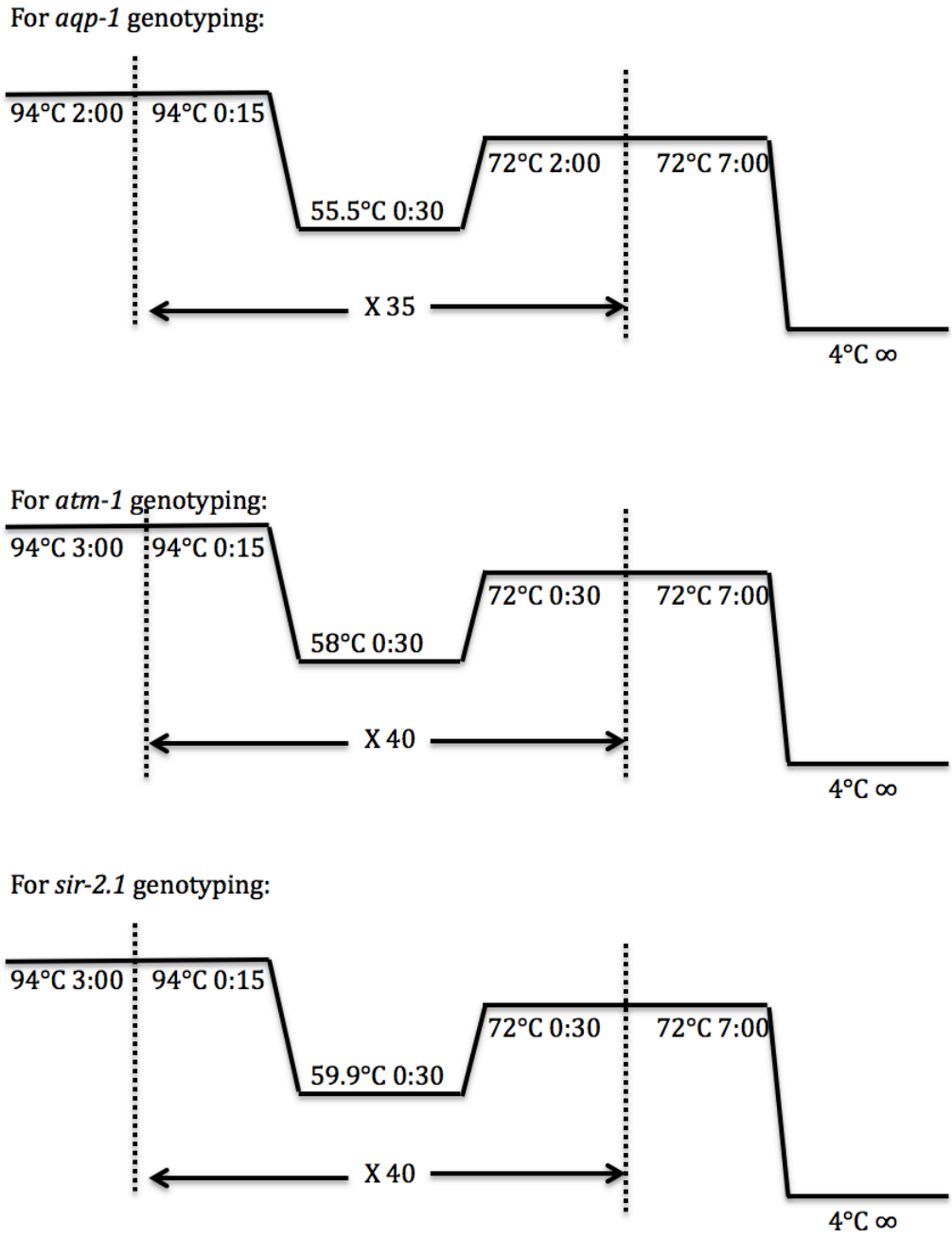

Figure 3.2: PCR Genotyping program. The fragments contain *aqp-1*, *atm-1*, *sir-2.1* mutants need to be genotyped for the confirmation of *aqp-1(-); atm-1(-)* and *aqp-1(-); sir-2.1(-)* double mutants. The difference for the three genes' genotyping appeared at the annealing temperature and the time for extension. For *aqp-1*, the 55°C annealing temperature, extension 2 min for 35 cycle; for *atm-1*, the PCR condition was 58°C annealing temperature, extension 30 sec for 40 cycle; for *sir-2.1*, the PCR condition was 59.9°C annealing temperature, extension 30 sec for 40 cycle.

3.2.5 DNA analysis by gel electrophoresis

1% agarose TAE gel electrophoresis was used to identify the specific DNA fragments resulting from PCR amplification. For this study, samples were the fragments contain *aqp-1*, *atm-1*, or *sir-2.1* genes. Fragments migrate towards the cathode in an electrical field due to the negative charge of DNA. The speed of migration is determined by the size of the fragments, the larger the fragment, the slower the fragment travels.

5µl loading buffer Orange G was added to each reaction mixture of 26.5µl (*sir-2.1* and *atm-1* PCR system) or 28.5µl (*aqp-1* PCR system) PCR products, of which, 5µl was loaded to a 1% agarose gel (agarose was dissolved in 1*TAE-buffer; heated and cooled before addition of 2µl 1.2% SYBR (Invitrogen) into each 50mL 1% agarose gel). To determine the size of the fragment, 5µl 100bp quick loading DNA ladders (BioLabs) were run together with the PCR products.

3.3 WMicroTracker (DesignPlus)

To solve the labor intensive problem of heat shock assay and drug toxicity assay, the WMicrotracker, as a automatic measuring machine, seemed to be a promising solution.

Locomotor activities in animal models is a common parameter in disease studies, drug quantification, toxicity assessment, and stress response, for example, oxidative stress. WMicroTracker provides the capability to measure the locomotor activities of small animals cultured in microtiter plates in an easy, fast and highly reproducible way. The system can be used in high-throughput screening assay to identify and evaluate the biological effects of new potential compounds, drugs, as well as mutant studies in the model organisms, like *C. elegans*.

WMicrotracker detects animal locomotor activities by infrared microbeam light scattering. Each microtiter well is crossed by at least one 150µm infrared microbeam, scanned more than 10 times per second. The detected signal is then digitally processed to register the amount of animal movement in a fixed period of time (Figure 3.3). The animals can be placed in the equipment within microtiter plates. All commercial sizes, 6, 12, 24, 48, 96 and 384 well plates are compatible with WMicrotrakcer. The range for operation temperature is from

4°C to 40°C. The software will record the activity of each well and the average activity of the group. The use of liquid media is preferred.

For experiments in this study, the 96-well microtiter plates were used. 100µl worms-suspension in M9 buffer in each well for heat shock assay. But, if it is a drug assay, 90µl worms-suspension is required for each well, added with 10µl drugs of different concentrations, according to the required final drug gradient. Normally, the worms are collected by washing the plates contain synchronized worms from bleaching method (the population from the egg laying synchronized method is to small for the high-throughput screening assay) with M9 buffer, 2-3 plates are required for each strain, according to the population of worms on each plate. In this study, WMicrotracker was used in heat shock assay and PQ survival assay.

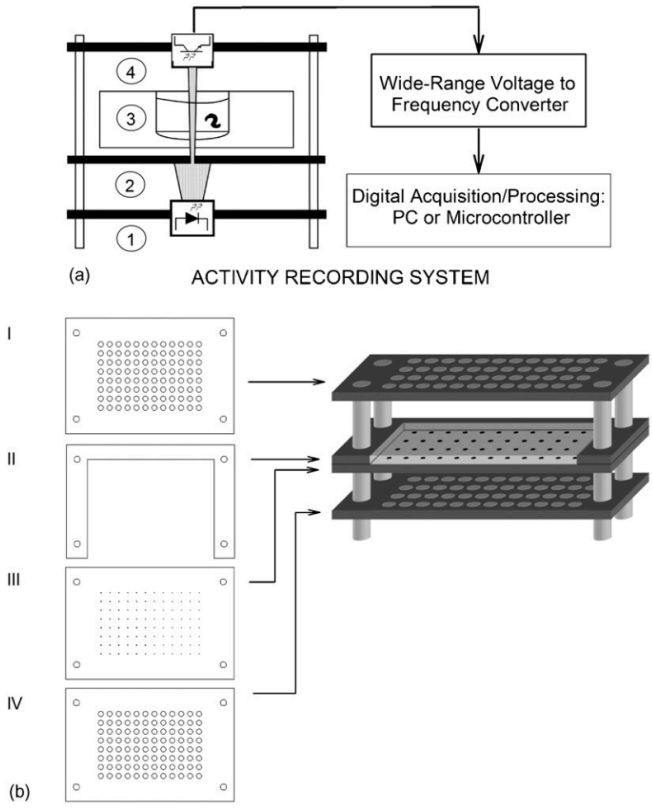

Figure 3.3: The structure and the principle for WMicrotracker. (a) Schematic diagram of the WMicrotracker: ① Bottom acrylic plate, where the infrared led is located; ② middle plate, with 100µm microholes for the light microbeam; ③ worm suspension receptacle; ④ top plate, where the phototransistor is located. The analogical output of the phototransistor is converted to a direct proportional (linear) frequency is captured by a PC sound board or microcontroller for

digital processing. (b) Mechanical design and assembling scheme. Left: diagram of the acrylic plates. From top to bottom: (I) plate for phototransistor mounting, with 5 mm holes; (II) guiding plate; (III) plate with microholes; (IV) plate for infrared diodes mounting. Right: scheme of the assembled apparatus. Taken from (Simonetta & Golombek, 2007)

3.4 Phenotypic characterization of Stress response deficient *C. elegans*

3.4.1 Brood size analysis

C. elegans is self fertilized, which produces a limited number of sperm first and then a larger number of oocytes from the same germ-line tissue. Therefore, self-progeny brood sizes are determined by the number of sperm, which produced prior to the irreversible onset of oogenesis, while most of the oocytes remain unfertilized (Hodgkin & Barnes, 1991). This results in a trade off between total fecundity and generation time: the more sperm produced, the longer the generation time (Cutter, 2004). The integrity of the genome is essential to both the health of the individual and to the reproductive success of a species. Published data shows that some UV-sensitive *C. elegans* strains, for example, *rad-1*, has the phenotype of reduced brood size (Hartman & Herman, 1982). Strains have the reduced growth rate phenotype, for example, *ubc-18*, show reduced brood size phenotype also (Fay, Large, Han, & Darland, 2003). Examination of the thermal sensitivity of *C. elegans* has revealed significant reduction in the brood size at temperatures above 25°C and almost complete sterility above 27°C (Petrella, 2014). Mutations, for example, *eat*, produce defects in pharyngeal pumping that lead to a reduction in food uptake and concomitant DR phenotypes, including a starved appearance, reduced brood size and extended lifespan. In conclusion, brood size is an essential phenotype might has connections with stress responses, such as heat, UV, and aging.

For the brood size analysis, virgin single worm from strains involved in this study were used, include the reference strain Bristol N2, *atm-1(-)*, *sir-2.1(-), aqp-1(-), aqp-1(-); atm-1(-),* and the *aqp-1(-); sir-2.1(-)* strains, were transferred to new 3.5cm OP50-seeded NGM plates, when they start to lay eggs, they are transferred to new small plates every day, until they stop laying eggs. The egg-laying period usually lasts 3 to 4 days, according to strain and incubating

temperature. The number of eggs laid on each plate were recorded, triplication for each strain.

3.4.2 Heat shock assay

Heat shock is a widely used method within *C. elegans* community to study the impact of stress on physiology, behavior, fecundity, and survival. Heat shock response (HSR) is a homeostatic response that maintains the proper protein-folding environment in the cell. This response is universal, and many of its components are well conserved from bacteria to humans (Guisbert, Yura, Rhodius, & Gross, 2008). Additionally, several longevity mutants of the *C. elegans* exhibit increased intrinsic thermo-tolerance as young adults (Lithgow, White, Melov, & Johnson, 1995). The study of stress response in *C. elegans* has provided great insight into many complex pathways and diseases. There is a growing interest in how stress responses are integrated to affect lifespan, and disease pathology, by using the widespread technique (Zevian & Yanowitz, 2014).

In this study, both manual counting and WMiortracker were used to measure the heat shock assay. But there were differences between these two methods. For the manual scoring, the 3.5cm OP50-seeded NGM plates was used, 15 synchronized L4 or L1 worms were transferred to each plate, followed by heat shock at 35°C (heat shock trials were performed at 32°C, 34°C, and 35°C condition), survival was scored once per hour; for the WMicrotracker method, 96-well microtiter plates were used, 100µl of synchronized L4 worm suspensions were transferred to each well, followed by heat shock at the same temperature 35°C (heat shock trial for WMicrotracker were at 32°C, 34°C, and 35°C) as the manual counting method, locomotor activities of worms were measured by WMicrotracker for every 30 minutes.

3.4.3 PQ sensitive assay

PQ, is a cation charged 2+, formed by two pyridine rings, is classified as a viologen. Viologen is a family of redox-active heterocycles, acts as a redox cycler with a great negative potential (E_0=-0.446 V). This feature restricts its interaction with strong reductant compounds. When dication of PQ (PQ^{2+})

accepts an electron from a reductant form the PQ monocation radical (PQ^+), which then rapidly reacts with oxygen (O_2 E_0=0.16 V) to initially produce superoxide radical (O_2^-) (k 7.7 x 108 M^{-1} s^{-1}) and subsequently the other reactive oxygen species (ROS) such as hydrogen peroxide (H_2O_2) and hydroxyl radical (OH). Studies show that PQ is toxic to human beings and organisms, for example, it is linked to development of Parkinson's disease (Tanner, et al., 2011; Kamel, 2013); in addition, PQ-induced oxidative stress in differentiated Human Neuroblastoma (SHSY-5Y) cells as indicated by an increase in the production of cellular reactive oxygen species (ROS) (McCarthy, Somayajulu, Sikorska, Borowy-Borowski, & Pandey, 2004).Thus, PQ is often used in science to catalyze the formation of ROS, more specifically, the superoxide anion, for the oxidative stress response for instance.

For PQ survival assay, both manual counting and WMicrotracker method were applied. For the manual scoring method, the 24-well PQ-containing NGM plates were used, 15 synchronized L1/L4 worms for each well, the L1 /L4 survival was scored after 48 hours; for the WMicrotracker method, 96-well flat bottom microtiter plates were used, 90µl L4 synchronized worm-suspension were needed, added with 10µl PQ of different concentration, so that can generate the gradient drug assay. The locomotor activities were counted during the 48-hour treatment.

3.4.4 IR assay

IR, for example x-ray radiation, is radiation that carries enough energy to free electrons from atoms or molecules. It is an important source for environmental DSBs. Thus, it can be used to do research in DNA repair and DDR. In this study, X-rays from a Faxitron CellRad, with the 130kV, 5mA dose rate, was used to set up the 50Gy, 70Gy, and 90Gy dose conditions for the IR sensitivity assay. 15 synchronized L4/L1 stage worms or embryos (according to the requirement of the experiment) were transferred to 3.5cm OP50-seeded NGM plates, then radiated by X-ray (Faxitron CellRad) for 50Gy, 70Gy, and 90Gy treatment respectively. The worms were inspected every day by stereomicroscopy (Zeiss stemi SV6). The L1 survival (brood lethality) was recorded 48 hours after the

treatment; the L4 percentage was counted after 72 hours after the eggs were laid; the embryo survival was scored 24 hours after the birth.

4. Results

4.1 Generation of double mutant strains

4.1.1 Annealing temperature optimization for *sir-2.1*

To optimize the annealing temperature for *sir-2.1*, the gradient test was run in Eppendorf Mastercycler ep Gradient S. The assessment of the best annealing temperature for *sir-2.1* was confirmed by agarose electrophoresis (Figure 4.1). 315bp fragment is the expected band from both *sir-2.1(-)* and *aqp-1(-); sir-2.1(-)*. The figure shows that, the nonspecific bands disappeared gradually for both *sir-2.1(-)* and *aqp-1(-); sir-2.1(-)* strains as the annealing temperature increased from 54.5°C to 59.9°C. Therefore, the optimized annealing temperature for genotyping *sir-2.1* is: 59.9°C. Annealing temperature are 58°C for *atm-1* and 55.5°C for *aqp-1* according to previous experience.

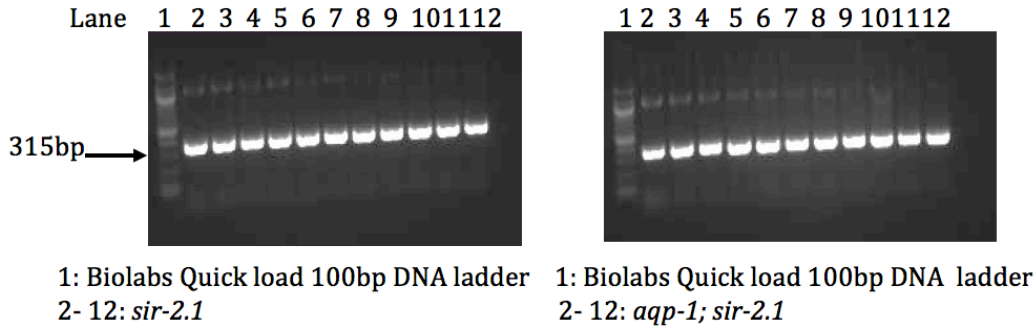

Figure 4.1 *sir-2.1* genotyping annealing temperature gradient test. There were 11 same PCR system for each strain, *sir-2.1* (left panel) and *sir-2.1; aqp-1*(right panel). The First lanes of both panels were loaded with 5µl Biolabs Quick load 100bp DNA ladder; 2-12 lanes were loaded with 5µl amplification products. The gradient annealing temperature for samples from lane 2 to lane 12 were: 54.6°C, 54.7°C, 55.0°C, 55.4°C, 56.0°C, 56.7°C, 57.4°C, 58.1°C, 58.7°C, 59.3°C, 59.7°C, 59.9°C respectively.

4.1.2 Primers for *atm-1*

Two different primer pairs were tested for *atm-1* genotyping. Triplicates for per strain per primer. The figure of gel electrophoresis for *atm-1(-)* and N2 strains shows that for the primer pair I (Table 3.1), both strains had the 874bp fragment products (N2 expected band: 874bp, *atm-1(-)* expected band: 326bp); for the primer pair II, both strains got the 820bp fragment products (N2 expected band: 820bp, *atm-1(-)* expected band: 272bp) (Figure 4.2). The outcome shows that

atm-1(-) was unfortunately mixed with N2. However, a new *atm-1(-)* strain was kindly provided by the Clare Hall Labs of Francis crick institute.

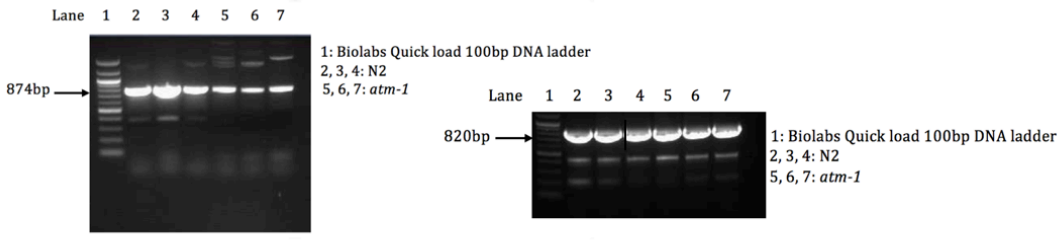

Figure 4.2: Primers for *atm-1.* The left panel shows the products amplified by primer pair I, the right panel shows the products amplified by primer pair II. For both panel, the first lane was loaded with 5µl Biolabs Quick load 100bp ladder; 2-4 lanes were loaded with 5µl products from N2 strain; 5-7 lanes were loaded with 5µl products from *atm-1(-)* strain.

4.1.3 Recovery rate for double mutant generation

In order to understand whether *aqp-1* functions as a mediator of the systemic homeostatic response in DNA repair deficient strain and genetic correlation between two genes. Firstly, the strain contains both mutants should be generated. In this study, *aqp-1(-); atm-1(-)* and *aqp-1(-); sir-2.1(-)* was generated. The generation of *aqp-1(-); atm-1(-)* double mutant is used as an example to illustrate the result.

To generate double mutants, mating system was set up (Chapter 3.2.1 & Chapter 3.2.2). For both cases, one mating system was kept in 20°C incubator as usual, and one mating system was kept in the 15°C incubator as back up. The F1 generation was inspected by using the Zeiss Stemi SV6, around 50% of the F1 population were males, which indicated the success of the sexual reproduction. The resulting F2 offspring, obtained from self-fertilization of singled F1 hermaphrodites, were analyzed by PCR genotyping to confirm the double deletions. As *aqp-1* and *atm-1* are located on separate chromosomes (*aqp-1 II*, *arm-1 I)* according to Mendelian segregation theory (Figure 4.3), worms homozygous for both mutants would be expected in one of sixteen offspring. In this study, however, we didn't get the *aqp-1(-); atm-1(-)* from the first 32 singled F2 generation hermaphrodite. But, we got 17 (among 32 single F2 generation hermaphrodites) with *atm-1* heterozygous, 8 samples (among the 17 *atm-1*

heterozygous) were chosen and genotyped. Luckily, 5 among the 8 *atm-1* heterozygous were with *aqp-1* homozygous mutant. 1 among the 5 plates was chosen, and 6 worms from the F3 generation of the chosen one, were single to 6 separate 3.5cm OP50-seeded plates, let them lay around 20 eggs (F4 generation), followed by being genotyped, 2 among 6 were the *aqp-1(-); atm-1(-)* homozygous double mutant. Therefore, the recovery rate for *aqp-1(-); atm-1(-)* is much lower than 1:32. As We got 3 *aqp-1(-); sir-2.1(-)* at the 32 singled worms in F2, the recover rate of *aqp-1(-); sir-2.1(-)* is around 3:32.

	II	I		II	I
	$aqp\text{-}1^-$	$atm\text{-}1^+$	x	$aqp\text{-}1^+$	$atm\text{-}1^-$
P0	$aqp\text{-}1^-$	$atm\text{-}1^+$		$aqp\text{-}1^+$	$atm\text{-}1^-$
	↓				
	$aqp\text{-}1^+$	$atm\text{-}1^+$	x	$aqp\text{-}1^+$	$atm\text{-}1^+$
F1	$aqp\text{-}1^-$	$atm\text{-}1^-$		$aqp\text{-}1^-$	$atm\text{-}1^-$
	↓				

F2

	$aqp\text{-}1^+$ $atm\text{-}1^+$	$aqp\text{-}1^+$ $atm\text{-}1^-$	$aqp\text{-}1^-$ $atm\text{-}1^+$	$aqp\text{-}1^-$ $atm\text{-}1^-$
$aqp\text{-}1^+$ $atm\text{-}1^+$	$aqp\text{-}1^+$ $atm\text{-}1^+$ $aqp\text{-}1^+$ $atm\text{-}1^+$	$aqp\text{-}1^+$ $atm\text{-}1^-$ $aqp\text{-}1^+$ $atm\text{-}1^+$	$aqp\text{-}1^-$ $atm\text{-}1^+$ $aqp\text{-}1^+$ $atm\text{-}1^+$	$aqp\text{-}1^-$ $atm\text{-}1^-$ $aqp\text{-}1^+$ $atm\text{-}1^+$
$aqp\text{-}1^+$ $atm\text{-}1^-$	$aqp\text{-}1^+$ $atm\text{-}1^+$ $aqp\text{-}1^+$ $atm\text{-}1^-$	$aqp\text{-}1^+$ $atm\text{-}1^-$ $aqp\text{-}1^+$ $atm\text{-}1^-$	$aqp\text{-}1^-$ $atm\text{-}1^+$ $aqp\text{-}1^+$ $atm\text{-}1^-$	$aqp\text{-}1^-$ $atm\text{-}1^-$ $aqp\text{-}1^+$ $atm\text{-}1^-$
$aqp\text{-}1^-$ $atm\text{-}1^+$	$aqp\text{-}1^+$ $atm\text{-}1^+$ $aqp\text{-}1^-$ $atm\text{-}1^+$	$aqp\text{-}1^+$ $atm\text{-}1^-$ $aqp\text{-}1^-$ $atm\text{-}1^+$	$aqp\text{-}1^-$ $atm\text{-}1^+$ $aqp\text{-}1^-$ $atm\text{-}1^+$	$aqp\text{-}1^-$ $atm\text{-}1^-$ $aqp\text{-}1^-$ $atm\text{-}1^+$
$aqp\text{-}1^-$ $atm\text{-}1^-$	$aqp\text{-}1^+$ $atm\text{-}1^+$ $aqp\text{-}1^-$ $atm\text{-}1^-$	$aqp\text{-}1^+$ $atm\text{-}1^-$ $aqp\text{-}1^-$ $atm\text{-}1^-$	$aqp\text{-}1^-$ $atm\text{-}1^+$ $aqp\text{-}1^-$ $atm\text{-}1^-$	**$aqp\text{-}1^-$ $aqp\text{-}1^-$** **$atm\text{-}1^-$ $atm\text{-}1^-$**

Figure 4.3: Mendelian segregation theory's application in genetic cross. The figure shows all the possible genotypes in F2 generation of self-fertilized heterozygous hermaphrodites from F1. The F1 hermaphrodites heterozygous for *aqp-1* and *atm-1* were obtained by genetic crossing *aqp-1(-)* with *atm-1(-/-)* (P0). According to Mendelian segregation theory, the *aqp-1(-); atm-1(-)* recovery rate suppose to be 1:16. The genotype we need was marked in red in the figure.

4.1.4 Genotyping of double mutant *C. elegans*

To confirm the expected double deletions in the single worms from the F2 generation, PCR genotyping was used to amplify the target fragments of double mutant worms. The binding sites of the primers for *atm-1, aqp-1*, and *sir-2.1* are (Figure 4.4, left panel) and the gel electrophoresis out come of *aqp-1(-); atm-1(-)* and *aqp-1(-); sir-2.1(-)* (Figure 4.4, right panel) are all showed below.

For the *aqp-1(-); atm-1(-)* double mutant genotyping (Figure 4.4, I), when it was amplified by the *aqp-1* primer pairs, the product segment was the same as *aqp-1(-)* strain, only 381bp segment, while N2 strain had 381bp and 125bp two segments; when it was amplified by the *atm-1* primer pair II, the product band was the same as *atm-1(-)* strain, 326bp, while N2 strain had 874bp segment instead. From the figure, the strain was confirmed to be *aqp-1(-); atm-1(-)* double mutant strain.

For the *aqp-1(-); sir-2.1(-)* double mutant genotyping (Figure 4.4, II), when it was amplified by the *aqp-1* primer pairs, the segments was the same as *aqp-1(-)* strain, only 381bp segment, while N2 strain had 381bp and 125bp two segments; when it was amplified by the *sir-2.1* primer pair, the product band was the same as *sir-2.1(-)* strain, 315bp, while N2 strain had 1083bp segment band instead. From the figure, the strain was confirmed to be *aqp-1(-); sir-2.1(-)* double mutant strain.

In conclusion, both *aqp-1(-); atm-1(-)* and *aqp-1(-); sir-2.1(-)* double mutant strains were generated successfully. And the old mixed *atm-1(-)* was replaced by the new *atm-1(-)* provided by the Clare Hall Labs of Francis crick institute.

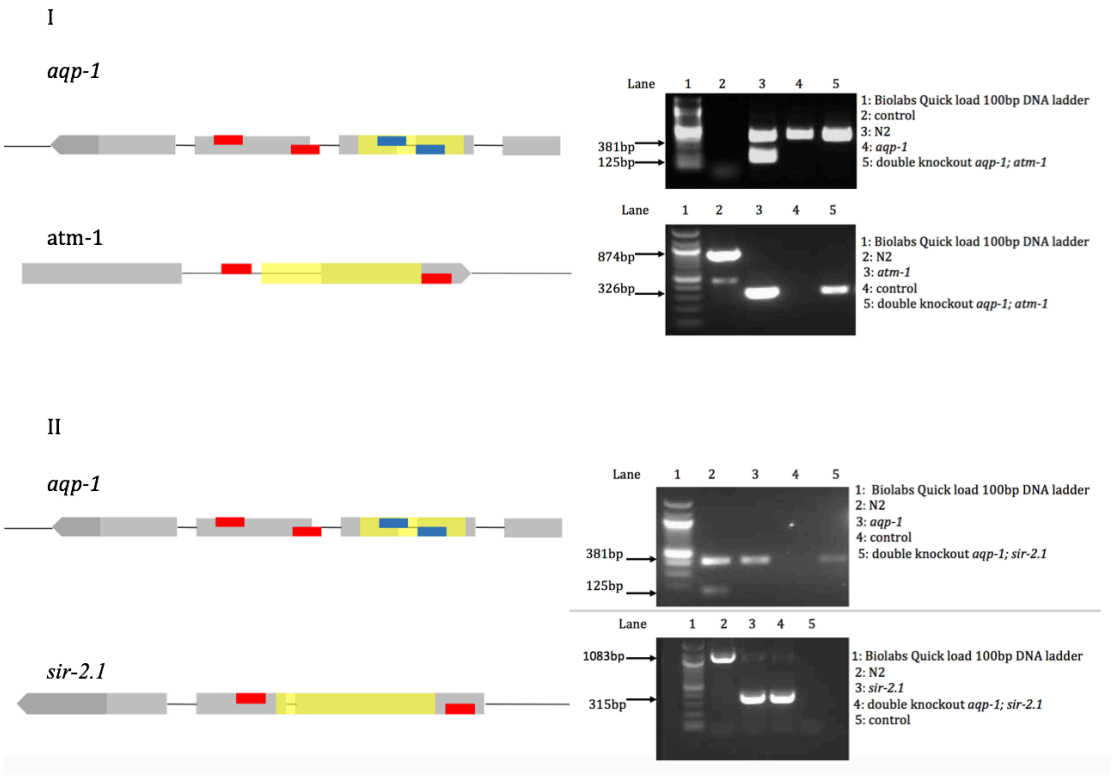

Figure 4.4: Genotyping of double mutant *C. elegans*. The red-marked sequences indicate the primers' binding sites which located outside the deletions; the blue-marked sequences are the primers' bind sites which located inside the deletion; the yellow-marked sequences show where the deletions are. Image (I) shows the genotyping outcome of *aqp-1(-); atm-1(-)* strain; image (II) shows the genotyping outcome of *aqp-1(-); sir-2.1(-)* strain.

4.2 WMicrotracker method establishment

Traditional manual scoring of the PQ toxicity assay and heat shock tolerance assay in *C. elegans* are quite time- and labor- consuming. Hence, in order to increase the efficiency, we wanted to exploit the automatic scoring system-WMcrotracker, which might be a promising alteration of manual scoring.

4.2.1 WMicrotracker buffer trial

To adapt the WMicrotracker to stress response assay. Firstly, a proper buffer for making *C. elegans* samples should be found, which should be suitable both for the WMicrotracker, so that the system can record the locomotor activities relatively accurate, and for the worms, so that the buffer would not influence the locomotor activities of worms and would not generate stress to the worms. It has been showed that both 3PY buffer and M9 buffer (Appendix 8.1) can be used to prepare *C. elegans* samples. But it is unclear which buffer is more mild to worms. Moreover, it is not known how many worms were required at least for each well so that worms can have a relatively stable locomotor activities curve.

To investigate this, 100µl worm suspension containing 10, 20 or 30 L4-stage synchronized worms from N2 strain respectively, were transferred to separate wells of the 96-well microtiter plate. One group of worm suspension was made by 3PY buffer, while the other group was made by M9 buffer. The locomotor activities of worms were measured by the WMicrotracker every 30 minutes for ten hours continuously.

For 10-worm 3PY suspension (Figure 4.5, a, blue), the locomotor activities of worms decreased to 34.6% during the first one and half hours, then it went up a bit, fluctuated around 55% until 3 hours after the measuring start. The locomotor activities of worms then increased abruptly at 3.5 hours to 134.6%, followed by a gentle dropping to around 100% then increased again to 176.9% at 6 hours after transfer, which was the point with the highest locomotor activities. After that, the locomotor activities of worms went down gradually, though there was a pump up to 90.4% at 7.5 hours.

For 10-worm M9 suspension (Figure 4.5, b, blue), the locomotor activities of

worms also decreased during the first 1.5 hours to 36.7%, which is a higher than the 10-worm 3PY suspension. Then the locomotor activities showed a dramatic increase to 140% at the first 2 hours and increase even more to 266.7% at the 3.5 hours, which was much higher than the highest locomotor activities the 10-worm 3PY worms had. The locomotor activities from 2 hours to 9 hours fluctuated between 100% (9 hours, lowest) to 266.7% (3.5 hours, highest), with the average locomotor activities around 156.4%, which was as the locomotor activities the worms-10 in 3PY had (around 78.6%) during the same period. Though the activities of 10-worm M9 suspension decreased a bit to 46.7% at the 9.5 hours, but it rebounded to 126.7% at the end of the measurement.

For 20-worm 3PY suspension (Figure 4.5, a, red), the locomotor activities curve of the worms was quite similar to the 10-worm 3PY suspension. The curve also showed the decrease and the fluctuation during the first 3 hours as the 10-worm 3PY suspension did, but higher, which was between 64,1% (1.5 hours) to 92.3% (3 hours). Then the locomotor activities of worms increased abruptly to 128.2% (4 hours) and to 130.8% (5.5 hours), which was the highest point during the whole measurement. After 6 hours, however, the locomotor activities dropped down really fast. The locomotor activities of worms totally disappeared after 8 hours, which means for the 20-worm condition, 3PY is not suitable to be used as the locomotor activities measuring buffer.

For 20-worm M9 buffer suspension (Figure 4.5, b, red), compared to the 10-worm M9 buffer suspension, it had a more stable locomotor activities curve, with the highest point 156.6% (5.5 hours) and the lowest point 73,6% (1 hours), and it still had 149.1% locomotor activities at the end of the measurement, which is quite ideal.

For the 30-worm 3PY suspension (Figure 4.5, a, black), compared to 10-worm and 20-worm 3PY suspension, it had a relatively stable locomotor activities curve during the whole 10-hour measurement, which is mostly between 16.9% (6 hours) and 76.8% (3 hours). However the average locomotor activities was too low, around 45.5%, for the measurement. In addition, it dropped down to 0,0% (10 hours).

For the 30-worm M9 suspension (Figure 4.5, b, black), however, the locomotor activities curve was quite steady during the whole 10-hour measurement, which fluctuated between 78.1% (5.5 hours) and 143.8% (10 hours) with the average locomotor activities around 115%.

In conclusion, comparing all the trial condition we have done, the 30-worm M9 buffer had the steadiest locomotor activities curve and with the smallest fluctuation interval (between 78.1% (5.5 hours) and 143.8% (10 hours)), and the average locomotor activities around 115%. According to previous experience, that 50 worms in each well is also suitable for the measurement. It suggests that at least 30 worms, up to around 50 worms, in each well for 100µl worm suspension in M9 buffer should be the ideal condition for WMicrotracker locomotor activities measurement.

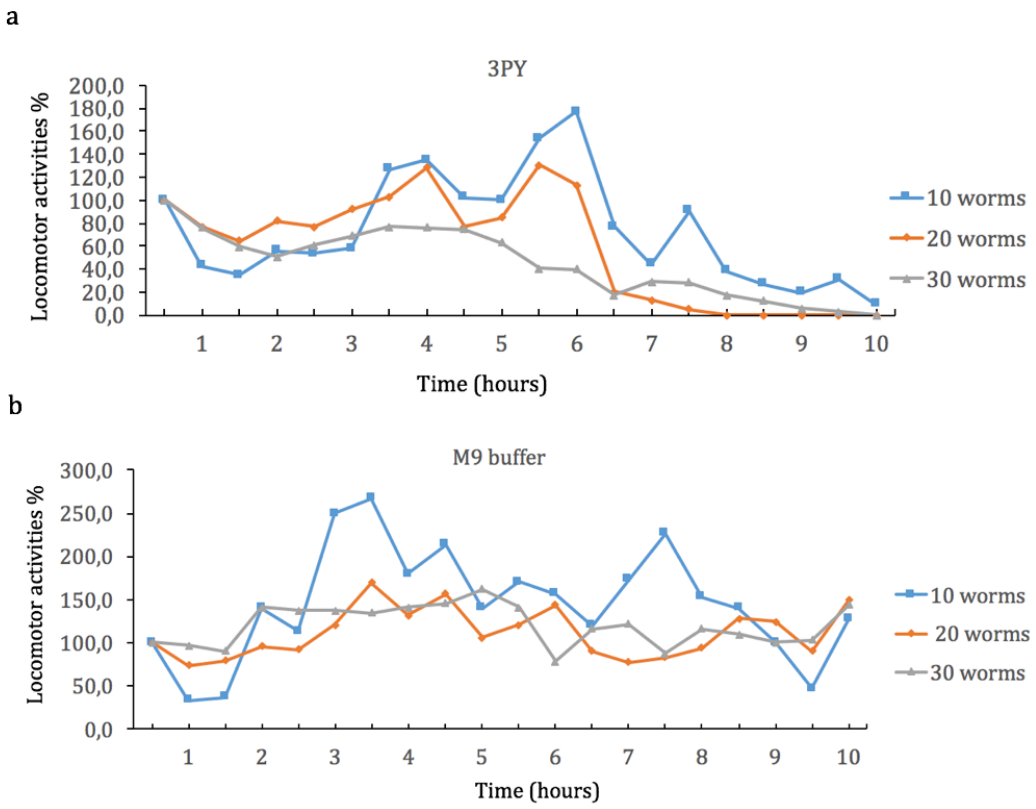

Figure 4.5: The WMicrotracker buffer trial. Figure shows the locomotor activities curve of 10-wrom(blue), 20-worm (red), and 30-worm (grey) per 100µl per well in 3PY buffer (a) and M9

buffer (b) respectively. The vertical axis shows values of the locomotor activities, while the first measurement is for the basal locomotor activities. The horizontal axis shows the time for the measurement.

4.2.2 WMicrotracker heat shock trail

It has been showed that WMicrotracker can be used to measure locomotor activities of *C. elegans*. But it has not been tested whether WMicrotracker can be used to measure heat shock tolerance assay and which temperature should be used for heat shock. In order to test this, reference strain Bristol N2, and *aqp-1(-)*, *sir-2.1(-)*, *atm-1(-)* strains were measured for heat shock tolerance at 32°C, 34°C, and 35°C respectively, by both manual scoring and WMicrotracker (Chapter 3.4.2).

When the worms were heat shocked at 32°C (Heraeus CO2 Incubator) and the locomotor activities were measured by the WMirotracker (Figure 4.6, I, a). The measurement lasted for 6 hours. The locomotor activities of the *sir-2.1(-)* worms dropped quickly from 100% to 42.7% during the first 2 hours. However, unlike the other three strains, the locomotor activities of *sir-2.1(-)* worms increased from 42.7% (2 hours) to 50.8% (3 hours), which was followed by a continuous decrease from 37.9% (4 hours) to 6.7% (6 hours). Compared to *sir-2.1(-)*, N2 strain showed stronger tolerance at the beginning, 71.7% (2 hours), but decreased faster afterwards, from 48.4% (3 hours) to 3.9% (6 hours). For *atm-1(-)*, in contrast to N2 strain, the locomotor activities went down fast at the beginning to 56.6% (2 hours), but became quite tolerant afterwards (30.3%, 3h; 31.4%, 5h), though the locomotor activities became 0,0% (6 hours). Different from the other three strains, the *aqp-1* strain was quite tolerant to heat shock during the first 4 hours (66.2%, 2h; 51.5%, 3h; 43.6%, 4h), but showed a dramatic drop after 4 hours, from 11.3% (5 hours) to 2.5% (6 hours). In conclusion, N2 strain and *aqp-1(-)* showed great tolerance to heat shock at the first four hours, while *atm-1(-)* and *sir-2.1(-)* appeared to have stronger tolerance at the later measuring time.

When the traditional manual scoring was used to record the heat shock tolerance at 32°C heat shock condition (Figure 4.6, I, b). The measurement lasted for 9 hours. However, the outcome was totally different from the WMicrotracker

measurement. The biggest difference was that, even after being heat shocked for 9 hours, the majority of the worm population were alive. The strain that first started to die was *aqp-1(-)*, to 98.8% (7 hours), and with the lowest survival after 9-hour heat shock 96.3% (9 hours) compared to the other three strain. Both *sir-2.1(-)* and *atm-1(-)* just started to die after 9-hour 32°C heat shock.

When the worms were heat shocked at 34°C (Heraeus CO2 Incubator) and the locomotor activities were measured by the WMirotracker (Figure 4.6, II, c). The measurement lasted for 8 hours. *sir-2.1(-)* showed the highest locomotor activities during the whole heat shock duration, with the highest locomoter activities 46.3% (2 hours) ended to 3.9% (8 hours). On the contrary, *aqp-1(-)* showed the least tolerance to heat shock, which showed the lowest locomotor activities during the whole measurement, with 24.2% (2 hours) at the beginning and ended up in 1.4% (8 hours). *atm-1(-)* had a big drop in locomotor activity at the beginning to 30.9 (2 hours) and decreased to 1.6% gradually. For N2 strain, it also dropped dramatically in locomotor activities at the first 2 hours to 35.1% (2 hours) and gradually decreased to 1.2% in the end.

When the traditional manual scoring was used to record the heat shock tolerance at 34°C heat shock condition (Figure 4.6, II, d). The measurement lasted for 9 hours. *aqp-1(-)* survival started to decrease from the first 2 hours to 81.2% (2 hours), while *atm-1(-)* started to decrease to 98.8% (4 hours). *aqp-1(-)* showed less tolerance to heat shock during the whole measuring process, from 77.5% survival (5 hours) to 60.0% survival (9 hours). For the *atm-1(-)* strain, though the survival started to drop at 4 hours, but it remained relatively higher survival towards heat shock during the next 5 hours, it still had 87.5% survival at the end of the measurement. For N2 strain and *sir-2.1(-)* strain, both of them showed stronger tolerance towards heat shock than the other two strains, as survival of both the strains started to drop down after 5-hour 34°C heat shock, which is 1 hour later than two other strains. At the end of the measurement, the survival of the N2 and *sir-2.1(-)* remained high at 86.3% (9 hours).

When the worms were heat shocked at 35°C (Heraeus CO2 Incubator) and the locomotor activities were measured by the WMirotracker (Figure 4.6, III, e). The measurement took 5 hours to accomplish. *aqp-1(-)* showed the lowest tolerance

towards heat shock, because first it had the biggest drop to 14.3% (2 hours) in locomotor activities, and it kept to decrease fast during the whole measurement from 4.4% (3 hours) to 0% (5 hours). For *sir-2.1(-)*, though the locomotor activities of it decreased to 18.7% (2 hours) but it showed strong tolerance during the next three hours, compared to the *atm-1(-).* Interestingly, though the *atm-1(-)* showed strong heat shock tolerance during the first two hours, 21.7% (2 hours), but the locomotor activities started to drop down dramatically from 5.4% (3 hours) to 0% (5 hours). The N2 had big drop at the first to hours and kept relatively stead dropping for the next three hours (18.6%, 2 hours; 5.8% 3 hours; 3.5%, 4 hours; 0%, 5 hours).

When the traditional manual scoring was used to record the heat shock tolerance at 35°C heat shock condition (Figure 4.6, III, f). the measurement took 14 hours to finish. *aqp-1(-)* showed the least tolerance to heat shock during the whole measurement, whose survival started to decrease to 96.3% (3 hours) and dramatically dropped to 2.5% (11 hours), while *atm-1(-)* survival decreased to 98.8% (4 hours), N2 decreased to 97.5% (4 hours), and for *sir-2.1(-)*, it started to decreased to in survival 97.5% after 5-hour heat shock, which showed the strongest resistance to heat shock during the whole process, it still had 17.5% survival (12 hours) and 8.8% (13 hours). When it came to *atm-1(-)*, though it showed weaker resistance towards heat shock than the N2 and *sir-2.1(-)*, but it showed stronger resistance than the *aqp-1(-)*.

In conclusion: firstly, the outcomes of WMicrotracker and manual scoring were highly inconsistent and both the WMcrotracker and manual scoring were not suitable for measuring when the heat shock temperature was at 32°C; secondly, when the heat shock temperature increased to 34°C, it showed some consistency between the manual- scoring survival and the WMicrotracker- scoring locomotor activities, though the values were totally different, but in both method, *sir-2.1(-)* showed the strongest resistance, while *apq-1(-)* showed the lowest heat shock tolerance. But 34°C was also not suitable for heat shock, as more than 60% of the worm population were still alive after 9-hour heat shock; thirdly, when the heat shock temperature was lifted up to 35°C, the manual scoring and the WMicrotracker scoring method had relatively high consistence in both the value and the connection between locomotor activities and survival percentage, which

indicates that 35°C supposes to be chosen as the heat shock temperature, at this temperature, both the manual recording and WMicrotraker can be used, though the consistence was low between the two different measuring methods.

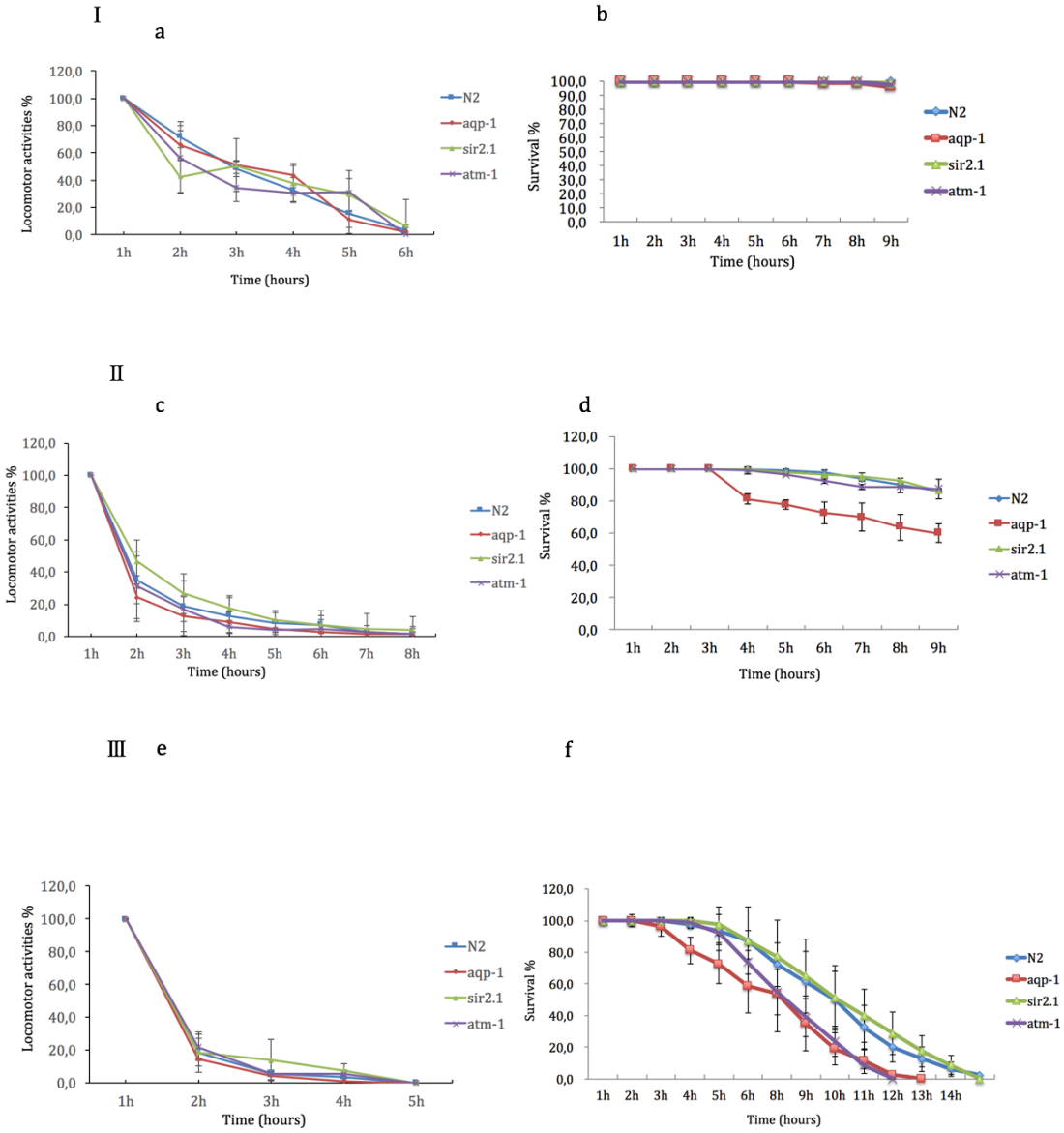

Figure 4.6: Heat-shock assay method establishment. The figure shows the outcomes of heat shock at 32°C (I), 34°C (II), and 35°C (III) by WMicrotracker method (a, c, e) and manual scoring method (b, d, f). Each condition was done for triplicates. Error bars represent the S.D. Worms from N2 (blue), *aqp-1(-)* (red), *atm-1(-)* (purple), and *sir-2.1(-)* (green) were assessed. For the WMcrotracker method, the locomotor activities were measured once per hour; for the manual scoring method, the survival was measured once per hour.

4.2.3 WMicrotracker PQ P0 survival assay trial

As we can see in the heat shock trial, WMicrotracker and manual scoring had very different results. To test if it will have the same circumstances for other types of toxicants, we tried to use the WMicrotracker measuring method for PQ sensitivity assay (Chapter 3.4.3).

N2 strain was used to perform the trial. 90µl worm suspension, containing L4 synchronized worms (around 50) were transferred and added with PQ for the final concentration range: 0mM, 5mM, 10mM, 15mM to 20mM. The measurement was once per 30min and took 48 hours to be done until all the worms didn't move anymore (Figure 4.7). The figure shows that, the locomotor activities of worms, decreased in a time-dependent manner. But the locomotor activities of worms during the first 2.5 hours is an exception, the worms treated with PQ, shows a transient increased to 106%-109% locomotor activities compared to the group without PQ, which didn't show obvious increase in locomotor activities. Also, locomotor activities of worms decreased in a PQ-concentration-dependent manner, which means, treated with higher-concentrated PQ, showed less locomotor activities than the ones treated with lower-concentrated PQ. The locomotor activities of the worms, treated with 20mM PQ, came to 0% at 32 hours, while for the worms treated with 15mM, 10mM, and 5mM PQ, the locomotor activities disappeared at 45 hours, 46 hours, and 48 hours after the treatment respectively.

Though the locomotor activity curves of worms fluctuated a lot, the trend of the time-dependent and drug-concentration-dependent locomotor activities manner shows that WMicrotracker might be a promising alternative of manual scoring for PQ toxicity assay.

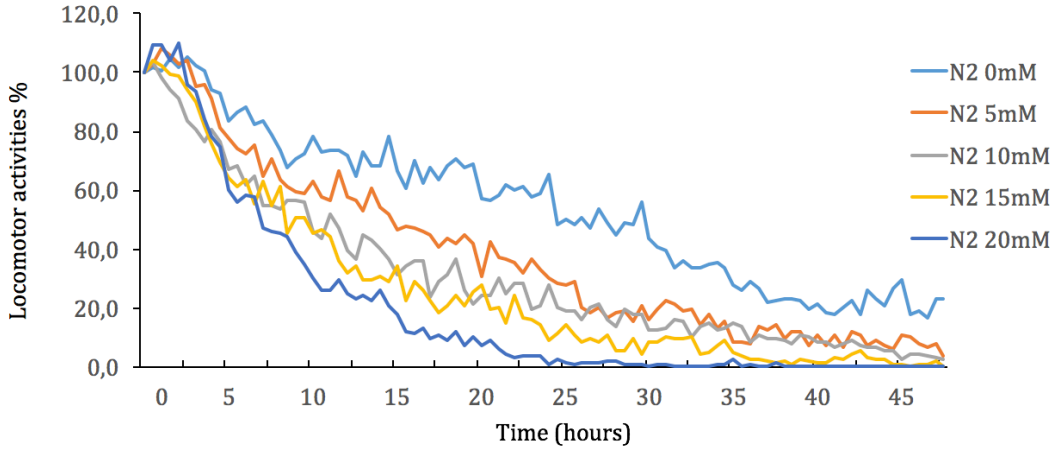

Figure 4.7 WMicrotracker PQ toxicity assay trial. The L4 synchronized worms from N2 strain and the 96-well microtiter plate were used in the trial. 100µl worm suspension (50 worms), containing PQ with different concentration 0mM (blue), 5mM (red), 10mM (black), 15mM (yellow), 20mM (deep blue), were transferred to separate wells respectively. Triplicates for each concentration. The locomotor activities were measured by WMicrotracker once per 30 minutes.

Concluding the experiments of WMicrotracker method establishment, M9 buffer was determined to be the *C. elegans* sample generation buffer for WMicrotraker; 30-50 worms per 100µl per well is suitable for the both WMicrotracker measurement and worms' locomotor activities stability; WMicrotracker automatic measuring system was suitable for PQ toxicity assay; though WMicrotracker didn't work well in heat shock assay, we can give another try by shifting the WMicrotracker into the incubator.

4.3 Phenotypic assessment of stress sensitivity of DNA repair mutants

The DNA repair double mutants generated in this thesis (*apq-1(-); atm-1(-)* and *aqp-1(-); sir-2.1(-)*) had not previously been functionally characterized. The present study, therefore, includes phenotypical analyses of these mutants.

4.3.1 Brood size assay

Brood size is a phenotype used to distinguish differences in fitness and stress sensitivity between mutant strains. Published evidence showed that the *atm-1* strain has smaller brood size compared to the N2 strain (Jones, Huang, Chua, Baillie, & Rose, 2012). But there was no evidence for the brood size phenotype of the *aqp-1(-)*. In this thesis, *aqp-1(-); atm-1(-)* and *aqp-1; sir-2.1* double mutant strains were generated and the brood size is unknown. To investigate the phenotypes of different mutants and to figure out if the *aqp-1* functions as a mediator in the cytoprotective homeostatic system of the DNA check point deficeint strain *atm-1(-)* and if these mutants would influence the brood size, the N2, *atm-1(-)*, *sir-2.1(-)*, *aqp-1(-)*, *aqp-1(-); atm-1(-)*, *aqp-1(-); sir-2.1(-)*) were used (Chapter 3.4.1)(Figure 4.8).

The figure shows the brood sizes of N2, *atm-1(-)*, *aqp-1(-)*, *sir-2.1(-)*, *aqp-1(-); atm-1(-)* and *aqp-1(-); sir-2.1(-)*. As expected, according to published literature (Jones, Huang, Chua, Baillie, & Rose, 2012), *atm-1(-)* strain had a smaller brood size compared to the other 5 strains. The Student's *t*-test, showed significant differences in brood size between N2 (230,7±23,4 (*n*=9)) and *atm-1(-)* (*188,5*±26,0 (*n*=8)). N2, *aqp-1(-)*, *sir-2.1(-)*, and *aqp-1(-); sir-2.1(-)* had almost the same size of brood, which was around 230 offspring per hermaphrodite, while *sir-2.1(-)* had a slightly, but not significant higher brood size than the other 3 strains. However, *aqp-1(-); atm-1(-)* double mutant strain had a brood size of around 250 offspring. By performing the Student's *t*-test, significant difference of brood size was also seen between *atm-1(-)* (188,5±26,0 (*n*=8)) and *aqp-1(-); atm-1(-)* (242,2±29,5 (n=5)), suggesting that aqp-1 might contribute to the low brood size of *atm-1(-)*. From this, we suspect that, *aqp-1* might be a mediator in the cytoprotective homeostatic system in the DNA repair deficient strain *atm-1(-)*.

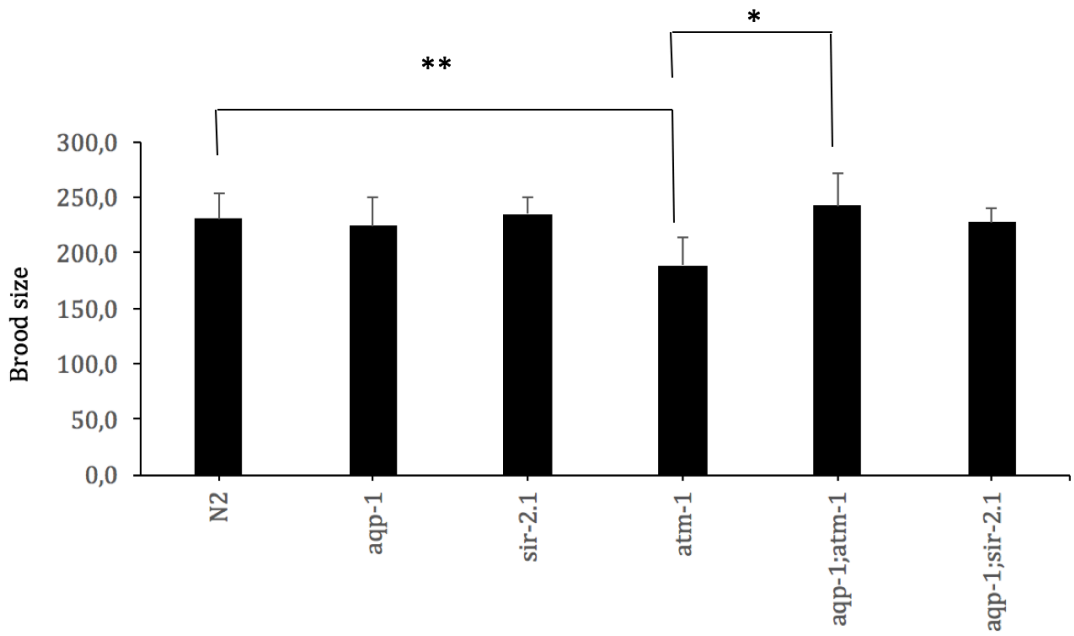

Figure 4.8: Brood size. The N2, *aqp-1(-), sir-2.1(-), atm-1(-), aqp-1(-); atm-1(-),* and *aqp-1(-); sir-2.1(-).* Data are mean ± S.D. N2=230,7±23,4 (*n*=9); *aqp-1(-)* =224,7±25,7 (*n*=10); *sir-2.1(-)* =235,1±15,7 (n=9); *atm-1(-)* =188,5±26,0 (*n*=8); *aqp-1; atm-1(-)* =242,2±29,5 (n=5); *aqp-1(-); sir-2.1(-)* =227,8±12,7 (n=5). Error bars represent the S.D. Student's *t*-test were performed to assess the significance between different strains, **P*<0.05; ***P*<0.01.

4.3.2 35°C Heat shock assay by manual and WMicrotracker

The PQ toxicity survival assay showed the potential of using the WMicrotracker as a method to score viability. We speculate that the initial trial (Chapter 4.2.2) was confounded by poor temperature control. In an attempt to improve temperature control and reduce temperature fluctuation during the experiment, we placed the WMicrotracker instrument into the incubator. The measurement took 7 hours to accomplish (Chapter 3.4.2).

For the WMicrotracker measurement (Figure 4.9, a), N2 showed the strongest tolerance to heat shock during the whole process. Interestingly, within the first hour of heat shock, the locomotor activities of N2 even increased to 105%. After that, the locomotor activities of the N2 worms started to decreased slowly to 77.7% (2 hours), which was followed by dramatic decrease in locomotor activities to 10.3% (4 hours), and then decreased slowly to 1.5% (6 hours). For other five strains, they showed much less tolerance to heat shock than N2 strain. Among the five strains, *aqp-1(-)* 86.8% (1 hour), *atm-1(-); aqp-1(-)* 88.4% (1

hour), and *aqp-1(-); sir-2.1(-)* 80.2% (1 hour) had relatively more locomotor activities than *atm-1(-)* 65.3% (1 hour) and *sir-2.1(-)* 75% (1 hour) at the beginning of the measurement. Interestingly, the *atm-1(-)* 1.1% (4 hours), the *sir-2.1(-)* 1.3% (4.5 hours) single mutant strains are the two strains, whose locomotor activities lasted for the longest, while the locomotor activities of *aqp-1;* atm-1 strain disappeared after 3.5 hours.

For the manual scoring measurement (Figure 4.9, b). The N2 was also the strain that showed the strongest tolerance to heat shock (this part was the same as the outcome of WMicrotracker), which still had survival after 11-hour heat shock at 35°C 2.2% (11 hours), while all the other strains didn't have any survival, and N2 strain had the highest survival during the whole measurement. But for *atm-1(-)* and *sir-2.1(-)* strains, the consequences were totally different from the records of WMicrotracker. This two single mutant strains showed strong tolerance in the manual measuring assay, while by the WMicrotracker, the outcomes were on the contrary. For *aqp-1(-)*, it showed the same trend as in WMicrotracker, firstly relatively strong tolerance (85.4%, 2 hours) then as heat shock went on, the tolerance to heat became weaker (3.4%, 8 hours). For *atm-1(-); aqp-1(-)* and *aqp-1(-); sir-2.1(-)* had the almost the same trend as the *aqp-1(-)*, which was quite similar to the outcome measured by WMicrotracker.

In conclusion, due to the outcomes from WMicrotracker and manual measurement were of big difference, WMicrotracker might not be a good alteration for heat shock assay measurement; by the WMicrotracker method (Figure 4.9, a), we can divide the 6 strains into two groups, N2 as one group is resistant to heat shock, while all the other 5 mutant strains were hypersensitive to heat shock, without big difference between the 5 strains, suggesting that *aqp-1*, *sir-2.1* and *atm-1* all required for the heat shock response; but by the manual scoring method (Figure 4.9, b), it showed that among *aqp-1*, *sir-2.1* and *atm-1*, only *aqp-1* is required for the heat shock response, concluding from that *atm-1(-)* and *sir-2.1(-)* was quite resistant to heat shock compared to *aqp-1(-).*

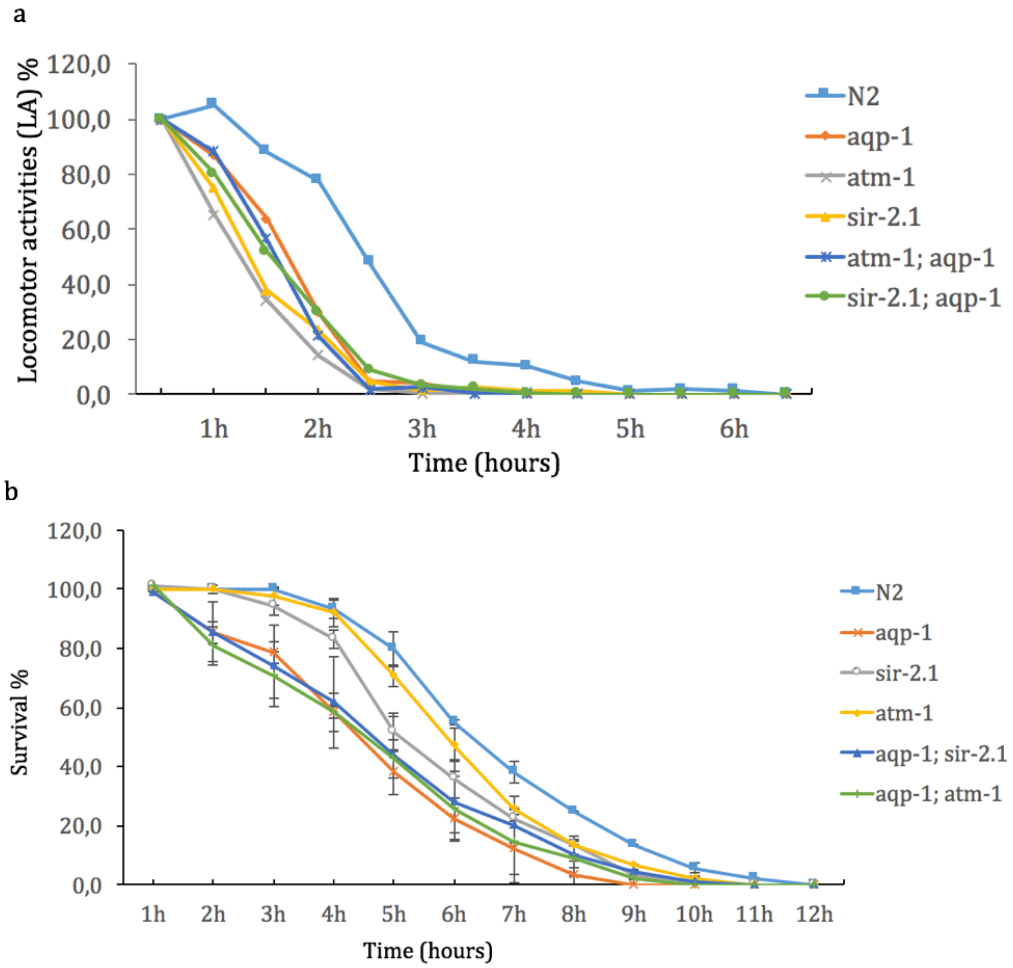

Figure 4.9: Heat shock at 35°C. The figure shows the heat shock assay measured by WMicrotracker (a) and manual scoring (b) respectively. N2 (blue), *aqp-1(-)* (red), *sir-2.1(-)* (black), *atm-1(-)* (yellow), *aqp-1(-); sir-2.1(-)* (deep blue), and *aqp-1(-); atm-1(-)* (green) were used. Error bars represent the S.D. The WMicrotracker measured the locomotor activities of worms, while the manual scoring measured the survival of worms.

4.3.3 Manual-scoring PQ toxicity trial

To settle the gradient range for manual-scoring PQ toxicity assay, the 24-well plates were used for the purpose. The NGM was dissolved then added with PQ with the resulting final concentrations range: 0µM, 100µM, 200µM, 300µM, 400µM, 500µM. In this trial. *aqp-1(-), atm-1(-), sir-2.1(-)* and N2 strain were used. 15 synchronized L1 worms from different strains were transferred to each wells containing different concentration of PQ (method detail: Chapter 3.4.3). The PQ sensitivity was assessed by manual scoring the adult percentage after 72 hours. The adult percentage was lower, when the worms from the same strain treated

with PQ with higher concentration and different strains showed different PQ sensitivities when they were treated with PQ, the lower the adult-percentage, the more sensitivity (Figure 4.10). In this trial, *sir-2.1(-)* showed the strongest resistance to PQ, the strain had 87.9% and 64.3% of adult with the treatment of 100µM and 200µM respectively. *atm-1(-)* displayed strong resistance to PQ when the concentration was lower than 200µM (70% adult, 100µM); but when the concentration came up to 200µM, the adult percentage of *atm-1(-)* dropped dramatically from 70% to 12.5%. *aqp-1(-)* had lower adult percentage than N2 from 0µM to 200µM.

In conclusion, as there was no adult worm was observed for any of the strains tested above when the concentration of PQ increased to 300µM, the up range of PQ-concentration for the manual-scored PQ assay was settled at 300µM and it was applied to the subsequent experiments; *sir-2.1(-)* showed strong resistance to PQ in the trial; *aqp-1(-)* showed relatively low resistance compared to the other 3 strains; *atm-1(-)* showed stronger resistance than *aqp-1(-)* when the concentration of PQ was lower than 100µM. To determine which gene plays the main role in PQ stress response, more experiments required.

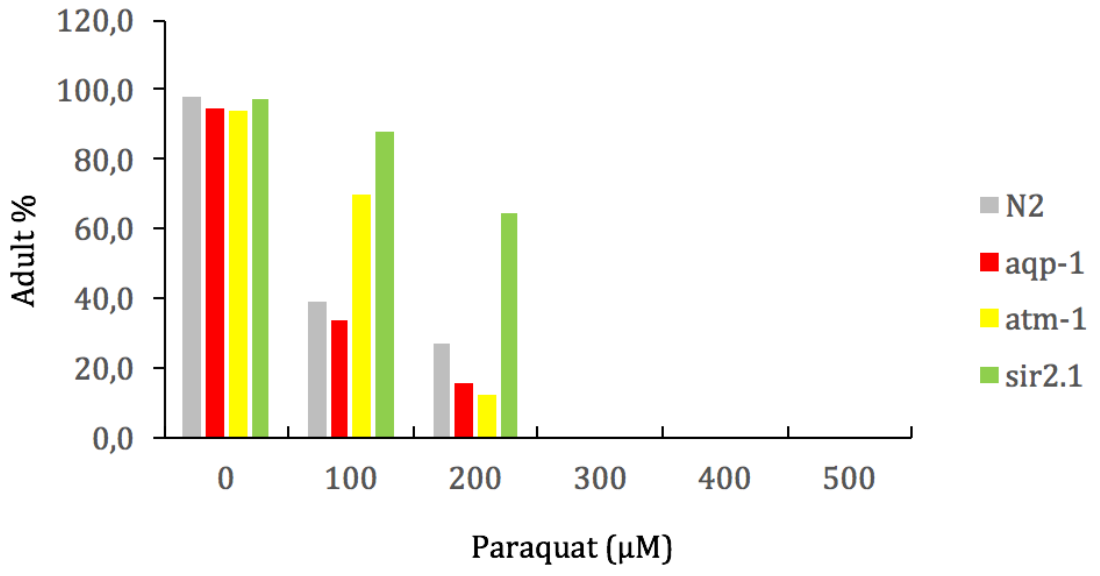

Figure 4.10: Manual-scored PQ P0 survival trial. *aqp-1(-)* (red), *atm-1(-)* (yellow), *sir-2.1(-)* (green) and N2 (grey) four strains were used in the trial. The PQ concentration range was: 0µM, 100µM, 200µM, 300µM, 400µM, 500µM. The vertical axis shows how many of the L1 worms, been transferred went to adult stage after 72 hours.

4.3.4 Manual-scoring PQ toxicity assay for double mutant

One of the study's purpose is to figure out the genetic interaction between *aqp-1* and *sir-2.1*, and the role of *aqp-1* in cytoprotective homeostatic response of the DNA damage checkpoint activation deficient strain *atm-1(-)*. In order to achieve this, we generated *aqp-1(-); atm-1(-)* and *aqp-1(-); sir-2.1(-)*, by comparing them with *aqp-1(-), atm-1(-), sir-2.1(-)* single mutant, to see what's the difference between the strains when they were treated with the ROS-generating agent PQ. Instead of bleaching method to generate synchronized worms, the egg laying method was adapted in this experiment. *aqp-1(-); atm-1(-), aqp-1(-); sir-2.1(-), aqp-1(-), atm-1(-), sir-2.1(-),* and N2 strains were used in this experiment. Three gravid worms were transferred to each well of 24-well PQ containing plates, after laying eggs for 3 hours, the gravid worms were removed. Triplicates were performed per strain per PQ concentration. The F1 survival was recorded (Figure 4.11).

For the control group, which were without PQ, the *atm-1(-)* strain and the *aqp-1(-); atm-1(-)* strain had lower F1 survival than the other four strains, they had 93.5% and 97.8% survival respectively. When the treatment concentration of PQ increased to 50μM, the F1 survival of *atm-1(-)* dropped dramatically to 55.6%, while the survival of *aqp-1(-); atm-1(-)* maintained at 97.2%, which was higher than *sir-2.1(-)* strain (85.3%) and *aqp-1(-); sir-2.1(-)* (94.6%). But, N2 and the *aqp-1(-)* still remained at 100% when the concentration of PQ is at 50 μM. When the concentration of PQ came to 100μM, the F1 survival of N2 and *aqp-1(-)* started to decrease, they decreased to 52.2% and 54.1% respectively, which is only lower than the survival of the *aqp-1(-); sir-2.1(-)* double mutant strain (75.0%). *atm-1(-)* seemed to be the most vulnerable strain towards PQ, which only had 14.3% of F1 survival. Interestingly, the *aqp-1(-); sir-2.1(-)* (75.0%) had higher L1 survival than both *sir-2.1(-)* (32.8%) and *aqp-1(-)* (54.1%), while the survival of another double mutant, *aqp-1(-); atm-1(-)* double mutant strain (43.2%), was between the *atm-1(-)* (14.3%) and *aqp-1(-)* (54.1%).

When the concentration of PQ increased to 150μM, the survival of *aqp-1(-); atm-1(-)* (14.3%) remained between the F1 survival of *aqp-1(-)* (52.6%) and *atm-1(-)* (2.3%). However, the F1 survival of *aqp-1(-); sir-2.1(-)* (75.0%) was

much higher than *sir-2.1(-)* (18.1%) and *aqp-1(-)* strain (52.6%). The F1 survival of N2 went down to 27.8%.

When the concentration of PQ increased to 200µM, there was no F1 survival of N2, *atm-1(-)*, and *aqp-1(-); atm-1(-)* strains. *aqp-1(-)*, however, which seemed to be the most resistant strain in this experiment, compared to the other five strains, still had 13.3% F1 survival while *aqp-1(-); sir-2.1(-)* and *sir-2.1(-)* had 9.3% and 4.2% F1 survival respectively.

For worms treated with 250µM PQ, *sir-2.1(-)* was the only strain still had a low fraction of F1 survival (3.8%).

From the manual-scoring PQ toxicity assay we can conclude that: *sir-2.1(-)* was the most resistant strain in this experiment, because it was the only strain had L1 survival when treated with 250µM PQ; but when the treatment PQ concentration is lower than 250µM, *aqp-1(-), aqp-1(-); sir-2.1(-)* showed higher L1 survival than *sir-2.1(-); atm-1(-)* was showed to be the least resistant strain to PQ.

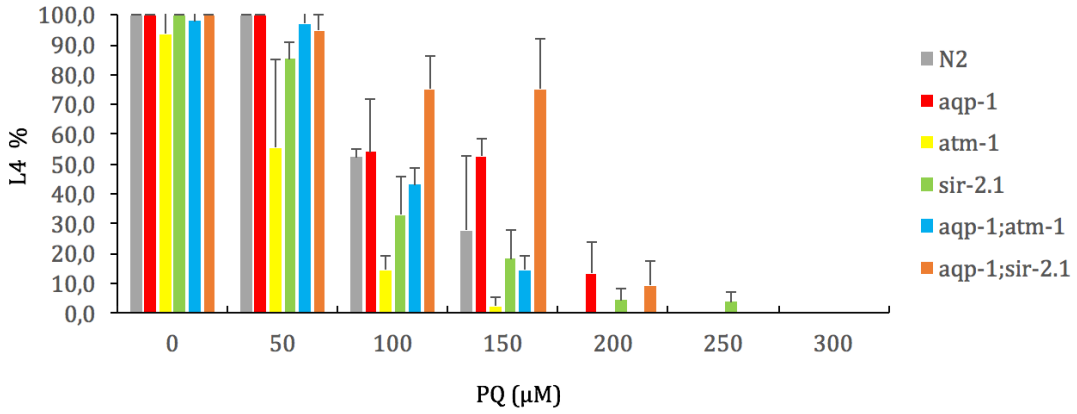

Figure 4.11 Manual-scored PQ F1 survival assay for double mutant. The figure shows the outcomes of PQ F1 survival assay for *aqp-1(-)*; *atm-1(-)* (blue), *aqp-1(-); sir-2.1(-)* (orange), *aqp-1(-)* (red), *atm-1(-)* (yellow), *sir-2.1(-)* (green), and N2 (grey). Triplicates for each condition. The horizontal axis shows the concentration of PQ, range: 0µM, 50µM, 100µM, 150µM, 200µM, 250µM, 300µM. The vertical axis shows manual-scored the L4 (L1 survival). Error bars represent the S.D. Data are mean ± S.D.

4.3.5 WMicrotracker PQ toxicity assay for double mutants

aqp-1(-); atm-1(-), aqp-1(-); sir-2.1(-), *aqp-1(-), atm-1(-), sir-2.1(-),* and N2 strains were used in this experiment. Measurement of the PQ P0 survival took 48 hours to accomplish, triplicates for each condition. Worms were washed down from the bleaching-synchronized worm plates for each strains, 90µl of the worm suspension, contains 30-50 worms, were transferred to 96-well plates, followed by adding PQ to achieve the final concentration range: 0mM, 5mM, 10mM, and 20mM. First, a trial has been done by testing N2 strain (Figure 4.7). It shows in the trail that as the concentration of PQ increased, the less locomotor activities N2 worms had. The locomotor activities decrease in a time-dependent and dose-dependent manner.

When the concentration of PQ is 0mM, which used as the control group, the locomotor activities of all the strains were relatively stable compared to the worms in the drug containing wells. But, there were certain characteristics for different strains (Figure 4.12, a). For *sir-2.1(-)*, during the first five hours after transfer, worms from this strain normally had much higher (140%) locomotor activities compared to the basal locomotor activities, which was measured right after the transfer. On the contrary, for *aqp-1(-)* and *aqp-1(-); atm-1(-)*, worms from this two strains had a drop during the first 5 hours after transfer, then recovered to the basal locomotor activities. For *atm-1(-)*, it showed a longer duration of drop than *aqp-1(-)* and *aqp-1(-); atm-1(-)* during the first 10 hours then recovered gradually. For N2 and *aqp-1(-); sir-2.1(-)*, they had a normal locomotor activities curve, it showed fluctuation and decreased a bit as the time went by after the transfer.

When the concentration of PQ was raised up to 5mM (Figure 4.12, b), at the first ten hours of the measurement, all the strains showed almost the same locomotor activities curve as the control group. For *sir-2.1(-),* the locomotor activities even went higher to 160% than the control group 140%. When the measurement lasted for more than ten hours, the locomotor activities of worms from all the strains started to drop down with different degree. Interestingly, *aqp-1(-); atm-1(-)* showed even more locomotor activities than the ones without the treatment of any drugs between the 10 hours to 30 hours. The *atm-1(-)* strain

showed higher sensitivity than the *aqp-1(-); atm-1(-)* double mutant strain but higher resistance than the four other strains to PQ.

Compare the locomotor activities curve of worms from different strains treated with 5mM, 10mM, and 20mM PQ (Figure 4.12, b, c, d): worms from *aqp-1(-); atm-1(-)* showed the strongest resistance to PQ all the time; while worms from *aqp-1(-)* showed the lowest resistance during the whole measurement; worms from *sir-2.1(-)* had higher locomotor activities during the first 5 hours after transfer, when treated with PQ with higher concentration, for example, they had 200% locomotor activities during the first five hours when the concentration of PQ was 20mM; the resistance to PQ of *aqp-1(-); sir-2.1(-)* was mainly between the resistance of *aqp-1(-)* and *sir-2.1(-).*

a

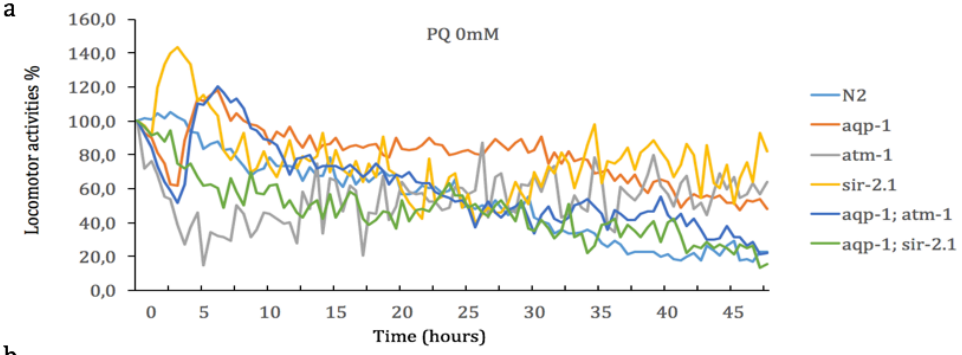
PQ 0mM
Locomotor activities %
160,0
140,0
120,0
100,0
80,0
60,0
40,0
20,0
0,0
0 5 10 15 20 25 30 35 40 45
Time (hours)
N2
aqp-1
atm-1
sir-2.1
aqp-1; atm-1
aqp-1; sir-2.1

b

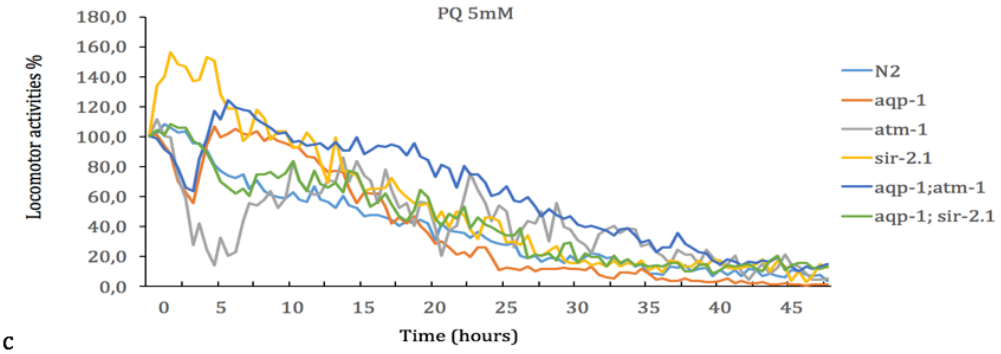
PQ 5mM
Locomotor activities %
180,0
160,0
140,0
120,0
100,0
80,0
60,0
40,0
20,0
0,0
0 5 10 15 20 25 30 35 40 45
Time (hours)
N2
aqp-1
atm-1
sir-2.1
aqp-1;atm-1
aqp-1; sir-2.1

c

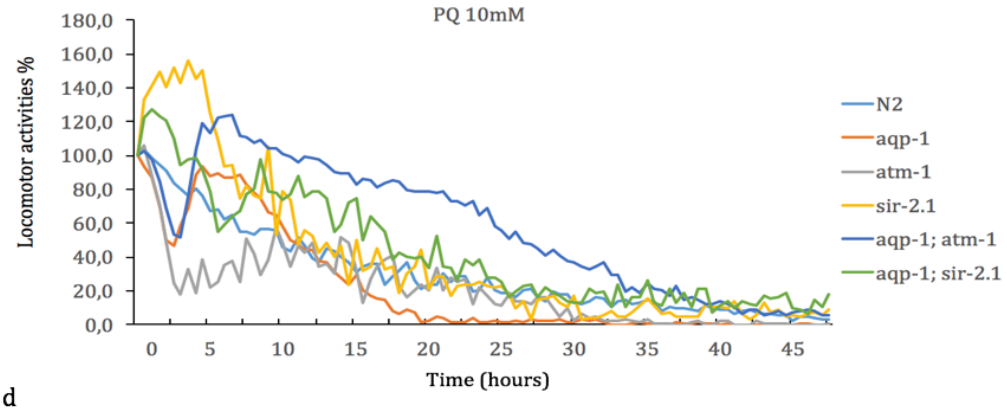
PQ 10mM
Locomotor activities %
180,0
160,0
140,0
120,0
100,0
80,0
60,0
40,0
20,0
0,0
0 5 10 15 20 25 30 35 40 45
Time (hours)
N2
aqp-1
atm-1
sir-2.1
aqp-1; atm-1
aqp-1; sir-2.1

d

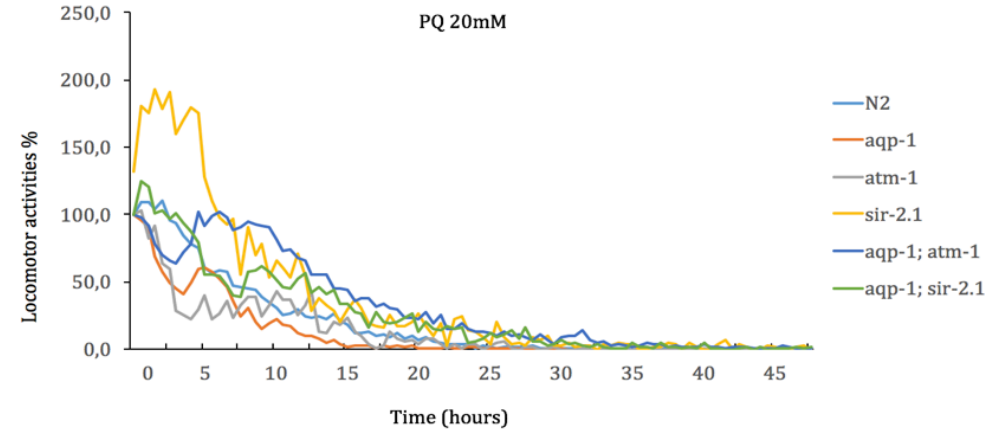
PQ 20mM
Locomotor activities %
250,0
200,0
150,0
100,0
50,0
0,0
0 5 10 15 20 25 30 35 40 45
Time (hours)
N2
aqp-1
atm-1
sir-2.1
aqp-1; atm-1
aqp-1; sir-2.1

Figure 4.12 WMicrotracker PQ toxicity assay for double mutants. *aqp-1(-)*; *atm-1(-)* (deep blue), *aqp-1(-); sir-2.1(-)* (green), *aqp-1(-)* (red), *atm-1(-)* (grey), sir-2.1(-) (yellow), and N2 (blue) measured by the WMicrotracker once per 30 minutes after being treated with 0mM (a), 5mM (b), 10mM (c) and 20mM (d) PQ respectively. The vertical axis shows the locomotor activities of worm. The horizontal axis shows the measuring time.

4.3.6 IR survival assay for *C. elegans* at different stages

To figure out how does IR, which used to generate DSBs in DNA, influence the stress response of DNA repair deficient strains and how does the general stress response pathways correlate with the classical DNA repair pathway, and if the worms would show different degree of IR resistance if they were treated at different developmental stages. To achieve this, worms at different developmental stages, in this experiment was L1 and embryo stage, were treated with 70Gy X-ray, which is generated from the CellRad (Faxitro) irradiator. Two types of assay were performed. For the egg assay, 3 gravid worms were transferred to 3.5cm OP50-seeded NGM plates for each strain, which were removed, after laying eggs for 3 hours. The number of the eggs left on the plates were scored, follow by 70Gy X-ray IR to the eggs, the L1 and L4 were recorded 24 hours or 72 hours after IR respectively; for the L1 assay, it is similar to the egg assay, the main difference is the timing of IR, the L4 was recorded after 48 hours.

When the x-ray IR was given to the L1-stage worms (Figure 4.13, a), N2 showed the highest L4, which was 38.2%, while the *sir-2.1(-)* showed the lowest L4, which was 4.5%. *aqp-1(-); sir-2.1(-)* and *aqp-1(-); atm-1(-)* had the L4 between two corresponding single mutant strains. For example, the L4 of *aqp-1(-); sir-2.1(-)* was 11.1, which is between the L4 of *aqp-1(-)* (17,0%) and *sir-2.1(-)* (4.5%).

When the 70Gy X-ray IR were exerted at the egg stage (egg assay) (Figure 4.13, b). Surprisingly, the F1 survival of N2 (4.3%), *aqp-1(-)* (3.8%), and *aqp-1(-); sir-2.1(-)* (7.3%) were extremely low, while the F1 survival of *sir-2.1(-)* strain, and *aqp-1(-); atm-1(-)* strain were 33.9% and 24.1% respectively. Interestingly, the *atm-1* strain was with the highest L1 (87.8%) and L4 (11.4%), compared to

other five strains. From the control group which was without IR treatment, only *sir-2.1(-)* and *atm-1(-)* had relatively lower L4, 88.9% and 81.7% respectively.

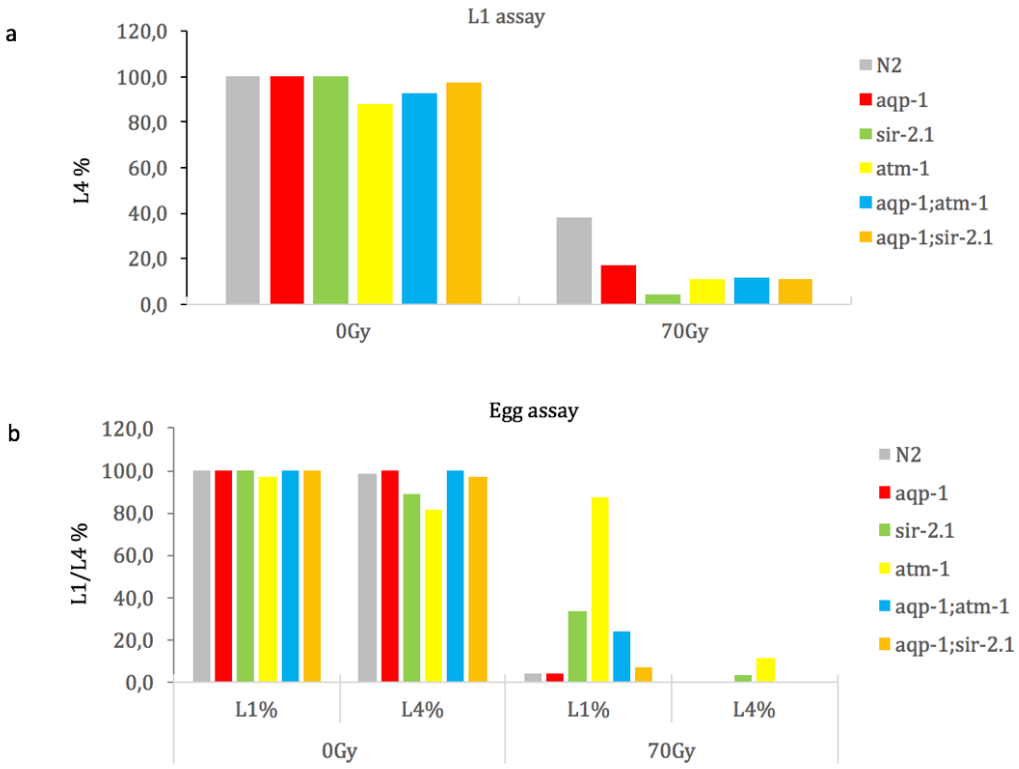

Figure 4.13: IR survival assay for *C. elegans* at different stages *aqp-1(-)*; *atm-1(-)* (blue), *aqp-1(-); sir-2.1(-)* (orange), *aqp-1(-)* (red), *atm-1(-)* (yellow), *sir-2.1*(-) (green), and N2 (grey) have been tested in the IR assay. Two different types of IR assay were measured: the the L1 assay (a), the egg assay (b), For the egg assay, both the L1 and the L4 were recorded, while for L1 assay, only L4 was recorded.

Compare the L1 assay and the egg assay, N2, *aqp-1(-)*, *aqp-1(-); atm-1(-)* and *aqp-1(-); sir-2.1(-)* showed big difference between the two circumstance. When they were treated at the L1 stage, they still have some worm can go to the L4 stage, 38.2% for N2, 17% for *aqp-1(-)*, 11.3% for *aqp-1(-); atm-1(-)* and 11.1% for *aqp-1(-); sir-2.1(-).* But when the IR were given at the egg stage, none of them have worms came to L4 stage, while the *atm-1(-)* showed almost the same percentage of L4 as the IR given at the L1 stage. We can conclude that, *sir-2.1*, *aqp-1*, and *atm-1* were required for the IR resistance, but about how they interact with each other requires more experiments.

5. Discussion

5.1 Summary of results

In the present study, we used genetic analysis to address the involvement of *aqp-1*, which is one of the downstream effectors in IIS pathway, in the DNA damage checkpoint activation deficient strain *atm-1(-)* and to investigate if there are genetic correlations between *sir-2.1* and *aqp*-1, as *sir-2.1* pathway is partially overlapping with IIS pathway.

To achieve these, *aqp-1(-); atm-1(-)* and *aqp-1(-); sir-2.1(-)* double mutant strains were generated successfully. Moreover, to solve the labor intensive problem of various stress response assay, we tested the WMicrotracker in both the heat shock assay and PQ toxicity assay. The double mutants *aqp-1(-); atm-1(-)* and *aqp-1(-); sir-2.1(-)*, were assessed together with reference strain N2, and *aqp-1(-), sir-2.1(-), atm-1(-)* single mutant strains by the PQ toxicity assay (by both the WMicrotracker and manual scoring), heat shock assay (by both the WMicrotracker and manual scoring), and IR sensitivity assay (only by manual scoring).

The rough conclusion about the WMicrotracker: it was suitable for the PQ toxicity assay, while it didn't show consistence with the manual scoring method for the heat shock assay. In the WMicrotracker PQ toxicity assay, as *aqp-1(-); atm-1(-)* showed a much stronger resistance to PQ than *aqp-1(-) and atm-1(-)* single mutant strains, and *aqp-1(-); sir-2.1(-)* showed stronger resistance than both *aqp-1(-)* and *sir-2.1(-)* single mutant strains after 15 hours, though it was less resistant to PQ than *sir-2.1(-)* but more resistant than *aqp-1(-)* during the first 15 hours. From this we suspect that the *aqp-1, sir-2.1* and *atm-1* don't work in the same stress response pathway, as they didn't have the exact same locomotor curves. But *aqp-1* might have genetic interactions with both *atm-1,* and *sir-2.1.* Additionally, *aqp-1* might function as a mediator of the cytoprotective homestatic response in the DNA checkpoint activation deficient strain *atm-1(-)*. To illustrate correlations between aqp-1, atm-1 and sir-2.1 in detail, more experiments are required.

5.2 Double mutant generation

5.2.1 Obtain double mutants according to Mendelian ratio?

According to Mendelian segregation theory (Figure 4.3), we suppose to get double mutant worm at a 1:16 rate. However, we got *aqp-1(-); atm-1(-)* at an even lower ratio than 1:32. We don't know the exact ratio is because, we didn't get the *aqp-1(-); atm-1(-)* at the 32 single F2 generation hermaphrodites. Instead, we only got strain with homozygous *aqp-1(-)* and heterozygous *atm-1(-)* at the F2 generation. Then we obtained *aqp-1(-); atm-1(-)* from the next generation of the self-fertilized F2 heterozygous. But for *aqp-1(-); sir-2.1(-)*, we succeeded in getting it at a ratio of 3:32, which is close to the Mendelian ratio.

As *aqp-1, sir-2.1* and *atm-1* are at different chromosomes, no difference in recovery ratio is expected in the efficiency of generating *aqp-1(-); sir-2.1(-)* and *aqp-1(-); atm-1(-)* double mutant. There are several possible reasons for this: firstly, it might because *aqp-1(-); atm-1(-)* is an unfavorable mutant, while *aqp-1(-); sir-2.1(-)* do not impact viability; another reason might be that the stress, for example, the heat-shock method for male generation at the beginning of the crossing, might influence the recovery ratio; also, as we have only done the mating experiment once for each double mutant, we cannot say the exact ratio for obtaining the double mutant in F2 generation.

5.2.2 Nonspecific bands in PCR genotyping

In this study, we got nonspecific bands for *sir-2.1* genotyping, and for *atm-1* genotyping. In the case of *sir-2.1*, we had the expected bands but also some nonspecific bands. So all we needed to do for the *sir-2.1* genotyping was to optimize the annealing temperature, so that, the primer pair for *sir-2.1* would not bind to other low affinity binding sites. In order to find the optimal temperature, the gradient PCR was run by the Eppendorf Mastercycler ep Gradient S.

But in the case of *atm-1*, it was quite different, because we didn't get the product of the right size, instead we got a bright band at the wrong size, which is the same size as the reference strain N2 (Figure 4.2). Then there were two possibilities: firstly, it might be a problem of primer pairs giving unspecific bands; or it might be the problem of the strain. We tested the first possibility, and tried to optimize the PCR conditions, but it still didn't work. For this case, we

used Primer 5 to design new primers altered reaction conditions and cycling conditions. The difference between this two pairs of primers, is 56bp binding sites moving and the newly designed primer contains less dimer and less hairpin. But for both primer pairs I got the same wrong results. Which means that *atm-1(-)* was somehow mixed with the reference strain N2, and we obtained a new stock of strain for which we could confirm the mutant allele.

5.3 WMicrotracker-a promising alternative to manual scoring?

5.3.1 M9 buffer vs 3PY buffer

To find the buffer can support worm viability and also be suitable for the scanning system of WMicrotracker was the first factor to consider in order to turn WMicrotracker into a worm assistant. There were two options for us, the M9 buffer, which is normally used to recovery worms from plates, and the 3PY buffer (Appendix 8.1), which is recommended by the WMicrotracker company. However, our results show that compared to 3PY buffer, which only contains peptone, worms in M9 buffer were tended to be more calm and have more stable locomotor activities.

Through the trial, we found out that the locomotor activities of worms in both M9 buffer and 3PY fluctuated all the time, no matter how many worms in each well. The reason for the fluctuation might be: the normal circadian rhythms of *C. elegans*; the stressful conditions in the well because of too many or too few worms; or worms don't like to stay in buffer, they would rather to stay on NGM solid plates.

Therefore, we wanted to find the condition where the worms had relatively stable locomotor activities. As we can see in the figure (Figure 4.5), the locomotor activities of worms decreased when they were kept in 3PY buffer, there were almost no movement in the end. This makes it difficult to use 3PY buffer for making the WMicrotracker samples. But for M9 buffer, when there were only 10 worms in each well, the locomotor activities were quite changeable, but when the amount of worms increased to 30 for each well, it seemed to have a much ideal locomotor activities curve and without decrease until the end of the measurement.

5.3.2 Not suitable for heat shock experiment?

Heat shock, briefly, means to give organism a living environment with a higher temperature than the ideal temperature for the organisms. It is normally 5 to 10 degrees higher than the highest point of the ideal range. For example, for *C. elegans*, normally we keep them in 20°C or 25°C incubator according to the requirements of different experiments. So for the heat shock, we can just keep them in the 35°C incubator to carry out heat shock. In this study, we run the trial at 32°C, 34°C, and 35°C respectively to find out the optimal heat shock temperature (Figure 4.6).

During the trial, we didn't put the WMicrotracker in the heat shock incubator directly. Which means, we have to move the plates from the heat shock incubator to the WMicrotracker, which would influence the outcome: first, it made the temperature controlling hard, because the room temperature was around 20°C, and the machine cannot control temperature; secondly, when we move the plates to the machine, we may shake the plates, and it would influence the locomotor activities of worms, which contributes to the inaccuracy to the measurement.

To solve the temperature controlling and transferring problem, we move the WMicrotracker into the incubator. Then we run the heat shock assay again measured by both WMicrotracker and manual scoring (Figure 4.9). Still we got different outcome from the WMicrotracker to the manual scoring.

Here are several reason for the inconsistence: Firstly, and the most importantly, the WMicrotracker is used to measure the locomotor activities, while the manual scoring is to score how many worms is still alive, that makes the two measurement essentially different. The worms don't have to move around all the time when they are alive, the consistence actually has to be built upon the hypothesis that if the worms don't move during the measuring time, then they are dead. But it is not the case. Secondly, it might be influenced by the different plates have been used in the two different measurements, for the WMicrotracker, worms were kept in M9 buffer in 96-well plates, while for the manual scoring, the 3.5cm NGM solid plates were used. As we all know that, worms are more stressed when they are kept in the liquid buffer than on the solid NGM. Thirdly, for the manual scoring, we still have to move the plates out of the heat shock

incubator to inspect and score by using the Zeiss Stemi SV6, which make the temperature controlling difficult for the manual scoring method. If it takes too long in the room temperature, the worms keep living.
Hence, we cannot say that WMicrotracker is not suitable for heat shock, it is a totally different system from the manual scoring, they measure different phenotypes. So, I would say that, both method works, but the outcomes from the two different measurement are not comparable.

5.3.3 Good choice for PQ assay?

For the PQ assay, as the heat shock assay, we didn't get the consistent outcomes from the manual scoring, we still believe that WMicrotracker is a pretty good choice for PQ assay (Figure 4.7).
We can see from the figure, when the concentration of the treatment drugs became higher, the locomotor activities of worms decreased faster. Which means if we know how fast the locomotor activities decrease, then we know which treatment drug concentration is higher. By the same token, if we use drugs with the same concentration on different strains, we would know which strain is more sensitive to the drug. That's what we suppose to measure in the drug sensitivity assay.
The difference between the WMicrotracker and the manual counting in drug sensitivity assay are (except for the reason in the last chapter): Firstly, we use different PQ concentration range, for the WMicrotracker, the concentration of PQ range: 0mM, 5mM, 10mM, 15mM to 20mM; while for manual scoring the concentration of PQ range: 0µM, 50µM, 100µM, 150µM, 200µM, 250µM, 300µM to 350µ. The reason for the big range difference is because PQ concentration in µM is enough to influence the growth of the worms but cannot influence the worms die and move less during the 48-hour measurement. Secondly, the two measurement measure different aspects of worms: the WMicrotracker is actually used to measure the acute toxicity of drugs, while the manual scoring is used to measure the chronic toxicity of drugs which would influence the growth of worms.

Therefore, in conclusion, M9 buffer, instead of 3PY, is a better choice for the WMicrotracker sample preparation; WMicrotracker can be used in both heat shock assay and PQ assay, but it is not comparable to the manual scoring.

5.4 Genetic correlations between IIS pathway gene *aqp-1* and DNA damage checkpoint activation gene *atm-1*

5.4.1 *apq-1* is required for cytoprotective homeostatic response

According to Kenyon and colleagues, *aqp-1* functions in the IIS pathway as the downstream target of FOXO family member *daf-16* (Lee, Murphy, & Kenyon, 2009). Further, AQP-1 expression is upregulated in *daf-2(-)*, and loss of AQP-1 function in *daf-2* mutant animals results in reduced lifespan. This suggest that *aqp-1* may act as a crucial effector for slow down aging and increase the stress response by activating downstream genes, as longevity is generally associated with stronger stress resistance.

In this study, *aqp-1(-)* were tested in heat shock tolerance assay, PQ toxicity assay, and IR assay. It's actually tested if *aqp-1* is required for the homeostatic regulation, oxidative DNA damage response, and DSBs repair.

From the outcome we got, we can see that *aqp-1(-)* strain is hypersensitive to heat shock, because it showed both in the trial (Figure 4.6, II, III) at 34°C and 35°C heat shock by manual scoring and the WMicrotracker, compared to N2, *atm-1(-),* and *sir-2.1(-)*. In the final heat shock experiment (Figure 4.9), even compared to *aqp-1(-); atm-1(-)* and *aqp-1(-); sir-2.1(-)* double mutant strains, *aqp-1(-)* showed stronger sensitivity to heat shock. But there was a exception, during the WMicrotracker measuring 35°C heat shock(Figure 4.9, a), *aqp-1(-)* had a lot of locomotor activities during the first two hours of heat shock than other mutant strains, but, still, locomotor activities of *aqp-1(-)* is much lower than the N2 reference strain. In addition, when we were doing manual scoring heat shock, we can distinguish *aqp-1(-)* from other strains by using Zeiss Stemi SV6, the shape of *aqp-1(-)* worms were soon became straight, and without so much movement. Further, during heat shock, *aqp-1(-)* showed a high rate of protruding vulva, which was much higher than other strains involved in this study.

For the manual-scoring PQ assay (Figure 4.10; Figure 4.11) and the WMicrotracker-measuring PQ assay (Figure 4.12), the outcomes from this two different methods showed strong consistent. In the PQ-WMicrotracker assay (Figure 4.12) it is obvious that the locomotor activities of *aqp-1(-)* worms decreased earlier and faster than all the other strains*: N2, atm-1(-), sir-2.1(-), aqp-1(-);sir-2.1(-), aqp-1(-);atm-1(-)* at all the PQ concentration: 5mM, 10mM, 20mM. In addition, the locomotor activities of *aqp-1(-)* worms were died out earlier as the PQ concentration increased. From this, we can conclude that *aqp-1* is crucial for the resistance against the ROS generating agent PQ.

For the IR assay (Figure 4.13), it is hard to say, because we only done the experiment once. As we inspected, when the L1 worms were treated with 70Gy IR, *aqp-1(-)* seemed to be more sensitive than the N2 strain, but more tolerance than other four mutant strains; when the embryos were treated with 70Gy IR, *aqp-1(-)* seemed to be the most sensitive strain, with the lowest L1 and L4 compared to all the other 5 strains. This indicates that aqp-1 plays an important role in the DSBs stress response during embryonic development, while there are might be other pathways were gradually completed during growth, which would then replace the *aqp-1* to response to DSBs.

In conclusion, from the present study, we can preliminary say that, *aqp-1* is required for the general stress response and oxidative DNA damage response. But to illustrate it in details, the further researches are required.

5.4.2 *aqp-1* functions as the mediator of system homeostatic response in DNA damage checkpoint deficient strain *atm-1(-)*?

atm-1 is known as one of the main orchestrators in DDR, which is important for DNA damage check point activation and induce cell cycle arrest or apoptosis. Interestingly and against our hypothesis, *aqp-1(-); atm-1(-)*, showed the highest resistance to PQ among the six strains in the WMicrotracker-measuring PQ toxicity assay(Figure 4.12), which supposed to show hypersensitivity to PQ as *aqp-1(-)* and *atm-1(-)* did. It means that when both *atm-1* and *aqp-1* were deleted, the organisms are with even stronger resistance to PQ. This made us suspect that, when the worms were exerted with high-concentration PQ treatment, though both the *aqp-1* and the *atm-1* are required for the stress

response pathway, *aqp*-1 might function as a mediator of the cytoprotective homeostatic response while *atm-1* acts at the DNA damage checkpoint activation, but the process might be cytotoxic if they were over-activated.

The *aqp-1*'s possible role of a mediator in cytoprotective homeostatic response was also implied by the brood size assay (Figure 4.8), *atm-1(-)* has 188,5±26,0 brood, while *aqp-1(-); atm-1(-)* has 242,2±29,5, which indicates that *aqp-1* might be the reason for the decreased brood size of the DNA damage checkpoing activation deficient strain *atm-1(-)*. To illustrate the genetic correlations detail between *aqp-1* and *atm-1*, further researches are required.

5.5 Perspective

WMicrotracker allows researchers to monitor the locomotor activities of small-size animals by scanning animals with infrared, however, it cannot control temperature and track the movement of worms, the application of WMicrotracker is quite limited. It would be amazing if the WMicrotracker carry its own temperature-controlling and camera system. I am also looking forwards to exploit the application of WMicrotracker to other research field such as in neurodegeneration, it can be used to track the movement disorder of worms and used together with the software called "Wormlab".

As we roughly suspect that *aqp-1* might works as a mediator in the cytoprotective homeostatic response pathway in the DNA repair checkpoint activation deficient strain *atm-1(-)*, but to investigate further,

In this study, what we mainly did is to check stress response of different different strain, as we already preliminary see that *aqp-1(-)*; *atm-1(-)* has strong resistance to PQ, it would be interesting to see if the strain has longer lifespan and test if ATM-1 and AQP-1 really have genetic interactions, to more precisely how *aqp-1* interact with *atm-1*, the transcriptional signatures should be done for the *atm-1(-)*, to see if there is a upregulation in *aqp-1*; and it would be interesting to see if the *aqp-1(-); atm-1(-)* double mutant strain is another longevity strain, as it is quite resistant to PQ. And what's the role of the *aqp-1* in the cytoprotective homeostatic response? Is it a central orchestrator which connect DNA repair with cytoprotective homeostatic response and initiate a whole

cascade? In addition, it is also interesting to generate the *aqp-1(-); atm-1(-); air-2.1(-)* triple mutant, to see if the *aqp-1* and *sir-2.1* have the synthetic liability in the DNA checkpoint activation mutant *atm-1(-)*. In addition, I roughly found out that *aqp-1(-)* strain might grow faster than N2 and other strains been used in this study, is that the reason for why the aqp-1(-) strain has a shorter lifespan? It is already amazing to see that the glycerol channel AQP-1 plays such an important role in aging and stress response, I'm looking forward to do more research about metabolism, stress response and aging.

6. Reference

Allen, C., Halbrook, J., & Nickoloff, J. A. (2003). Interactive competition between homologous recombination and non-homologous end joining. *Mollecular cancer reserach: MCR , 1* (12), 913-920.

Ames, B. N., Shigenaga, M. K., & Hagen, T. M. (1993). Oxidants, antioxidants, and the degenerative diseases of aging. *Proceedings of the National Academy of Sciences of the United States of America , 90* (17), 7915-7922.

Amrit, F. R., Ratnappan, R., Keith, S. A., & Ghazi, A. (2014). The C. elegans lifespan assay toolkit. *Methods (San Diego, Calif.) , 68* (3), 465-475.

Anderson, J. L., Morran, L. T., & Phillips, P. C. (2010). Outcrossing and the Maintenance of Males within C. elegans Populations. *Journal of Heredity , 101* (Suppl 1), S62-S74.

Anindya, R., Mari, P.-O., Kristensen, U., Kool, H., Giglia-Mari, G., Mullenders, L. H., et al. (2010). A Ubiquitin-Binding Domain in Cockayne Syndrome B Required for Transcription-Coupled Nucleotide Excision Repair. *Molecular Cell , 38* (5), 637-648.

Arczewska, K. D., Tomazella, G. G., Lindvall, J. M., Kassahun, H., Maglioni, s., Torgovnick, A., et al. (2013). Active transcriptomic and proteomic reprogramming in the C. elegans nucleotide excision repair mutant xpa-1. *Nucleic Acid Research , 41* (10), 5368-5381.

Aas, P. A., Otterlei, M., Falnes, P. Ø., Vågbø, C. B., Skorpen, F., Akbari, M., et al. (2003). Human and bacterial oxidative demethylases repair alkylation damage in both RNA and DNA. *Nature , 421* (6925), 859-863.

Barrière, A., & Félix, M.-A. (2014). Isolation of C. elegans and related nematodes. *WormBook: The Online Review of C. Elegans Biology* , 1-19.

Bartek, J., & Lukas, J. (2003). Chk1 and Chk2 kinases in checkpoint control and cancer. *Cancer Cell , 3* (5), 421-429.

Bartek, J., & Lukas, J. (2007). DNA damage checkpoints: from initiation to recovery or adaptation. *Current Opinion in Cell Biology , 19* (2), 238-245.

Bjelland, S., & Seeberg, E. (2003). Mutagenicity, toxicity and repair of DNA base damage induced by oxidation. *Mutation Research , 531* (1-2), 37-80.

Bont, R. D., & Larebeke, N. v. (2004). Endogenous DNA damage in humans: a review of quantitative data. *Mutagenesis , 19* (3), 169-185.

Brenner, S. (1974). The genetics of Caenorhabditis elegans. *Genetics , 77* (1), 71-94.

Burma, S., Chen, B. P., Murphy, M., Kurimasa, A., & Chen, D. J. (2001). ATM phosphorylates histone H2AX in response to DNA double-strand breaks. *The Journal of Biological Chemistry , 276* (45), 42462-42467.

Byrne, S., Cunniffe, S., O'Neill, P., & Lomax, M. E. (2009). 5,6-Dihydrothymine impairs the base excision repair pathway of a closely opposed AP site or single-strand break. *radiation research , 172* (5), 537-549.

Chapman, J. R., Taylor, M. R., & Boulton, s. J. (2012). Playing the End Game: DNA Double-Strand Break Repair Pathway Choice. *Molecular Cell , 47* (4), 497-510.

Christmann, M., Verbeek, B., Roos, W. P., & Kaina, B. (2011). O(6)-Methylguanine-DNA methyltransferase (MGMT) in normal tissues and tumors: enzyme activity, promoter methylation and immunohistochemistry. *Biochimica Et Biophysica Acta , 1816* (2), 179-190.

Clancy, s. (2008). DNA damage & repair: mechanisms for maintaining DNA integrity. *Nature education , 1* (1), 103.

Clark, A. B., Cook, M. E., Tran, H. T., Gordenin, D. A., Resmick, M. A., & Kunkel, T. A. (1999). Functional analysis of human MutSα and MutSβ complexes in yeast. *Nucleic Acids Research , 27* (3), 736-742.

Costanzo, V., Robertson, K., Ying, C. Y., Kim, E., Avvedimento, E., Gottesman, M., et al. (2000). Reconstitution of an ATM-dependent checkpoint that inhibits chromosomal DNA replication following DNA damage. *Molecular Cell , 6* (3), 649-659.

Courgeon, A.-M., Maisonhaute, C., & Best-Belpomme, M. (1984). Heat shock proteins are induced by cadmium in Drosophila cells. *Experimental Cell Research , 153* (2), 515-521.

Cutter, A. D. (2004). Sperm-limited fecundity in nematodes: how many sperm are enough? *Evolution; International Journal of Organic Evolution , 58* (3), 651-655.

de Boer, J., & Hoeijmakers, J. H. (2000). Nucleotide excision repair and human syndromes. *Carcinogenesis , 21* (3), 453-460.

Dengg, M., Garcia-Muse, T., Gill, S. G., Ashcroft, N., Boulton, S. J., & Nilsen, H. (2006). Abrogation of the CLK-2 checkpoint leads to tolerance to base-excision repair intermediates. *EMBO reports , 7* (10), 1046-1051.

Enserink, J. M. (2015). Sumo and the cellular stress response. *Cell Division , 10*, 4.
Ercal, N., Gurer-Orhan, H., & Aykin-Burns, N. (2001). Toxic metals and oxidative stress part I: mechanisms involved in metal-induced oxidative damage. *Current Topics in Medicinal Chemistry , 1* (6), 529-539.
Ermolaeva, M. A., & Schumacher, B. (2014). Systemic DNA damage responses: Organismal adaptations to genome instability. *Trends in genetics : TIG , 30* (3), 95-102.
Ermolaeva, M. A., Segref, A., Dakhovnik, A., Ou, H.-L., Schneider, J. I., Utermohlen, O., et al. (2013). DNA damage in germ cells induces an innate immune response that triggers systemic stress resistance. *Nature , 501* (7467), 416-420.
Errol, F. C., Graham, W. C., Wolfram, s., Richard , W. D., Roger, S. A., & Tom , E. (2006). *DNA repair and Mutagenesis* (Second edition ed.).
Falck, J., Coates, J., & Jackson, S. P. (2005). Conserved modes of recruitment of ATM, ATR and DNA-PKcs to sites of DNA damage. *Nature , 434* (7033), 605-611.
Falck, J., Mailand, N., Syljuåsen, R. G., Bartek, J., & Lukas, J. (2001). The ATM-Chk2-Cdc25A checkpoint pathway guards against radioresistant DNA synthesis. *Nature , 410* (6830), 842-847.
Fan, C.-H., Liu, W.-L., Cao, H., Wen, C., Chen, L., & Jiang, G. (2013). O6-methylguanine DNA methyltransferase as a promising target for the treatment of temozolomide-resistant gliomas. *Cell Death & Disease , 4* (10), e876.
Fang, E. F., Scheibye-Knudsen, M., Brace, L. R., Kassahun, H., SenGupta, T., Nilsen, H., et al. (2014). Defective mitophagy in XPA via PARP-1 hyperactivation and NAD(+)/SIRT1 reduction. *Cell , 157* (4), 882-896.
Fanning, E., Klimovich, V., & Nager, A. R. (2006). A dynamic model for replication protein A (RPA) function in DNA processing pathways. *Nucleic Acids Research , 34* (15), 4126-4137.
Fay, D. S., Large, R., Han, M., & Darland, M. (2003). lin-35/Rb and ubc-18, an E2 ubiquitin-conjugating enzyme, function redundantly to control pharyngeal morphogenesis in C. elegans. *Development (Cambridge, England) , 130* (14), 3319-3330.
Fekairi, S., Scaglione, S., Chahwan, C., Taylor, E. R., Tissier, A., Coulon, S., et al. (2009). Human SLX4 is a Holliday Junction Resolvase Subunit that Binds Multiple DNA Repair/Recombination Endonucleases. *Cell , 138* (1), 78-89.

Fensgård, Ø., Kassahun, H., Bombik, I., Rognes, T., Lindvall, J. M., & Nilsen, H. (2010). A Two-tiered compensatory response to loss of DNA repair modulates aging and stress response pathways. *Aging (Albany NY) , 2* (3), 133-159.

Fraga, C. G., Shigenaga, M. K., Park, J. W., Degan, P., & Ames, B. N. (1990). Oxidative damage to DNA during aging: 8-hydroxy-2'-deoxyguanosine in rat organ DNA and urine. *Proceedings of the National Academy of Sciences of the United States of America , 87* (12), 4533-4537.

Francis, D. B., Kozlov, M., Chavez, J., Chu, J., Malu, S., Hanna, M., et al. (2014). DNA Ligase IV regulates XRCC4 nuclear localization. *DNA repair , 21*, 36-42.

Freund, A., Patil, C. K., & Campisi, J. (2011). p38MAPK is a novel DNA damage response-independent regulator of the senescence-associated secretory phenotype. *The EMBO journal , 30* (8), 1536-1548.

Friedberg, E. C., Aguilera, A., Gellert, M., Hanawalt, P. C., Hays, J. B., Lehmann, A. R., et al. (2006). DNA repair: from molecular mechanism to human disease. *DNA repair , 5* (8), 986-996.

Friedberg, E. C., Walker, G. C., & Siede, W. (1995). *DNA Repair and Mutagenesis.*

Fromme, J., & Verdine, G. L. (2003). Structure of a trapped endonuclease III–DNA covalent intermediate. *The EMBO Journal , 22* (13), 3461-3471.

Gartner, A., MacQueen, A. J., & Villeneuve, A. M. (2004). Methods for analyzing checkpoint responses in Caenorhabditis elegans. *Methods in Molecular Biology (Clifton, N.J.) , 280*, 257-274.

Gems, D., & Partridge, L. (2015). Genetics of Longevity in Model Organisms: Debates and Paradigm Shifts. *Annual Review of Physiology , 75* (1), 621-644.

Gilca, M., Stoian, I., Atanasiu, V., & Virgolici, B. (2007). The oxidative hypothesis of senescence. *Journal of postgraduate Medicine , 53* (3), 207-213.

Guisbert, E., Yura, T., Rhodius, V. A., & Gross, C. A. (2008). Convergence of Molecular, Modeling, and Systems Approaches for an Understanding of the Escherichia coli Heat Shock Response. *Microbiology and Molecular Biology Reviews , 72* (3), 545-554.

Hakim, J. (1993). [Reactive oxygen species and inflammation]. *Comptes Rendus Des Séances De La Société De Biologie Et De Ses Filiales , 187* (3), 286-295.

Hartman, P. S., & Herman, R. K. (1982). Radiation-sensitive mutants of Caenorhabditis elegans. *Genetics , 102* (2), 159-178.

Hashmi, S., Tawa, W., & Lustigman, S. (2001). Caenorhabditis elegans and the study of gene function in parasites. *Trends in Parasitology , 17* (8), 387-393.
Hegde, M. L., Hazra, T. K., & Mitra, S. (2008). Early Steps in the DNA Base Excision/Single-Strand Interruption Repair Pathway in Mammalian Cells. *Cell research , 18* (1), 27-47.
Hodgkin, J., & Barnes, T. M. (1991). More is not better: brood size and population growth in a self-fertilizing nematode. *Proceedings. Biological Sciences / The Royal Society , 246* (1315), 19-24.
Hoeijmakers, J. H. (2001). Genome maintenance mechanisms for preventing cancer. *Nature , 411* (6835), 366-374.
Hu, J., Souza-Pinto, N. C., Haraguchi, K., Hogue, B. A., Jaruga, P., Greenberg, M. M., et al. (2005). Repair of Formamidopyrimidines in DNA Involves Different Glycosylases ROLE OF THE OGG1, NTH1, AND NEIL1 ENZYMES. *Journal of Biological Chemistry , 280* (49), 40544-40551.
Hybertson, B. M., Gao, B., Bose, S. K., & McCord, J. M. (2011). Oxidative stress in health and disease: The therapeutic potential of Nrf2 activation. *Molecular Aspects of Medicine , 32* (4-6), 234-246.
Jackson, A. L., & Loeb, L. A. (2001). The contribution of endogenous sources of DNA damage to the multiple mutations in cancer. *Mutation Research , 477* (1-2), 7-21.
Jackson, S. P. (2002). Sensing and repairing DNA double-strand breaks. *Carcinogenesis , 23* (5), 687-696.
Jacobs, A. L., & Schär, P. (2012). DNA glycosylases: in DNA repair and beyond. *Chromosoma , 121* (1), 1-20.
Jazayeri, A., Falck, J., Lucas, C., Bartek, J., Smith, G. C., Lukas, J., et al. (2006). ATM- and cell cycle-dependent regulation of ATR in response to DNA double-strand breaks. *Nature Cell Biology , 8* (1), 37-45.
Jazayeri, A., Falck, J., Lukas, C., Bartek, J., Smith, G. C., Lukas, J., et al. (2006). ATM- and cell cycle-dependent regulation of ATR in response to DNA double-strand breaks. *Nature Cell Biology , 8* (1), 37-45.
Jiang, J., Briedé, J. J., Jennen, D. G., Van Summeren, A., Saritas-Brauers, K., Schaart, G., et al. (2015). Increased mitochondrial ROS formation by acetaminophen in human hepatic cells is associated with gene expression changes suggesting

disruption of the mitochondrial electron transport chain. *Toxicilogy letters , 234* (2), 139-150.
Jones, M. R., Huang, J. C., Chua, S. Y., Baillie, D. L., & Rose, A. M. (2012). The atm-1 gene is required for genome stability in Caenorhabditis elegans. *Molecular Genetics and Genomics , 287* (4), 325-335.
Kamel, F. (2013). Paths from Pesticides to Parkinson's. *Science , 341* (6147), 722-723.
Kenyon, C. J. (2010). The genetics of ageing. *Nature , 464* (7288), 504-512.
Kenyon, C., Chang, J., Gensch, E., Rudner, A., & Tabtiang, R. (1993). A C. elegans mutant that lives twice as long as wild type. *Nature , 366* (6456), 461-464.
Khazaeli, A. A., Tatar, M., Pletcher, S. D., & Curtsinger, C. (1997). Heat-Induced Longevity Extension in Drosophila. I. Heat Treatment, Mortality, and Thermotolerance. *The Journals of Gerontology Series A: Biological Sciences and Medical Sciences , 52A* (1), B48-B52.
Kim, Y.-J., & Wilson, D. M. (2012). Overview of Base Excision Repair Biochemistry. *Current molecular pharmacology , 5* (1), 3-13.
Kitagawa, R., Bakkenist, C. J., McKinnon, P. J., & Kastan, M. B. (2004). Phosphorylation of SMC1 is a critical downstream event in the ATM-NBS1-BRCA1 pathway. *Genes & Development , 18* (12), 1423-1438.
Krejci, L., Altmannova, V., Spirek, M., & Zhao, X. (2012). Homologous recombination and its regulation. *Nucleic Acids Research , 40* (13), 5795-5818.
Krokan, H. E., & Bjørås, M. (2013). Base Excision Repair. *Cold Spring Harbor Perspective in Biology , 5* (4), a012583.
Krokan, H. H., Standal, R., & Slupphaug, G. (1997). DNA glycosylases in the base excision. *The Biochemical Journal , 325 (Pt 1)*, 1-12.
Landis, J. N., & Murphy, C. T. (2010). Integration of diverse inputs in the regulation of C. elegans DAF- 16/FOXO. *Developmental dynamics : an official publication of the American Association of Anatomists , 239* (5).
Lans, H., Lindvall, J. M., Thijssen, K., Karambelas, A. E., Cupac, D., Fensgård, Ø., et al. (2013). DNA damage leads to progressive replicative decline but extends the life span of long-lived mutant animals. *Cell Death & Differentiation , 20* (12), 1709-1718.
Lant, B., & Storey, K. B. (2010). An Overview of Stress Response and

Hypometabolic Strategies in Caenorhabditis elegans: Conserved and Contrasting Signals with the Mammalian System. *International Journal of Biological Sciences , 6* (1), 9-50.

Lapenna, S., & Giordano, A. (2009). Cell cycle kinases as therapeutic targets for cancer. *Nature Review Drug Discovery , 8* (7), 547-566.

Larsen, P. L. (1993). Aging and resistance to oxidative damage in Caenorhabditis elegans. *Proceedings of the National Academy of Sciences of the United States of America , 90* (19), 8905-8909.

Laat, W. L., Jaspers, N. G., & Hoeijmakers, J. H. (1999). Molecular mechanism of nucleotide excision repair. *Genes & Development , 13* (7), 768-785.

Lee, J.-H., & Paull, T. T. (2005). ATM activation by DNA double-strand breaks through the Mre11-Rad50-Nbs1 complex. *Science (New York, N.Y.) , 308* (5721), 551-554.

Lee, S.-J., Murphy, C. T., & Kenyon, C. (2009). Glucose shortens the life span of C. elegans by downregulating DAF-16/FOXO activity and aquaporin gene expression. *Cell metabolism , 10* (5), 379-391.

Li, G.-M. (2008). Mechanisms and functions of DNA mismatch repair. *Cell Research , 18* (1), 85-98.

Li, J., Liu, Z., Tan, C., Guo, X., Wang, L., Sancar, A., et al. (2010). Dynamics and mechanism of repair of ultraviolet-induced (6-4) photoproduct by photolyase. *Nature , 466* (7308), 887-890.

Lieber, M. R. (2010). The Mechanism of Double-Strand DNA Break Repair by the Nonhomologous DNA End Joining Pathway. *Annual review of biochemistry , 79*, 181-211.

Lindahl, T. (1993). Instability and decay of the primary structure of DNA. *Nature , 362* (6422), 709-715.

Lindahl, T., & Wood, R. D. (1999). Quality control by DNA repair. *Science , 286* (5446), 1897-1905.

Link, C. D., Cypser, J. R., Johnson, C. J., & Johnson, T. E. (1999). Direct observation of stress response in Caenorhabditis elegans using a reporter transgene. *Cell stress & Chaperones , 4* (4), 235-242.

Lithgow, G. J., White, T. M., Melov, S., & Johnson, T. E. (1995). Thermotolerance and extended life-span conferred by single-gene mutations and induced by thermal

stress. *Proceedings of the National Academy of Sciences of the United States of America , 92* (16), 7540-7544.
Lloyd, D. R., Carmichael, P. L., & Phillips, D. H. (1998). Comparison of the formation of 8-hydroxy-2'-deoxyguanosine and single- and double-strand breaks in DNA mediated by fenton reactions. *Chemical Research in Toxicology , 11* (5), 420-427.
López-Otín, C., Blasco, M. A., Partridge, L., Serrano, M., & Kroemer, G. (2013). The Hallmarks of Aging. *Cell , 153* (6), 1194-1217.
López-Otín, C., Blasco, M. A., Partridge, L., Serrano, M., & Kroemer, G. (2013). The Hallmarks of Aging. *Cell , 153* (6), 1194-1127.
Mair, W., & Dillin, A. (2008). Aging and survival: the genetics of life span extension by dietary restriction. *Annual Review of Biochemistry , 77*, 727-754.
Manelyte, L., Urbanke, C., Giron-Monzon, L., & Friedhoff, P. (2006). Structural and functional analysis of the MutS C-terminal tetramerization domain. *Nucleic Acid Research , 34* (18), 5270-5279.
Maréchal, A., & Zou, L. (2013). DNA Damage Sensing by the ATM and ATR Kinases. *Cold Spring Harbor Perspectives in Biology , 5* (9), a012716.
Matsuoka, S., Huang, M., & Elledge, S. J. (1998). Linkage of ATM to cell cycle regulation by the Chk2 protein kinase. *Science (New York, N.Y.) , 282* (5395), 1893-1897.
McCarthy, S., Somayajulu, M., Sikorska, M., Borowy-Borowski, H., & Pandey, S. (2004). Paraquat induces oxidative stress and neuronal cell death; neuroprotection by water-soluble Coenzyme Q10. *Toxicology and Applied Pharmacology , 201* (1), 21-31.
Meyers, M., Hwang, A., Wagner, M. W., Bruening, A. J., Veigl, M. L., Sedwick, W. D., et al. (2003). A role for DNA mismatch repair in sensing and responding to fluoropyrimidine damage. *Oncogene , 22* (47), 7376-7388.
Minois, N. (2000). Longevity and aging: beneficial effects ofexposure to mild stress. *Biogerontology , 1* (1), 15-29.
Morley, J. F., & Morimoto, R. I. (2004). Regulation of Longevity in Caenorhabditis elegans by Heat Shock Factor and Molecular Chaperones. *Molecular Biology of the Cell , 15* (2), 657-664.
Mouchiroud, L., Houtkooper, R. H., Moullan, N., Katsyuba, E., Ryu, D., Cantó, C., et

al. (2013). The NAD(+)/Sirtuin Pathway Modulates Longevity through Activation of Mitochondrial UPR and FOXO Signaling. *Cell , 154* (2), 430-441.
Muñoz, M. J. (2003). Longevity and heat stress regulation in Caenorhabditis elegans. *Mechanisms of Ageing and Development , 124* (1), 43-48.
Murakami, S., & Johnson, T. E. (1996). A Genetic Pathway Conferring Life Extension and Resistance to Uv Stress in Caenorhabditis Elegans. *Genetics , 143* (3), 1207-1218.
Murphy, C. T. (2013, December 26). Insulin/insulin-like growth factor signaling in C. elegans. *WormBook* , 1-43.
Murphy, C. T., McCarroll, S. A., Bargmann, C. I., Fraser, A., Kamath, R. S., Ahringer, J., et al. (2003). Genes that act downstream of DAF-16 to influence the lifespan of Caenorhabditis elegans. *Nature , 424* (6946), 277-283.
Ni, Z., & Lee, S. S. (2010). RNAi screens to identify components of gene networks that modulate aging in Caenorhabditis elegans. *Briefings in Functional Genomics , 9* (1), 53-64.
Nimonkar, A. V., Genschel, J., Kinoshita, E., Polaczek, P., Campbell, J. L., Wyman, C., et al. (2011). BLM–DNA2–RPA–MRN and EXO1–BLM–RPA–MRN constitute two DNA end resection machineries for human DNA break repair. *Genes & Development , 25* (4), 350-362.
Obsil, T., & Obsilova, V. (2011). Structural basis for DNA recognition by FOXO proteins. *Biochimica et Biophysica Acta (BBA) - Molecular Cell Research , 1813* (11), 1946-1953.
Ortega, j., Li, J. Y., Lee, S., Tong, D., Gu, L., & Li, G.-M. (2015). Phosphorylation of PCNA by EGFR inhibits mismatch repair and promotes misincorporation during DNA synthesis. *Proceedings of the National Academy of Sciences of the United States of America , 112* (18), 5667-5672.
Panowski, S. H., & Dillin, A. (2009). Signals of youth: endocrine regulation of aging in Caenorhabditis elegans. *Trends in endocrinology and metabolism: TEM , 20* (6), 259-264.
Paradis, S., & Ruvkun, G. (1998). Caenorhabditis elegans Akt/PKB transduces insulin receptor-like signals from AGE-1 PI3 kinase to the DAF-16 transcription factor. *Genes & Development , 12* (16), 2488-2498.
Petrella, L. N. (2014). Natural Variants of C. elegans Demonstrate Defects in Both

Sperm Function and Oogenesis at Elevated Temperatures. *PLOS ONE , 9* (11), e112377.

Poljsak, B., Šuput, D., & Milisav, I. (2013, April 29). Achieving the Balance between ROS and Antioxidants: When to Use the Synthetic Antioxidants. *Oxidative Medicine and Cellular longevity* , e956792.

Polyak, K., Xia, Y., Zweier, J. L., Kinzler, K. W., & Vogelstein, B. (1997). A model for p53-induced apoptosis. *Nature , 389* (6648), 300-305.

Richter, K., Haslbeck, M., & Buchner, J. (2010). The Heat Shock Response: Life on the Verge of Death. *Molecular Cell , 40* (2), 253-266.

Rilay, P. A. (1994). Free Radicals in Biology: Oxidative Stress and the Effects of Ionizing Radiation. *International Journal of Radiation Biology , 65* (1), 27-33.

Sandor, S., Yvette, T., & Arpad, S. (2012). The legacy of Hans Selye and the origins of stress research: A retrospective 75 years after his landmark brief “Letter” to the Editor # of Nature. *Informa Healthcare USA, Inc. , 15* (5), 472-478.

Schlesinger, M. J. (1990). Heat shock proteins. *Journal of Biological Chemistry , 265* (21), 12111-12114.

Sertic, S., Pizzi, S., Cloney, R., Lehmann, A. R., Marini, F., Plevani, P., et al. (2011). Human exonuclease 1 connects nucleotide excision repair (NER) processing with checkpoint activation in response to UV irradiation. *Proceedings of the National Academy of Sciences of the United States of America , 108* (33), 13647-13652.

Shama, S., Lai, C.-Y., Antoniazzi, J. M., Jiang, J. C., & Jazwinski, S. M. (1998). Heat Stress-Induced Life Span Extension in Yeast. *Experimental Cell Research , 245* (2), 379-388.

Shankaracharya, n., Das, S., & Vidyarthi, A. S. (2011). Homology modeling and function prediction of hABH1, involving in repair of alkylation damaged DNA. *Interdisciplinary Sciences, Computational Life Sciences , 3* (3), 175-181.

Simonetta, S. H., & Golombek, D. A. (2007). An automated tracking system for Caenorhabditis elegans locomotor behavior and circadian studies application. *Journal of Neuroscience Methods , 161* (2), 273-280.

Soulas-Sprauel, P., Rivera-Munoz, P., Malivert, L., Le Guyader, G., Abramowski, V., Revy, P., et al. (2007). V(D)J and immunoglobulin class switch recombinations: a paradigm to study the regulation of DNA end-joining. *Oncogene , 26* (56), 7780-7791.

Stergiou, L., & Hengartner, M. O. (2001). Death and more: DNA damage response pathways in the nematode C. elegans. *Cell Death and Differentiation , 11* (1), 21-28.

Stringham, E. G., Dixon, D. K., Jones, D., & Candido, E. P. (1992). Temporal and spatial expression patterns of the small heat shock (hsp16) genes in transgenic Caenorhabditis elegans. *Molecular Biology of the Cell , 3* (2), 221-233.

Sugasawa, K., Ng, J. M., Masutani, C., Iwai, S., van der Spek, P. J., Eker, A. P., et al. (1998). Xeroderma pigmentosum group C protein complex is the initiator of global genome nucleotide excision repair. *Molecular Cell , 2* (2), 223-232.

Sulston, J. E. (1983). Neuronal cell lineages in the nematode Caenorhabditis elegans. *Cold Spring Harbor Symposia on Quantitative Biology , 48 Pt 2*, 443-452.

Tanner, C. M., Kamal, F., Ross, G. W., Hoppin, J. A., Goldman, S. M., Korell, M., et al. (2011). Rotenone, Paraquat, and Parkinson's Disease. *Environmental Health Perspective , 119* (6), 866-872.

Tater, M., Bartke, A., & Antebi, A. (2003). The endocrine regulation of aging by insulin-like signals. *Science (New York, N.Y.) , 299* (5611), 1346-1351.

Tissenbaum, H. A., & Guarente, L. (2001). Increased dosage of a sir-2 gene extends lifespan in Caenorhabditis elegans. *Nature , 410* (6825), 227-230.

Tullet, J. M., Hertweck, M., Hyung An, J., Baker, J., Hwang, J. Y., Liu, S., et al. (2008). Direct inhibition of the longevity promoting factor SKN-1 by Insulin-like signaling in C. elegans. *Cell , 132* (6), 1025-1038.

van den Boch, M., Bree, R. T., & Lowndes, N. F. (2003). The MRN complex: coordinating and mediating the response to broken chromosomes. *EMBO Reports , 4* (9), 844-849.

Viswanathan, M., Kim, S. K., Berdichevsky, A., & Guarente, L. (2005). A role for SIR-2.1 regulation of ER stress response genes in determining C. elegans life span. *Developmental Cell , 9* (5), 605-615.

You, C., Swanson, A. L., Dai, X., Yuan, B., Wang, J., & Wang, Y. (2013). Translesion synthesis of 8,5'-cyclopurine-2'-deoxynucleosides by DNA polymerases η, ι, and ζ. *The Journal of Biological Chemistry , 288* (40), 28548-28556.

Zevian, S. C., & Yanowitz, J. L. (2014). Methodological considerations for heat shock of the nematode Caenorhabditis elegans. *Methods (San Diego, Calif.) , 68* (3), 450-457.

Zhao, H., & Piwnica-Worms, H. (2001). ATR-mediated checkpoint pathways regulate phosphorylation and activation of human Chk1. *Molecular and Cellular Biology , 21* (12), 4129-4139.

Zhou, B. B., & Elledge, S. J. (2000). The DNA damage response: putting checkpoints in perspective. *Nature , 408* (6811), 433-439.

Zhou, K. I., Pincus, Z., & Slack, F. J. (2011). Longetivity and stress in Caenorhabditis elegans. *Aging (Albany NY) , 3* (8), 733-753.

Zhu, j., Zhou, y., Wang, G.-N., Tai, G., & Ye, X.-S. (2014). Cell cycle arrest, apoptosis and autophagy induced by iminosugars on K562 cells. *European Journal of Pharmacology , 731*, 65-72.

Zou, L., & Elledge, S. J. (2003). Sensing DNA damage through ATRIP recognition of RPA-ssDNA complexes. *Science (New York, N.Y.) , 300* (5625), 1542-1548.

7. Appendix

7.1 Buffer

All the buffers and solutions have been used are autoclaved at 121^{0}C for 15min and stored at room temperature, unless otherwise stated.

3PY buffer
3% yeast extract
3% soy peptone

Bleaching solution
1.5ml bleaching solution for 3.5ml sample:
384µl sodium hypochlorite
500µl 5M NaOH
616µl H2O or M9 buffer

Freezing solution
100mM NaCl
50mM KH2PO4 (PH6.0)
30% glycerol
2,5 mg/ml cholesterol
0.3mM MgSO4

LB agar (pH 7.5)
10g Bacto-tryptone
5g Bacto-yeast
5g NaCl
15g agar
H2O to 1 liter

M9 buffer (1L)
3g KH2PO4
6g Na2HPO4
5g NaCl

1ml 1M $MgSO_4$

NGM (Nematode growth medium):
3 g NaCl
17g agar
2,5g peptone
975 ml H2O
Cover mouth of the flask with aluminum foil. Then, autoclave it for 50 min. Use water bath to cool it gradually to 56˚C. Add 1ml 1M CaCl2, 1ml 5mg/ml cholesterol in ethanol, 1ml 1M MgSO4 and 25ml 1M KPO4 buffer for 1L NGM.

Single worm lysis buffer (Stored at -20 ˚C)
50mM KCl
10mM Tris PH8.3
2.5mM Mgcl2
0.45% NP-40
0.45% Tween 20
+800µg/mL proteinase K

S medium (4L)
23.2 g NaCl
200 ml 1M potassium phosphate, pH 6.0 (136.1 g KH2PO4 per 1000 ml; start with 800 ml and adjust to pH 6.0 with solid KOH (approx. 15g) before bringing up to volume.)
3.8 L dH20
4 ml 5 mg/ml cholesterol in 95% EtOH. Warm to 37°C to dissolve.
Aliquot 400 ml into each of 10 bottles.

7.2 Equipment

ZEISS Stemi SV6

Axio zoom. V16

Zeiss Lumar. V12

Grant water bath

Thermostatschrank incubator

Sanyo incubator

Heraeus incubator

RSbiotech Galaxy S+

Phylum Tech Wmicrotracker-one

Infors ONEMED incubation shaker

Eppendorf Mastercycler ep Gradient S

CellRad X-ray Faxitro DetecMedico

BioRAD Trans UV

Bio RAD powerpac Basic

7.3 Raw data

Egg assay raw data

Strain	Brood size										AV	SD
N2	246	218	236	172	242	228	253	251	230		230,7	23,4
aqp-1	269	244	205	214	183	243	209	208	247		224,7	25,7
sir-2.1	237	223	265	237	249	234	217	211	243		235,1	15,7
atm-1	152	188	204	238	192	212	161	161			188,5	26,0
aqp-1;atm-1	278	231	236	270	196						242,2	29,5
aqp-1;sir-2.1	234	206	226	228	245						227,8	12,7

32°C heat shock-manual scoring trial raw data

Hours	N2	Survival%	aqp-1	Survival%	sir-2.1	Survival%	atm-1	Survival%
1	160	100,0	160	100,0	160	100,0	160	100,0
2	160	100,0	160	100,0	160	100,0	160	100,0
3	160	100,0	160	100,0	160	100,0	160	100,0
4	160	100,0	160	100,0	160	100,0	160	100,0
5	160	100,0	160	100,0	160	100,0	160	100,0
6	160	100,0	160	100,0	160	100,0	160	100,0
7	160	100,0	158	98,8	160	100,0	160	100,0
8	160	100,0	158	98,8	160	100,0	160	100,0
9	160	100,0	154	96,3	158	98,8	156	97,5

34°C heat shock-manual scoring trial raw data

Hours	N2	Survival%	aqp-1	Survival%	sir-2.1	Survival%	atm-1	Survival%
1	160	100,0	160	100,0	160	100,0	160	100,0
2	160	100,0	160	100,0	160	100,0	160	100,0
3	160	100,0	160	100,0	160	100,0	160	100,0
4	160	100,0	130	81,3	160	100,0	158	98,8
5	158	98,8	124	77,5	156	97,5	154	96,3
6	156	97,5	116	72,5	154	96,3	148	92,5
7	150	93,8	112	70,0	152	95,0	142	88,8
8	144	90,0	102	63,8	148	92,5	140	87,5
9	138	86,3	96	60,0	138	86,3	138	86,3

35°C heat shock-manual scoring trial raw data

Hours	N2	Survival%	aqp-1	Survival%	sir-2.1	Survival%	atm-1	Survival%
1	160	100,0	160	100,0	160	100,0	160	100,0
2	160	100,0	160	100,0	160	100,0	160	100,0
3	160	100,0	154	96,3	160	100,0	160	100,0
4	156	97,5	130	81,3	160	100,0	158	98,8
5	150	93,8	116	72,5	156	97,5	148	92,5
6	140	87,5	94	58,8	140	87,5	118	73,8
7	116	72,5	86	53,8	124	77,5	88	55,0
8	98	61,3	56	35,0	104	65,0	62	38,8
9	80	50,0	30	18,8	82	51,3	38	23,8
10	52	32,5	18	11,3	64	40,0	14	8,8
11	32	20,0	4	2,5	46	28,8	0	0,0
12	20	12,5	0	0,0	28	17,5		
13	10	6,3			14	8,8		
14	4	2,5			0	0,0		

Heat shock-WMicrotracker for double mutant raw data

Strain/Time (min)	30	60	90	120	150	180	210	240	270	300	330	360	390
N2	457	480	404	355	220	88	55	47	21	5	9	7	0
Locomotor activities%	100,0	105,0	88,4	77,7	48,1	19,3	12,0	10,3	4,6	1,1	2,0	1,5	0,0
aqp-1	453	393	289	134	21	19	3	0	0	0	0	0	0
Locomotor activities%	100,0	86,8	63,8	29,6	4,6	4,2	0,7	0,0	0,0	0,0	0,0	0,0	0,0
atm-1	268	175	92	38	5	1	0	3	0	0	0	0	0
Locomotor activities%	100,0	65,3	34,3	14,2	1,9	0,4	0,0	1,1	0,0	0,0	0,0	0,0	0,0
sir-2.1	240	180	91	56	11	4	7	3	3	0	0	0	0
Locomotor activities%	100,0	75,0	37,9	23,3	4,6	1,7	2,9	1,3	1,3	0,0	0,0	0,0	0,0
atm-1; aqp-1	456	403	257	97	9	12	2	0	0	0	0	0	0
Locomotor activities%	100,0	88,4	56,4	21,3	2,0	2,6	0,4	0,0	0,0	0,0	0,0	0,0	0,0
sir-2.1; aqp-1	479	384	248	143	42	17	11	2	0	0	0	0	0
Locomotor activities%	100,0	80,2	51,8	29,9	8,8	3,5	2,3	0,4	0,0	0,0	0,0	0,0	0,0

Heat shock-manual scoring for double mutant raw data

Time (hours)	N2	Survival%	aqp-1	Survival%	sir-2.1	Survival%	atm-1	Survival%	aqp-1; sir-2.1	Survival%	aqp-1; atm-1	Survival%
1	44,5	100,0	44	98,9	45	101,1	44,5	100,0	44	98,9	45	101,1
2	44,5	100,0	38	85,4	44,5	100,0	44,5	100,0	38	85,4	36	80,9
3	44,5	100,0	35	78,7	42	94,4	43,5	97,8	33	74,2	31,5	70,8
4	41,5	93,3	26	58,4	37	83,1	41	92,1	27,5	61,8	26	58,4
5	35,5	79,8	17	38,2	23	51,7	31,5	70,8	19,5	43,8	19	42,7
6	24,5	55,1	10	22,5	16	36,0	21	47,2	12,5	28,1	11,5	25,8
7	17	38,2	5,5	12,4	10	22,5	11,5	25,8	9	20,2	6,5	14,6
8	11	24,7	1,5	3,4	6	13,5	6	13,5	4,5	10,1	4	9,0
9	6	13,5	0	0,0	1,5	3,4	3	6,7	2	4,5	1	2,2
10	2,5	5,6		0,0	0,5	1,1	1	2,2	0,5	1,1	0	0,0
11	1	2,2		0,0	0	0,0	0	0,0	0	0,0		0,0
12	0	0,0		0,0		0,0		0,0		0,0		0,0

PQ-manual scoring trial raw data

	0µM			100µM			200µM			300µM			400µM			500µM		
	brood	adults	Survival%	brood	adults	Survival%	brood	adults	Survival%	brood	adults	Survival%	brood	adults	Survival%	brood	adults	Survival%
N2	43	42	97,7	31	12	38,7	22	6	27,3	27	0	0,0	32	0	0,0	34	0	0,0
aqp-1	36	34	94,4	30	10	33,3	19	3	15,8	31	0	0,0	16	0	0,0	31	0	0,0
atm-1	16	15	93,8	20	14	70,0	24	3	12,5	18	0	0,0	19	0	0,0	20	0	0,0
sir2.1	36	35	97,2	33	29	87,9	14	9	64,3	25	0	0,0	10	0	0,0	31	0	0,0

PQ-manual scoring raw data

	0µM			50µM			100µM			150µM			200µM			250µM			300µM		
	brood	L4	Survival%	brood	L4	Survival%	brood	L4	Survival%	brood	L4	Survival%	brood	L4	Survival%	brood	L4	Survival%	brood	L4	Survival%
N2	24	24	100,0	24	24	100,0	24	12	52,2	18	6	27,8	24	0	0,0	27	0	0,0	27	0	0,0
aqp-1	27	27	100,0	33	33	100,0	36	21	54,1	39	21	52,6	15	3	13,3	33	0	0,0	29	0	0,0
atm-1	30	30	93,5	36	21	55,6	36	6	14,3	45	0	2,3	45	0	0,0	24	0	0,0	27	0	0,0
sir-2.1	78	78	100,0	69	57	85,3	60	21	32,8	42	8	18,1	51	3	4,2	51	3	3,8	42	0	0,0
aqp-1; atm-1	45	45	97,8	36	36	97,2	45	18	43,2	48	6	14,3	39	0	0,0	27	0	0,0	48	0	0,0
aqp-1;sir-2.1	57	57	100,0	57	54	94,6	51	39	75,0	51	39	75,0	42	3	9,3	45	0	0,0	48	0	0,0

WMicrotracker buffer trial raw data:

/Time (min)	30	60	90	120	150	180	210	240	270	300	330	360	390	420	450	480	510	540	570	60
worms	30	10	11	42	34	75	80	54	64	42	51	47	36	52	68	46	42	30	14	3
otor activitise %	100,0	33,3	36,7	140,0	113,3	250,0	266,7	180,0	213,3	140,0	170,0	156,7	120,0	173,3	226,7	153,3	140,0	100,0	46,7	126,7
worms	52	22	18	29	28	30	66	70	53	52	80	92	40	23	47	20	14	10	16	5
otor activitise %	100,0	42,3	34,6	55,8	53,8	57,7	126,9	134,6	101,9	100,0	153,8	176,9	76,9	44,2	90,4	38,5	26,9	19,2	30,8	9,4
worms	53	39	42	51	49	64	90	70	83	56	64	76	48	41	44	50	68	66	48	7
otor activitise %	100,0	73,6	79,2	96,2	92,5	120,8	169,8	132,1	156,6	105,7	120,8	143,4	90,6	77,4	83,0	94,3	128,3	124,5	90,6	149,1
20 worms	39	30	25	32	30	36	40	50	30	33	51	44	8	5	2	0	0	0	0	0
otor activitise %	100,0	76,9	64,1	82,1	76,9	92,3	102,6	128,2	76,9	84,6	130,8	112,8	20,5	12,8	5,1	0,0	0,0	0,0	0,0	0,0
worms	64	62	58	90	88	88	86	90	93	104	90	50	74	78	56	74	70	64	66	9
otor activitise %	100,0	96,9	90,6	140,6	137,5	137,5	134,4	140,6	145,3	162,5	140,6	78,1	115,6	121,9	87,5	115,6	109,4	100,0	103,1	143,8
) worms	142	108	84	72	86	98	109	108	106	89	58	56	24	41	40	25	17	8	4	0
otor activitise %	100,0	76,1	59,2	50,7	60,6	69,0	76,8	76,1	74,6	62,7	40,8	39,4	16,9	28,9	28,2	17,6	12,0	5,6	2,8	0,0

PQ-WMicrotracker trial for N2 raw data

Time (min)	30	60	90	120	150	180	210	240	270	300	330	360	390	420	480	510	540	570	600	630	660	690	720	750	780	810	840	870	900	930	960	990	1020	1050	1080	1110	1140	1170	1200	1230	1260	1290	1320	1350	1380	1410	1
el	350	355	352	366	355	369	358	351	329	326	293	303	308	289	293	276	258	236	248	253	274	256	258	257	252	227	255	238	238	274	232	213	246	218	237	223	238	248	237	240	199	198	204	217	211	214	202	2
tor activities%	100,0	101,4	100,6	104,6	101,4	105,4	102,3	100,3	94,0	93,1	83,7	86,6	88,0	82,6	83,7	78,9	73,7	67,4	70,9	72,3	78,3	73,1	73,7	73,4	72,0	64,9	72,9	68,0	68,0	78,3	66,3	60,9	70,3	62,3	67,7	63,7	68,0	70,9	67,7	68,6	56,9	56,6	58,3	62,0	60,3	61,1	57,7	5
el	426	439	461	450	439	442	406	407	388	345	330	316	308	320	277	301	270	261	253	252	269	246	241	284	247	241	225	259	231	222	198	204	202	195	191	173	186	179	191	179	131	180	159	157	152	137	157	1
tor activities%	100,0	103,1	108,2	105,6	103,1	103,8	95,3	95,5	91,1	81,0	77,5	74,2	72,3	75,1	65,0	70,7	63,4	61,3	59,4	59,2	63,1	57,7	56,6	66,7	58,0	56,6	52,8	60,8	54,2	52,1	46,5	47,9	47,4	45,8	44,8	40,6	43,7	42,0	44,8	42,0	30,8	42,3	37,3	36,9	35,7	32,2	36,9	3
1M	387	401	380	364	352	323	312	295	311	295	259	264	240	251	213	213	207	218	218	216	177	169	200	182	153	142	173	167	156	142	121	132	139	139	92	112	122	141	102	83	93	93	116	97	111	110	77	
tor activities%	100,0	103,6	98,2	94,1	91,0	83,5	80,6	76,2	80,4	76,2	66,9	68,2	62,0	64,9	55,0	55,0	53,5	56,3	56,3	55,8	45,7	43,7	51,7	47,0	39,5	36,7	44,7	43,2	40,3	36,7	31,3	34,1	35,9	35,9	23,8	28,9	31,5	36,4	26,4	21,4	24,0	24,0	30,0	25,1	28,7	28,4	19,9	2
1M	377	393	386	374	372	354	339	309	286	262	243	230	239	209	238	206	230	171	190	190	172	176	166	136	121	130	112	112	116	110	130	85	109	99	86	70	79	91	78	96	105	74	76	56	92	64	61	
tor activities%	100,0	104,2	102,4	99,2	98,7	93,9	89,9	82,0	75,9	69,5	64,5	61,0	63,4	55,4	63,1	54,6	61,0	45,4	50,4	50,4	45,6	46,7	44,0	36,1	32,1	34,5	29,7	29,7	30,8	29,2	34,5	22,5	28,9	26,3	22,8	18,6	21,0	24,1	20,7	25,5	27,9	19,6	20,2	14,9	24,4	17,0	16,2	1
1M	372	407	407	388	409	356	348	312	290	279	224	209	216	214	175	172	169	164	144	130	112	96	98	111	92	86	91	83	98	78	67	45	43	50	37	41	33	44	28	38	27	33	22	16	13	14	14	
tor activities%	100,0	109,4	109,4	104,3	109,9	95,7	93,5	83,9	78,0	75,0	60,2	56,2	58,1	57,5	47,0	46,2	45,4	44,1	38,7	34,9	30,1	25,8	26,3	29,8	24,7	23,1	24,5	22,3	26,3	21,0	18,0	12,1	11,6	13,4	9,9	11,0	8,9	11,8	7,5	10,2	7,3	8,9	5,9	4,3	3,5	3,8	3,8	
Time (min)	1470	1500	1530	1560	1590	1620	1650	1680	1710	1740	1770	1800	1830	1860	1890	1920	1950	1980	2010	2040	2070	2100	2130	2160	2190	2220	2250	2280	2310	2340	2370	2400	2430	2460	2490	2520	2550	2580	2610	2640	2670	2700	2730	2760	2790	2820	2850	2
el	229	170	176	169	177	166	187	172	157	172	170	195	152	142	139	117	126	117	117	121	125	118	97	91	102	94	76	79	81	80	79	69	75	65	62	71	78	63	92	82	73	93	103	62	66	59	80	
tor activities%	65,4	48,6	50,3	48,3	50,6	47,4	53,4	49,1	44,9	49,1	48,6	55,7	43,4	40,6	39,7	33,4	36,0	33,4	33,4	34,6	35,7	33,7	27,7	26,0	29,1	26,9	21,7	22,6	23,1	22,9	22,6	19,7	21,4	18,6	17,7	20,3	22,3	18,0	26,3	23,4	20,9	26,6	29,4	17,7	18,9	16,9	22,9	2
el	128	121	118	124	86	79	87	71	79	80	66	89	69	83	95	92	82	83	62	77	57	65	36	35	33	58	53	61	42	51	52	30	46	32	45	29	51	45	30	38	30	26	47	43	34	28	33	
tor activities%	30,0	28,4	27,7	29,1	20,2	18,5	20,4	16,7	18,5	18,8	15,5	20,9	16,2	19,5	22,3	21,6	19,2	19,5	14,6	18,1	13,4	15,3	8,5	8,2	7,7	13,6	12,4	14,3	9,9	12,0	12,2	7,0	10,8	7,5	10,6	6,8	12,0	10,6	7,0	8,9	7,0	6,1	11,0	10,1	8,0	6,6	7,7	
1M	108	79	74	74	63	79	82	62	53	76	68	68	49	48	52	63	59	40	54	57	48	51	57	53	32	41	37	38	35	30	43	39	33	33	25	31	35	29	26	26	22	21	10	17	18	15	13	
tor activities%	27,9	20,4	19,1	19,1	16,3	20,4	21,2	16,0	13,7	19,6	17,6	17,6	12,7	12,4	13,4	16,3	15,2	10,3	14,0	14,7	12,4	13,2	14,7	13,7	8,3	10,6	9,6	9,8	9,0	7,8	11,1	10,1	8,5	8,5	6,5	8,0	9,0	7,5	6,7	6,7	5,7	5,4	2,6	4,4	4,7	3,9	3,4	
1M	35	43	55	40	33	36	32	41	22	21	37	17	31	32	38	37	36	38	16	18	27	35	19	15	10	9	8	6	7	3	9	7	5	5	12	10	16	20	12	9	9	3	3	1	3	3	7	
tor activities%	9,3	11,4	14,6	10,6	8,8	9,5	8,5	10,9	5,8	5,6	9,8	4,5	8,2	8,5	10,1	9,8	9,5	10,1	4,2	4,8	7,2	9,3	5,0	4,0	2,7	2,4	2,1	1,6	1,9	0,8	2,4	1,9	1,3	1,3	3,2	2,7	4,2	5,3	3,2	2,4	2,4	0,8	0,8	0,3	0,8	0,8	1,9	
1M	4	10	6	3	6	5	6	7	8	3	3	3	1	3	4	0	0	0	1	2	3	4	9	1	3	0	0	5	1	0	0	0	0	0	1	2	1	0	0	1	0	0	2	0	1	1	1	
tor activities%	1,1	2,7	1,6	0,8	1,6	1,3	1,6	1,9	2,2	0,8	0,8	0,8	0,3	0,8	1,1	0,0	0,0	0,0	0,3	0,5	0,8	1,1	2,4	0,3	0,8	0,0	0,0	1,3	0,3	0,0	0,0	0,0	0,0	0,0	0,3	0,5	0,3	0,0	0,0	0,3	0,0	0,0	0,5	0,0	0,3	0,3	0,3	

PQ-WMicrotracker control group for double mutant: (0mM, 5mM, 10mM, and 20mM) raw data

Group/Time (min)	30	60	90	120	150	180	210	240	270	300	330	360	390	420	450	480	510	540	570	600	630	660	690	720	750	780	810	840	870	900	930	960	990	1020	1050	1080	1110	1140	1170	1200	1230	1260	1290	1320	1350	1380	1410	1440
N2 0mM	350	355	352	366	355	369	358	351	329	326	293	303	308	289	293	276	258	236	248	253	274	256	258	257	252	227	255	238	238	274	232	213	246	218	237	223	238	248	237	240	199	198	204	217	211	214	202	206
Locomotor activities%	100,0	101,4	100,6	104,6	101,4	105,4	102,3	100,3	94,0	93,1	83,7	86,6	88,0	82,6	83,7	78,9	73,7	67,4	70,9	72,3	78,3	73,1	73,7	73,4	72,0	64,9	72,9	68,0	68,0	78,3	66,3	60,9	70,3	62,3	67,7	63,7	68,0	70,9	67,7	68,6	56,9	56,6	58,3	62,0	60,3	61,1	57,7	58,9
Group/Time (min)	1470	1500	1530	1560	1590	1620	1650	1680	1710	1740	1770	1800	1830	1860	1890	1920	1950	1980	2010	2040	2070	2100	2130	2160	2190	2220	2250	2280	2310	2340	2370	2400	2430	2460	2490	2520	2550	2580	2610	2640	2670	2700	2730	2760	2790	2820	2850	2880
N2 0mM	229	170	176	169	177	166	187	172	157	172	170	195	152	142	139	117	126	117	117	121	125	118	97	91	102	94	76	79	81	80	79	69	75	65	62	71	78	63	92	82	73	93	103	62	66	59	80	81
Locomotor activities%	65,4	48,6	50,3	48,3	50,6	47,4	53,4	49,1	44,9	49,1	48,6	55,7	43,4	40,6	39,7	33,4	36,0	33,4	33,4	34,6	35,7	33,7	27,7	26,0	29,1	26,9	21,7	22,6	23,1	22,9	22,6	19,7	21,4	18,6	17,7	20,3	22,3	18,0	26,3	23,4	20,9	26,6	29,4	17,7	18,9	16,9	22,9	23,1
Group/Time (min)	30	60	90	120	150	180	210	240	270	300	330	360	390	420	450	480	510	540	570	600	630	660	690	720	750	780	810	840	870	900	930	960	990	1020	1050	1080	1110	1140	1170	1200	1230	1260	1290	1320	1350	1380	1410	1440
aqp-1 0mM	413	385	373	335	308	259	257	365	412	466	461	476	488	455	414	432	415	406	403	390	357	387	374	399	366	347	379	339	355	356	372	342	351	354	348	353	358	331	323	371	346	343	344	354	373	356	354	331
Locomotor activities%	100,0	93,2	90,3	81,1	74,6	62,7	62,2	88,4	99,8	112,8	111,6	115,3	118,2	110,2	100,2	104,6	100,5	98,3	97,6	94,4	86,4	93,7	90,6	96,6	88,6	84,0	91,8	82,1	86,0	86,2	90,1	82,8	85,0	85,7	84,3	85,5	86,7	80,1	78,2	89,8	83,8	83,1	83,3	85,7	90,3	86,2	85,7	80,1
Group/Time (min)	1470	1500	1530	1560	1590	1620	1650	1680	1710	1740	1770	1800	1830	1860	1890	1920	1950	1980	2010	2040	2070	2100	2130	2160	2190	2220	2250	2280	2310	2340	2370	2400	2430	2460	2490	2520	2550	2580	2610	2640	2670	2700	2730	2760	2790	2820	2850	2880
aqp-1 0mM	333	338	342	334	329	348	370	356	342	360	368	335	341	374	308	335	309	340	316	321	319	285	289	295	267	282	263	283	257	239	265	270	265	240	203	220	234	226	231	225	233	215	215	196	220	217	222	199
Locomotor activities%	80,6	81,8	82,8	80,9	79,7	84,3	89,6	86,2	82,8	87,2	89,1	81,1	82,6	90,6	74,6	81,1	74,8	82,3	76,5	77,7	77,2	69,0	70,0	71,4	64,6	68,3	63,7	68,5	62,2	57,9	64,2	65,4	64,2	58,1	49,2	53,3	56,7	54,7	55,9	54,5	56,4	52,1	52,1	47,5	53,3	52,5	53,8	48,2
Group/Time (min)	30	60	90	120	150	180	210	240	270	300	330	360	390	420	450	480	510	540	570	600	630	660	690	720	750	780	810	840	870	900	930	960	990	1020	1050	1080	1110	1140	1170	1200	1230	1260	1290	1320	1350	1380	1410	1440
atm-1 0mM	137	99	105	94	76	74	53	37	51	63	20	47	44	43	40	69	62	43	49	63	62	58	54	55	38	80	66	103	46	91	89	64	85	81	28	63	62	93	57	68	88	80	78	79	72	72	65	67
Locomotor activities%	100,0	72,3	76,6	68,6	55,5	54,0	38,7	27,0	37,2	46,0	14,6	34,3	32,1	31,4	29,2	50,4	45,3	31,4	35,8	46,0	45,3	42,3	39,4	40,1	27,7	58,4	48,2	75,2	33,6	66,4	65,0	46,7	62,0	59,1	20,4	46,0	45,3	67,9	41,6	49,6	64,2	58,4	56,9	57,7	52,6	52,6	47,4	48,9
Group/Time (min)	1470	1500	1530	1560	1590	1620	1650	1680	1710	1740	1770	1800	1830	1860	1890	1920	1950	1980	2010	2040	2070	2100	2130	2160	2190	2220	2250	2280	2310	2340	2370	2400	2430	2460	2490	2520	2550	2580	2610	2640	2670	2700	2730	2760	2790	2820	2850	2880
atm-1 0mM	84	83	78	81	119	59	92	95	67	63	86	85	93	80	97	101	59	62	77	67	64	108	91	52	47	84	78	73	79	94	110	85	78	68	87	93	66	71	61	80	95	82	92	75	78	87	78	88
Locomotor activities%	61,3	60,6	56,9	59,1	86,9	43,1	67,2	69,3	48,9	46,0	62,8	62,0	67,9	58,4	70,8	73,7	43,1	45,3	56,2	48,9	46,7	78,8	66,4	38,0	34,3	61,3	56,9	53,3	57,7	68,6	80,3	62,0	56,9	49,6	63,5	67,9	48,2	51,8	44,5	58,4	69,3	59,9	67,2	54,7	56,9	63,5	56,9	64,2
Group/Time (min)	30	60	90	120	150	180	210	240	270	300	330	360	390	420	450	480	510	540	570	600	630	660	690	720	750	780	810	840	870	900	930	960	990	1020	1050	1080	1110	1140	1170	1200	1230	1260	1290	1320	1350	1380	1410	1440
sir-2.1 0mM	171	166	156	205	228	239	246	236	228	191	197	185	176	142	132	141	159	120	123	141	126	115	133	151	123	136	131	135	159	119	142	122	116	131	109	128	114	155	122	117	101	89	80	73	133	91	95	114
Locomotor activities%	100,0	97,1	91,2	119,9	133,3	139,8	143,9	138,0	133,3	111,7	115,2	108,2	102,9	83,0	77,2	82,5	93,0	70,2	71,9	82,5	73,7	67,3	77,8	88,3	71,9	79,5	76,6	78,9	93,0	69,6	83,0	71,3	67,8	76,6	63,7	74,9	66,7	90,6	71,3	68,4	59,1	52,0	46,8	42,7	77,8	53,2	55,6	66,7
Group/Time (min)	1470	1500	1530	1560	1590	1620	1650	1680	1710	1740	1770	1800	1830	1860	1890	1920	1950	1980	2010	2040	2070	2100	2130	2160	2190	2220	2250	2280	2310	2340	2370	2400	2430	2460	2490	2520	2550	2580	2610	2640	2670	2700	2730	2760	2790	2820	2850	2880
sir-2.1 0mM	118	84	97	67	77	83	79	79	88	110	99	87	119	105	125	118	139	128	103	125	146	167	108	131	128	133	144	122	139	145	152	141	131	115	127	148	137	93	146	108	103	127	87	113	129	109	159	141
Locomotor activities%	69,0	49,1	56,7	39,2	45,0	48,5	46,2	46,2	51,5	64,3	57,9	50,9	69,6	61,4	73,1	69,0	81,3	74,9	60,2	73,1	85,4	97,7	63,2	76,6	74,9	77,8	84,2	71,3	81,3	84,8	88,9	82,5	76,6	67,3	74,3	86,5	80,1	54,4	85,4	63,2	60,2	74,3	50,9	66,1	75,4	63,7	93,0	82,5
Group/Time (min)	30	60	90	120	150	180	210	240	270	300	330	360	390	420	450	480	510	540	570	600	630	660	690	720	750	780	810	840	870	900	930	960	990	1020	1050	1080	1110	1140	1170	1200	1230	1260	1290	1320	1350	1380	1410	1440
aqp-1; atm-1 0mM	418	385	353	307	267	246	216	261	383	462	457	478	504	489	464	472	449	402	396	372	369	357	322	286	325	327	334	302	306	306	308	297	309	297	281	293	312	294	261	286	281	292	267	264	265	243	236	228
Locomotor activities%	100,0	92,1	84,4	73,4	63,9	58,9	51,7	62,4	91,6	110,5	109,3	114,4	120,6	117,0	111,0	112,9	107,4	96,2	94,7	89,0	88,3	85,4	77,0	68,4	77,8	78,2	79,9	72,2	73,2	73,2	73,7	71,1	73,9	71,1	67,2	70,1	74,6	70,3	62,4	68,4	67,2	69,9	63,9	63,2	63,4	58,1	56,5	54,5
Group/Time (min)	1470	1500	1530	1560	1590	1620	1650	1680	1710	1740	1770	1800	1830	1860	1890	1920	1950	1980	2010	2040	2070	2100	2130	2160	2190	2220	2250	2280	2310	2340	2370	2400	2430	2460	2490	2520	2550	2580	2610	2640	2670	2700	2730	2760	2790	2820	2850	2880
aqp-1; atm-1 0mM	219	222	207	157	197	219	191	180	197	208	219	176	140	185	207	177	167	179	210	217	224	207	189	149	197	188	174	173	188	195	195	230	187	171	188	158	176	151	127	125	128	160	133	131	112	121	90	92
Locomotor activities%	52,4	53,1	49,5	37,6	47,1	52,4	45,7	43,1	47,1	49,8	52,4	42,1	33,5	44,3	49,5	42,3	40,0	42,8	50,2	51,9	53,6	49,5	45,2	35,6	47,1	45,0	41,6	41,4	45,0	46,7	46,7	55,0	44,7	40,9	45,0	37,8	42,1	36,1	30,4	29,9	30,6	38,3	31,8	31,3	26,8	28,9	21,5	22,0
Group/Time (min)	30	60	90	120	150	180	210	240	270	300	330	360	390	420	450	480	510	540	570	600	630	660	690	720	750	780	810	840	870	900	930	960	990	1020	1050	1080	1110	1140	1170	1200	1230	1260	1290	1320	1350	1380	1410	1440
aqp-1; sir-2.1 0mM	226	219	206	210	199	213	169	162	169	151	140	141	137	110	150	132	114	157	130	129	140	142	110	121	104	97	113	121	96	128	97	113	131	127	95	88	94	105	104	83	120	93	107	109	105	117	130	143
Locomotor activities%	100,0	96,9	91,2	92,9	88,1	94,2	74,8	71,7	74,8	66,8	61,9	62,4	60,6	48,7	66,4	58,4	50,4	69,5	57,5	57,1	61,9	62,8	48,7	53,5	46,0	42,9	50,0	53,5	42,5	56,6	42,9	50,0	58,0	56,2	42,0	38,9	41,6	46,5	46,0	36,7	53,1	41,2	47,3	48,2	46,5	51,8	57,5	63,3
Group/Time (min)	1470	1500	1530	1560	1590	1620	1650	1680	1710	1740	1770	1800	1830	1860	1890	1920	1950	1980	2010	2040	2070	2100	2130	2160	2190	2220	2250	2280	2310	2340	2370	2400	2430	2460	2490	2520	2550	2580	2610	2640	2670	2700	2730	2760	2790	2820	2850	2880
aqp-1; sir-2.1 0mM	126	126	111	115	104	99	114	121	107	92	120	83	79	94	82	70	79	115	72	76	50	60	88	90	96	72	87	80	72	84	92	65	91	95	73	50	60	57	65	57	61	57	49	62	56	60	30	35
Locomotor activities%	55,8	55,8	49,1	50,9	46,0	43,8	50,4	53,5	47,3	40,7	53,1	36,7	35,0	41,6	36,3	31,0	35,0	50,9	31,9	33,6	22,1	26,5	38,9	39,8	42,5	31,9	38,5	35,4	31,9	37,2	40,7	28,8	40,3	42,0	32,3	22,1	26,5	25,2	28,8	25,2	27,0	25,2	21,7	27,4	24,8	26,5	13,3	15,5
Group/Time (min)	30	60	90	120	150	180	210	240	270	300	330	360	390	420	450	480	510	540	570	600	630	660	690	720	750	780	810	840	870	900	930	960	990	1020	1050	1080	1110	1140	1170	1200	1230	1260	1290	1320	1350	1380	1410	1440
N2 5mM	426	439	461	450	439	442	406	407	388	345	330	316	308	320	277	301	270	261	253	252	269	246	241	284	247	241	225	259	231	222	198	204	202	195	191	173	186	179	191	179	131	180	159	157	152	137	157	140
Locomotor activities%	100,0	103,1	108,2	105,6	103,1	103,8	95,3	95,5	91,1	81,0	77,5	74,2	72,3	75,1	65,0	70,7	63,4	61,3	59,4	59,2	63,1	57,7	56,6	66,7	58,0	56,6	52,8	60,8	54,2	52,1	46,5	47,9	47,4	45,8	44,8	40,6	43,7	42,0	44,8	42,0	30,8	42,3	37,3	36,9	35,7	32,2	36,9	32,9
Group/Time (min)	1470	1500	1530	1560	1590	1620	1650	1680	1710	1740	1770	1800	1830	1860	1890	1920	1950	1980	2010	2040	2070	2100	2130	2160	2190	2220	2250	2280	2310	2340	2370	2400	2430	2460	2490	2520	2550	2580	2610	2640	2670	2700	2730	2760	2790	2820	2850	2880
N2 5mM	128	121	118	124	86	79	87	71	79	80	66	89	69	83	95	92	82	83	62	77	57	65	36	35	33	58	53	61	42	51	52	30	46	32	45	29	51	45	30	38	30	26	47	43	34	28	33	15
Locomotor activities%	30,0	28,4	27,7	29,1	20,2	18,5	20,4	16,7	18,5	18,8	15,5	20,9	16,2	19,5	22,3	21,6	19,2	19,5	14,6	18,1	13,4	15,3	8,5	8,2	7,7	13,6	12,4	14,3	9,9	12,0	12,2	7,0	10,8	7,5	10,6	6,8	12,0	10,6	7,0	8,9	7,0	6,1	11,0	10,1	8,0	6,6	7,7	3,5
Group/Time (min)	30	60	90	120	150	180	210	240	270	300	330	360	390	420	450	480	510	540	570	600	630	660	690	720	750	780	810	840	870	900	930	960	990	1020	1050	1080	1110	1140	1170	1200	1230	1260	1290	1320	1350	1380	1410	1440
aqp-1 5mM	412	417	387	365	287	260	228	306	391	439	409	420	434	421	418	426	401	412	400	392	383	379	357	355	333	315	317	314	268	228	260	255	255	219	172	191	172	194	168	147	118	123	107	87	93	80	109	107
Locomotor activities%	100,0	101,2	93,9	88,6	69,7	63,1	55,3	74,3	94,9	106,6	99,3	101,9	105,3	102,2	101,5	103,4	97,3	100,0	97,1	95,1	93,0	92,0	86,7	86,2	80,8	76,5	76,9	76,2	65,0	55,3	63,1	61,9	61,9	53,2	41,7	46,4	41,7	47,1	40,8	35,7	28,6	29,9	26,0	21,1	22,6	19,4	26,5	26,0
Group/Time (min)	1470	1500	1530	1560	1590	1620	1650	1680	1710	1740	1770	1800	1830	1860	1890	1920	1950	1980	2010	2040	2070	2100	2130	2160	2190	2220	2250	2280	2310	2340	2370	2400	2430	2460	2490	2520	2550	2580	2610	2640	2670	2700	2730	2760	2790	2820	2850	2880
aqp-1 5mM	80	45	51	47	44	56	41	49	47	47	53	50	49	45	56	32	25	22	37	40	35	50	36	20	23	16	16	23	15	14	13	12	17	22	8	16	8	9	12	6	5	9	5	5	3	7	7	4
Locomotor activities%	19,4	10,9	12,4	11,4	10,7	13,6	10,0	11,9	11,4	11,4	12,9	12,1	11,9	10,9	13,6	7,8	6,1	5,3	9,0	9,7	8,5	12,1	8,7	4,9	5,6	3,9	3,9	5,6	3,6	3,4	3,2	2,9	4,1	5,3	1,9	3,9	1,9	2,2	2,9	1,5	1,2	2,2	1,2	1,2	0,7	1,7	1,7	1,0
Group/Time (min)	30	60	90	120	150	180	210	240	270	300	330	360	390	420	450	480	510	540	570	600	630	660	690	720	750	780	810	840	870	900	930	960	990	1020	1050	1080	1110	1140	1170	1200	1230	1260	1290	1320	1350	1380	1410	1440
atm-1 5mM	143	159	143	142	103	84	40	60	35	20	46	29	33	63	79	77	83	91	75	84	119	101	92	87	89	101	100	123	100	120	106	101	79	112	92	75	80	58	81	79	56	29	53	58	85	108	92	80
Locomotor activities%	100,0	111,2	100,0	99,3	72,0	58,7	28,0	42,0	24,5	14,0	32,2	20,3	23,1	44,1	55,2	53,8	58,0	63,6	52,4	58,7	83,2	70,6	64,3	60,8	62,2	70,6	69,9	86,0	69,9	83,9	74,1	70,6	55,2	78,3	64,3	52,4	55,9	40,6	56,6	55,2	39,2	20,3	37,1	40,6	59,4	75,5	64,3	55,9
Group/Time (min)	1470	1500	1530	1560	1590	1620	1650	1680	1710	1740	1770	1800	1830	1860	1890	1920	1950	1980	2010	2040	2070	2100	2130	2160	2190	2220	2250	2280	2310	2340	2370	2400	2430	2460	2490	2520	2550	2580	2610	2640	2670	2700	2730	2760	2790	2820	2850	2880
atm-1 5mM	63	77	72	37	52	62	60	71	43	79	57	55	44	40	32	50	55	58	51	56	54	38	41	33	29	21	35	31	30	21	35	28	20	21	29	15	6	16	21	12	18	31	21	19	12	7	6	8
Locomotor activities%	44,1	53,8	50,3	25,9	36,4	43,4	42,0	49,7	30,1	55,2	39,9	38,5	30,8	28,0	22,4	35,0	38,5	40,6	35,7	39,2	37,8	26,6	28,7	23,1	20,3	14,7	24,5	21,7	21,0	14,7	24,5	19,6	14,0	14,7	20,3	10,5	4,2	11,2	14,7	8,4	12,6	21,7	14,7	13,3	8,4	4,9	4,2	5,6
Group/Time (min)	30	60	90	120	150	180	210	240	270	300	330	360	390	420	450	480	510	540	570	600	630	660	690	720	750	780	810	840	870	900	930	960	990	1020	1050	1080	1110	1140	1170	1200	1230	1260	1290	1320	1350	1380	1410	1440
sir-2.1 5mM	175	234	245	273	259	256	240	241	267	264	224	207	208	170	177	206	196	171	181	181	161	163	180	169	145	121	174	135	133	130	111	114	114	116	127	113	105	98	95	97	76	87	70	88	84	66	55	81
Locomotor activities%	100,0	133,7	140,0	156,0	148,0	146,3	137,1	137,7	152,6	150,9	128,0	118,3	118,9	97,1	101,1	117,7	112,0	97,7	103,4	103,4	92,0	93,1	102,9	96,6	82,9	69,1	99,4	77,1	76,0	74,3	63,4	65,1	65,1	66,3	72,6	64,6	60,0	56,0	54,3	55,4	43,4	49,7	40,0	50,3	48,0	37,7	31,4	46,3
Group/Time (min)	1470	1500	1530	1560	1590	1620	1650	1680	1710	1740	1770	1800	1830	1860	1890	1920	1950	1980	2010	2040	2070	2100	2130	2160	2190	2220	2250	2280	2310	2340	2370	2400	2430	2460	2490	2520	2550	2580	2610	2640	2670	2700	2730	2760	2790	2820	2850	2880
sir-2.1 5mM	80	76	51	52	49	60	38	36	41	47	31	27	28	30	25	27	23	30	23	27	25	31	19	24	16	30	29	23	24	30	23	32	31	22	20	22	23	26	32	18	31	23	7	18	5	12	26	22
Locomotor activities%	45,7	43,4	29,1	29,7	28,0	34,3	21,7	20,6	23,4	26,9	17,7	15,4	16,0	17,1	14,3	15,4	13,1	17,1	13,1	15,4	14,3	17,7	10,9	13,7	9,1	17,1	16,6	13,1	13,7	17,1	13,1	18,3	17,7	12,6	11,4	12,6	13,1	14,9	18,3	10,3	17,7	13,1	4,0	10,3	2,9	6,9	14,9	12,6
Group/Time (min)	30	60	90	120	150	180	210	240	270	300	330	360	390	420	450	480	510	540	570	600	630	660	690	720	750	780	810	840	870	900	930	960	990	1020	1050	1080	1110	1140	1170	1200	1230	1260	1290	1320	1350	1380	1410	1440
aqp-1;atm-1 5mM	447	442	408	395	353	295	284	379	442	524	500	556	534	526	524	498	484	473	455	458	431	433	420	423	426	409	429	404	405	444	396	406	419	417	425	416	392	426	388	377	326	362	351	294	360	333	333	310
Locomotor activities%	100,0	98,9	91,3	88,4	79,0	66,0	63,5	84,8	98,9	117,2	111,9	124,4	119,5	117,7	117,2	111,4	108,3	105,8	101,8	102,5	96,4	96,9	94,0	94,6	95,3	91,5	96,0	90,4	90,6	99,3	88,6	90,8	93,7	93,3	95,1	93,1	87,7	95,3	86,8	84,3	72,9	81,0	78,5	65,8	80,5	74,5	74,5	69,4
Group/Time (min)	1470	1500	1530	1560	1590	1620	1650	1680	1710	1740	1770	1800	1830	1860	1890	1920	1950	1980	2010	2040	2070	2100	2130	2160	2190	2220	2250	2280	2310	2340	2370	2400	2430	2460	2490	2520	2550	2580	2610	2640	2670	2700	2730	2760	2790	2820	2850	2880
aqp-1;atm-1 5mM	271	277	300	256	252	267	238	209	230	214	204	210	186	178	181	175	165	154	170	174	154	130	138	104	117	116	160	129	117	103	100	76	65	80	73	64	73	71	77	74	87	53	59	46	61	53	60	67
Locomotor activities%	60,6	62,0	67,1	57,3	56,4	59,7	53,2	46,8	51,5	47,9	45,6	47,0	41,6	39,8	40,5	39,1	36,9	34,5	38,0	38,9	34,5	29,1	30,9	23,3	26,2	26,0	35,8	28,9	26,2	23,0	22,4	17,0	14,5	17,9	16,3	14,3	16,3	15,9	17,2	16,6	19,5	11,9	13,2	10,3	13,6	11,9	13,4	15,0
Group/Time (min)	30	60	90	120	150	180	210	240	270	300	330	360	390	420	450	480	510	540	570	600	630	660	690	720	750	780	810	840	870	900	930	960	990	1020	1050	1080	1110	1140	1170	1200	1230	1260	1290	1320	1350	1380	1410	1440
aqp-1; sir-2.1 5mM	248	259	251	269	263	262	241	235	222	197	173	164	154	162	150	185	185	189	179	187	208	176	157	191	170	164	171	156	191	188	158	132	140	153	136	116	108	126	160	148	112	100	120	113	133	96	114	103
Locomotor activities%	100,0	104,4	101,2	108,5	106,0	105,6	97,2	94,8	89,5	79,4	69,8	66,1	62,1	65,3	60,5	74,6	74,6	76,2	72,2	75,4	83,9	71,0	63,3	77,0	68,5	66,1	69,0	62,9	77,0	75,8	63,7	53,2	56,5	61,7	54,8	46,8	43,5	50,8	64,5	59,7	45,2	40,3	48,4	45,6	53,6	38,7	46,0	41,5
Group/Time (min)	1470	1500	1530	1560	1590	1620	1650	1680	1710	1740	1770	1800	1830	1860	1890	1920	1950	1980	2010	2040	2070	2100	2130	2160	2190	2220	2250	2280	2310	2340	2370	2400	2430	2460	2490	2520	2550	2580	2610	2640	2670	2700	2730	2760	2790	2820	2850	2880
aqp-1; sir-2.1 5mM	99	90	85	85	96	46	52	50	54	42	70	72	40	54	49	48	33	50	39	44	35	37	33	36	34	39	40	26	25	36	37	22	28	35	33	35	37	29	25	42	50	28	35	39	40	32	30	33
Locomotor activities%	39,9	36,3	34,3	34,3	38,7	18,5	21,0	20,2	21,8	16,9	28,2	29,0	16,1	21,8	19,8	19,4	13,3	20,2	15,7	17,7	14,1	14,9	13,3	14,5	13,7	15,7	16,1	10,5	10,1	14,5	14,9	8,9	11,3	14,1	13,3	14,1	14,9	11,7	10,1	16,9	20,2	11,3	14,1	15,7	16,1	12,9	12,1	13,3
Group/Time (min)	30	60	90	120	150	180	210	240	270	300	330	360	390	420	450	480	510	540	570	600	630	660	690	720	750	780	810	840	870	900	930	960	990	1020	1050	1080	1110	1140	1170	1200	1230	1260	1290	1320	1350	1380	1410	1440
N2 10mM	387	401	380	364	352	323	312	295	311	295	259	264	240	251	213	213	207	218	218	216	177	169	200	182	153	142	173	167	156	142	121	132	139	139	92	112	122	141	102	83	93	93	116	97	111	110	77	80
Locomotor activities%	100,0	103,6	98,2	94,1	91,0	83,5	80,6	76,2	80,4	76,2	66,9	68,2	62,0	64,9	55,0	55,0	53,5	56,3	56,3	55,8	45,7	43,7	51,7	47,0	39,5	36,7	44,7	43,2	40,3	36,7	31,3	34,1	35,9	35,9	23,8	28,9	31,5	36,4	26,4	21,4	24,0	24,0	30,0	25,1	28,7	28,4	19,9	20,7
Group/Time (min)	1470	1500	1530	1560	1590	1620	1650	1680	1710	1740	1770	1800	1830	1860	1890	1920	1950	1980	2010	2040	2070	2100	2130	2160	2190	2220	2250	2280	2310	2340	2370	2400	2430	2460	2490	2520	2550	2580	2610	2640	2670	2700	2730	2760	2790	2820	2850	2880
N2 10mM	108	79	74	74	63	79	82	62	53	76	68	68	49	48	52	63	59	40	54	57	48	51	57	53	32	41	37	38	35	30	43	39	33	33	25	31	35	29	26	26	22	21	10	17	18	15	13	11
Locomotor activities%	27,9	20,4	19,1	19,1	16,3	20,4	21,2	16,0	13,7	19,6	17,6	17,6	12,7	12,4	13,4	16,3	15,2	10,3	14,0	14,7	12,4	13,2	14,7	13,7	8,3	10,6	9,6	9,8	9,0	7,8	11,1	10,1	8,5	8,5	6,5	8,0	9,0	7,5	6,7	6,7	5,7	5,4	2,6	4,4	4,7	3,9	3,4	2,8
Group/Time (min)	30	60	90	120	150	180	210	240	270	300	330	360	390	420	450	480	510	540	570	600	630	660	690	720	750	780	810	840	870	900	930	960	990	1020	1050	1080	1110	1140	1170	1200	1230	1260	1290	1320	1350	1380	1410	1440
aqp-1 10mM	477	447	416	331	239	223	276	328	423	447	420	426	413	413	421	395	370	354	315	308	278	240	227	211	210	179	175	148	133	112	142	99	80	74	69	37	32	41	33	7	11	21	18	7	8	9	17	7
Locomotor activities%	100,0	93,7	87,2	69,4	50,1	46,8	57,9	68,8	88,7	93,7	88,1	89,3	86,6	86,6	88,3	82,8	77,6	74,2	66,0	64,6	58,3	50,3	47,6	44,2	44,0	37,5	36,7	31,0	27,9	23,5	29,8	20,8	16,8	15,5	14,5	7,8	6,7	8,6	6,9	1,5	2,3	4,4	3,8	1,5	1,7	1,9	3,6	1,5
Group/Time (min)	1470	1500	1530	1560	1590	1620	1650	1680	1710	1740	1770	1800	1830	1860	1890	1920	1950	1980	2010	2040	2070	2100	2130	2160	2190	2220	2250	2280	2310	2340	2370	2400	2430	2460	2490	2520	2550	2580	2610	2640	2670	2700	2730	2760	2790	2820	2850	2880
aqp-1 10mM	8	10	8	6	12	6	13	12	10	10	16	6	8	15	12	13	7	1	1	0	3	6	2	2	2	1	9	3	2	7	3	2	0	2	1	1	1	1	0	2	2	0	1	2	2	0	1	0
Locomotor activities%	1,7	2,1	1,7	1,3	2,5	1,3	2,7	2,5	2,1	2,1	3,4	1,3	1,7	3,1	2,5	2,7	1,5	0,2	0,2	0,0	0,6	1,3	0,4	0,4	0,4	0,2	1,9	0,6	0,4	1,5	0,6	0,4	0,0	0,4	0,2	0,2	0,2	0,2	0,0	0,4	0,4	0,0	0,2	0,4	0,4	0,0	0,2	0,0
Group/Time (min)	30	60	90	120	150	180	210	240	270	300	330	360	390	420	450	480	510	540	570	600	630	660	690	720	750	780	810	840	870	900	930	960	990	1020	1050	1080	1110	1140	1170	1200	1230	1260	1290	1320	1350	1380	1410	1440
atm-1 10mM	152	161	134	107	75	37	27	50	28	59	34	38	53	57	38	77	63	45	59	87	74	52	71	65	74	52	55	46	78	73	48	20	41	52	59	62	35	25	31	36	31	51	31	42	39	41	19	34
Locomotor activities%	100,0	105,9	88,2	70,4	49,3	24,3	17,8	32,9	18,4	38,8	22,4	25,0	34,9	37,5	25,0	50,7	41,4	29,6	38,8	57,2	48,7	34,2	46,7	42,8	48,7	34,2	36,2	30,3	51,3	48,0	31,6	13,2	27,0	34,2	38,8	40,8	23,0	16,4	20,4	23,7	20,4	33,6	20,4	27,6	25,7	27,0	12,5	22,4
Group/Time (min)	1470	1500	1530	1560	1590	1620	1650	1680	1710	1740	1770	1800	1830	1860	1890	1920	1950	1980	2010	2040	2070	2100	2130	2160	2190	2220	2250	2280	2310	2340	2370	2400	2430	2460	2490	2520	2550	2580	2610	2640	2670	2700	2730	2760	2790	2820	2850	2880
atm-1 10mM	26	18	17	27	21	21	18	25	25	15	7	15	3	10	6	7	4	3	4	5	4	2	5	1	1	1	0	0	2	4	0	0	3	3	0	0	0	3	1	1	1	1	0	0	0	0	0	1
Locomotor activities%	17,1	11,8	11,2	17,8	13,8	13,8	11,8	16,4	16,4	9,9	4,6	9,9	2,0	6,6	3,9	4,6	2,6	2,0	2,6	3,3	2,6	1,3	3,3	0,7	0,7	0,7	0,0	0,0	1,3	2,6	0,0	0,0	2,0	2,0	0,0	0,0	0,0	2,0	0,7	0,7	0,7	0,7	0,0	0,0	0,0	0,0	0,0	0,7
Group/Time (min)	30	60	90	120	150	180	210	240	270	300	330	360	390	420	450	480	510	540	570	600	630	660	690	720	750	780	810	840	870	900	930	960	990	1020	1050	1080	1110	1140	1170	1200	1230	1260	1290	1320	1350	1380	1410	1440
sir-2.1 10mM	147	196	208	220	206	223	210	229	214	221	183	160	138	139	110	120	112	110	154	78	116	108	70	82	77	62	71	59	69	35	73	47	51	66	48	51	27	44	50	65	31	42	42	25	34	35	35	37
Locomotor activities%	100,0	133,3	141,5	149,7	140,1	151,7	142,9	155,8	145,6	150,3	124,5	108,8	93,9	94,6	74,8	81,6	76,2	74,8	104,8	53,1	78,9	73,5	47,6	55,8	52,4	42,2	48,3	40,1	46,9	23,8	49,7	32,0	34,7	44,9	32,7	34,7	18,4	29,9	34,0	44,2	21,1	28,6	28,6	17,0	23,1	23,8	23,8	25,2
Group/Time (min)	1470	1500	1530	1560	1590	1620	1650	1680	1710	1740	1770	1800	1830	1860	1890	1920	1950	1980	2010	2040	2070	2100	2130	2160	2190	2220	2250	2280	2310	2340	2370	2400	2430	2460	2490	2520	2550	2580	2610	2640	2670	2700	2730	2760	2790	2820	2850	2880
sir-2.1 10mM	33	32	33	26	14	20	5	21	23	25	19	16	25	4	6	6	8	12	7	7	11	17	23	17	9	11	7	7	7	7	18	16	16	14	20	9	5	8	19	11	13	7	8	7	10	11	8	13
Locomotor activities%	22,4	21,8	22,4	17,7	9,5	13,6	3,4	14,3	15,6	17,0	12,9	10,9	17,0	2,7	4,1	4,1	5,4	8,2	4,8	4,8	7,5	11,6	15,6	11,6	6,1	7,5	4,8	4,8	4,8	4,8	12,2	10,9	10,9	9,5	13,6	6,1	3,4	5,4	12,9	7,5	8,8	4,8	5,4	4,8	6,8	7,5	5,4	8,8
Group/Time (min)	30	60	90	120	150	180	210	240	270	300	330	360	390	420	450	480	510	540	570	600	630	660	690	720	750	780	810	840	870	900	930	960	990	1020	1050	1080	1110	1140	1170	1200	1230	1260	1290	1320	1350	1380	1410	1440
aqp-1; atm-1 10mM	403	413	393	341	276	215	207	303	415	479	457	494	497	499	451	446	432	440	419	421	408	400	386	399	398	393	380	363	360	359	335	346	344	328	338	345	339	321	316	317	316	315	316	293	294	285	294	261
Locomotor activities%	100,0	102,5	97,5	84,6	68,5	53,3	51,4	75,2	103,0	118,9	113,4	122,6	123,3	123,8	111,9	110,7	107,2	109,2	104,0	104,5	####	99,3	95,8	99,0	98,8	97,5	94,3	90,1	89,3	89,1	83,1	85,9	85,4	81,4	83,9	85,6	84,1	79,7	78,4	78,7	78,4	78,2	78,4	72,7	73,0	70,7	73,0	64,8
Group/Time (min)	1470	1500	1530	1560	1590	1620	1650	1680	1710	1740	1770	1800	1830	1860	1890	1920	1950	1980	2010	2040	2070	2100	2130	2160	2190	2220	2250	2280	2310	2340	2370	2400	2430	2460	2490	2520	2550	2580	2610	2640	2670	2700	2730	2760	2790	2820	2850	2880
aqp-1; atm-1 10mM	278	233	225	205	222	196	192	181	166	178	164	151	150	139	131	139	148	119	120	79	90	76	99	85	83	68	93	59	66	58	48	49	55	48	41	25	35	35	22	26	32	24	28	32	37	34	21	23
Locomotor activities%	69,0	57,8	55,8	50,9	55,1	48,6	47,6	44,9	41,2	44,2	40,7	37,5	37,2	34,5	32,5	34,5	36,7	29,5	29,8	19,6	22,3	18,9	24,6	21,1	20,6	16,9	23,1	14,6	16,4	14,4	11,9	12,2	13,6	11,9	10,2	6,2	8,7	8,7	5,5	6,5	7,9	6,0	6,9	7,9	9,2	8,4	5,2	5,7
Group/Time (min)	30	60	90	120	150	180	210	240	270	300	330	360	390	420	450	480	510	540	570	600	630	660	690	720	750	780	810	840	870	900	930	960	990	1020	1050	1080	1110	1140	1170	1200	1230	1260	1290	1320	1350	1380	1410	1440
aqp-1; sir-2.1 10mM	163	199	208	200	197	179	154	159	161	150	129	89	96	104	110	125	131	159	128	127	120	126	143	123	129	128	122	90	96	118	121	82	104	97	90	63	70	66	64	66	55	86	56	54	43	63	58	63
Locomotor activities%	100,0	122,1	127,6	122,7	120,9	109,8	94,5	97,5	98,8	92,0	79,1	54,6	58,9	63,8	67,5	76,7	80,4	97,5	78,5	77,9	73,6	77,3	87,7	75,5	79,1	78,5	74,8	55,2	58,9	72,4	74,2	50,3	63,8	59,5	55,2	38,7	42,9	40,5	39,3	40,5	33,7	52,8	34,4	33,1	26,4	38,7	35,6	38,7
Group/Time (min)	1470	1500	1530	1560	1590	1620	1650	1680	1710	1740	1770	1800	1830	1860	1890	1920	1950	1980	2010	2040	2070	2100	2130	2160	2190	2220	2250	2280	2310	2340	2370	2400	2430	2460	2490	2520	2550	2580	2610	2640	2670	2700	2730	2760	2790	2820	2850	2880
aqp-1; sir-2.1 10mM	45	45	41	26	32	37	39	26	36	31	28	23	21	21	34	31	32	17	39	17	27	26	42	21	19	35	21	30	17	34	34	12	18	22	16	22	20	19	28	25	27	31	16	14	10	24	17	29
Locomotor activities%	27,6	27,6	25,2	16,0	19,6	22,7	23,9	16,0	22,1	19,0	17,2	14,1	12,9	12,9	20,9	19,0	19,6	10,4	23,9	10,4	16,6	16,0	25,8	12,9	11,7	21,5	12,9	18,4	10,4	20,9	20,9	7,4	11,0	13,5	9,8	13,5	12,3	11,7	17,2	15,3	16,6	19,0	9,8	8,6	6,1	14,7	10,4	17,8
Group/Time (min)	30	60	90	120	150	180	210	240	270	300	330	360	390	420	450	480	510	540	570	600	630	660	690	720	750	780	810	840	870	900	930	960	990	1020	1050	1080	1110	1140	1170	1200	1230	1260	1290	1320	1350	1380	1410	1440
N2 20mM	372	407	407	388	409	356	348	312	290	279	224	209	216	214	175	172	169	164	144	130	112	96	98	111	92	86	91	83	98	78	67	45	43	50	37	41	33	44	28	38	27	33	22	16	13	14	14	15
Locomotor activities%	100,0	109,4	109,4	104,3	109,9	95,7	93,5	83,9	78,0	75,0	60,2	56,2	58,1	57,5	47,0	46,2	45,4	44,1	38,7	34,9	30,1	25,8	26,3	29,8	24,7	23,1	24,5	22,3	26,3	21,0	18,0	12,1	11,6	13,4	9,9	11,0	8,9	11,8	7,5	10,2	7,3	8,9	5,9	4,3	3,5	3,8	3,8	4,0
Group/Time (min)	1470	1500	1530	1560	1590	1620	1650	1680	1710	1740	1770	1800	1830	1860	1890	1920	1950	1980	2010	2040	2070	2100	2130	2160	2190	2220	2250	2280	2310	2340	2370	2400	2430	2460	2490	2520	2550	2580	2610	2640	2670	2700	2730	2760	2790	2820	2850	2880
N2 20mM	4	10	6	3	6	5	6	7	8	3	3	3	1	3	4	0	0	0	1	2	3	4	9	1	3	0	0	5	1	0	0	0	0	0	1	2	1	0	0	1	0	0	2	0	1	1	1	1
Locomotor activities%	1,1	2,7	1,6	0,8	1,6	1,3	1,6	1,9	2,2	0,8	0,8	0,8	0,3	0,8	1,1	0,0	0,0	0,0	0,3	0,5	0,8	1,1	2,4	0,3	0,8	0,0	0,0	1,3	0,3	0,0	0,0	0,0	0,0	0,0	0,3	0,5	0,3	0,0	0,0	0,3	0,0	0,0	0,5	0,0	0,3	0,3	0,3	0,3
Group/Time (min)	30	60	90	120	150	180	210	240	270	300	330	360	390	420	450	480	510	540	570	600	630	660	690	720	750	780	810	840	870	900	930	960	990	1020	1050	1080	1110	1140	1170	1200	1230	1260	1290	1320	1350	1380	1410	1440
aqp-1 20mM	425	408	386	291	244	209	193	174	211	255	259	243	220	197	150	103	130	88	66	82	95	78	73	52	44	42	31	18	27	14	6	13	13	11	3	11	7	12	6	12	3	1	1	1	6	4	2	5
Locomotor activities%	100,0	96,0	90,8	68,5	57,4	49,2	45,4	40,9	49,6	60,0	60,9	57,2	51,8	46,4	35,3	24,2	30,6	20,7	15,5	19,3	22,4	18,4	17,2	12,2	10,4	9,9	7,3	4,2	6,4	3,3	1,4	3,1	3,1	2,6	0,7	2,6	1,6	2,8	1,4	2,8	0,7	0,2	0,2	0,2	1,4	0,9	0,5	1,2
Group/Time (min)	1470	1500	1530	1560	1590	1620	1650	1680	1710	1740	1770	1800	1830	1860	1890	1920	1950	1980	2010	2040	2070	2100	2130	2160	2190	2220	2250	2280	2310	2340	2370	2400	2430	2460	2490	2520	2550	2580	2610	2640	2670	2700	2730	2760	2790	2820	2850	2880
aqp-1 20mM	5	4	2	1	1	2	1	0	0	0	1	1	1	0	0	0	0	0	0	0	0	0	0	0	0	0	0	0	0	0	0	0	0	0	0	0	0	0	0	0	0	0	0	0	0	0	0	0
Locomotor activities%	1,2	0,9	0,5	0,2	0,2	0,5	0,2	0,0	0,0	0,0	0,2	0,2	0,2	0,0	0,0	0,0	0,0	0,0	0,0	0,0	0,0	0,0	0,0	0,0	0,0	0,0	0,0	0,0	0,0	0,0	0,0	0,0	0,0	0,0	0,0	0,0	0,0	0,0	0,0	0,0	0,0	0,0	0,0	0,0	0,0	0,0	0,0	0,0
Group/Time (min)	30	60	90	120	150	180	210	240	270	300	330	360	390	420	450	480	510	540	570	600	630	660	690	720	750	780	810	840	870	900	930	960	990	1020	1050	1080	1110	1140	1170	1200	1230	1260	1290	1320	1350	1380	1410	1440
atm-1 20mM	127	131	105	116	81	76	36	32	28	37	51	28	33	45	29	42	49	49	31	42	54	47	47	32	41	54	16	15	26	23	30	17	13	4	1	3	16	10	7	9	5	10	10	4	1	4	1	4
Locomotor activities%	100,0	103,1	82,7	91,3	63,8	59,8	28,3	25,2	22,0	29,1	40,2	22,0	26,0	35,4	22,8	33,1	38,6	38,6	24,4	33,1	42,5	37,0	37,0	25,2	32,3	42,5	12,6	11,8	20,5	18,1	23,6	13,4	10,2	3,1	0,8	2,4	12,6	7,9	5,5	7,1	3,9	7,9	7,9	3,1	0,8	3,1	0,8	3,1
Group/Time (min)	1470	1500	1530	1560	1590	1620	1650	1680	1710	1740	1770	1800	1830	1860	1890	1920	1950	1980	2010	2040	2070	2100	2130	2160	2190	2220	2250	2280	2310	2340	2370	2400	2430	2460	2490	2520	2550	2580	2610	2640	2670	2700	2730	2760	2790	2820	2850	2880
atm-1 20mM	5	0	3	6	7	1	0	2	2	0	1	2	0	0	0	1	0	0	0	0	0	0	0	0	0	0	0	0	0	0	1	0	1	0	0	0	1	1	0	0	2	1	1	1	1	0	1	0
Locomotor activities%	3,9	0,0	2,4	4,7	5,5	0,8	0,0	1,6	1,6	0,0	0,8	1,6	0,0	0,0	0,0	0,8	0,0	0,0	0,0	0,0	0,0	0,0	0,0	0,0	0,0	0,0	0,0	0,0	0,0	0,0	0,8	0,0	0,8	0,0	0,0	0,0	0,8	0,8	0,0	0,0	1,6	0,8	0,8	0,8	0,8	0,0	0,8	0,0
Group/Time (min)	30	60	90	120	150	180	210	240	270	300	330	360	390	420	450	480	510	540	570	600	630	660	690	720	750	780	810	840	870	900	930	960	990	1020	1050	1080	1110	1140	1170	1200	1230	1260	1290	1320	1350	1380	1410	1440
sir-2.1 20mM	115	157	153	168	155	166	139	148	156	153	111	96	85	81	84	48	79	61	68	46	57	53	46	62	47	25	33	28	25	18	26	32	27	17	15	14	22	15	15	18	23	15	9	17	2	19	21	12
Locomotor activities%	132,0	180,2	175,6	192,8	177,9	190,5	159,5	169,9	179,1	175,6	127,4	110,2	97,6	93,0	96,4	55,1	90,7	70,0	78,1	52,8	65,4	60,8	52,8	71,2	53,9	28,7	37,9	32,1	28,7	20,7	29,8	36,7	31,0	19,5	17,2	16,1	25,3	17,2	17,2	20,7	26,4	17,2	10,3	19,5	2,3	21,8	24,1	13,8
Group/Time (min)	1470	1500	1530	1560	1590	1620	1650	1680	1710	1740	1770	1800	1830	1860	1890	1920	1950	1980	2010	2040	2070	2100	2130	2160	2190	2220	2250	2280	2310	2340	2370	2400	2430	2460	2490	2520	2550	2580	2610	2640	2670	2700	2730	2760	2790	2820	2850	2880
sir-2.1 20mM	11	8	3	18	8	3	4	2	8	6	9	2	2	4	1	2	2	0	3	2	4	3	3	0	0	1	1	4	3	0	4	1	0	0	3	6	0	3	1	0	0	2	1	0	0	1	2	0
Locomotor activities%	12,6	9,2	3,4	20,7	9,2	3,4	4,6	2,3	9,2	6,9	10,3	2,3	2,3	4,6	1,1	2,3	2,3	0,0	3,4	2,3	4,6	3,4	3,4	0,0	0,0	1,1	1,1	4,6	3,4	0,0	4,6	1,1	0,0	0,0	3,4	6,9	0,0	3,4	1,1	0,0	0,0	2,3	1,1	0,0	0,0	1,1	2,3	0,0
Group/Time (min)	30	60	90	120	150	180	210	240	270	300	330	360	390	420	450	480	510	540	570	600	630	660	690	720	750	780	810	840	870	900	930	960	990	1020	1050	1080	1110	1140	1170	1200	1230	1260	1290	1320	1350	1380	1410	1440
aqp-1; atm-1 20mM	399	390	367	313	280	262	252	287	313	408	364	395	408	389	353	363	376	371	364	363	324	289	296	272	261	220	222	221	180	178	174	144	149	150	124	136	120	119	92	93	90	109	77	100	61	58	77	60
Locomotor activities%	100,0	97,7	92,0	78,4	70,2	65,7	63,2	71,9	78,4	102,3	91,2	99,0	102,3	97,5	88,5	91,0	94,2	93,0	91,2	91,0	81,2	72,4	74,2	68,2	65,4	55,1	55,6	55,4	45,1	44,6	43,6	36,1	37,3	37,6	31,1	34,1	30,1	29,8	23,1	23,3	22,6	27,3	19,3	25,1	15,3	14,5	19,3	15,0
Group/Time (min)	1470	1500	1530	1560	1590	1620	1650	1680	1710	1740	1770	1800	1830	1860	1890	1920	1950	1980	2010	2040	2070	2100	2130	2160	2190	2220	2250	2280	2310	2340	2370	2400	2430	2460	2490	2520	2550	2580	2610	2640	2670	2700	2730	2760	2790	2820	2850	2880
aqp-1; atm-1 20mM	51	53	49	41	53	41	44	37	28	42	29	15	35	38	39	54	29	20	24	12	16	12	8	11	19	13	13	7	9	5	7	6	15	6	5	2	5	7	5	4	3	1	2	9	7	3	4	3
Locomotor activities%	12,8	13,3	12,3	10,3	13,3	10,3	11,0	9,3	7,0	10,5	7,3	3,8	8,8	9,5	9,8	13,5	7,3	5,0	6,0	3,0	4,0	3,0	2,0	2,8	4,8	3,3	3,3	1,8	2,3	1,3	1,8	1,5	3,8	1,5	1,3	0,5	1,3	1,8	1,3	1,0	0,8	0,3	0,5	2,3	1,8	0,8	1,0	0,8
Group/Time (min)	30	60	90	120	150	180	210	240	270	300	330	360	390	420	450	480	510	540	570	600	630	660	690	720	750	780	810	840	870	900	930	960	990	1020	1050	1080	1110	1140	1170	1200	1230	1260	1290	1320	1350	1380	1410	1440
aqp-1; sir-2.1 20mM	262	327	316	265	269	254	263	246	229	207	145	145	142	123	104	102	151	152	160	151	134	122	117	138	149	109	120	107	116	88	88	71	68	43	72	52	50	54	61	70	35	52	39	36	46	40	42	11
Locomotor activities%	100,0	124,8	120,6	101,1	102,7	96,9	100,4	93,9	87,4	79,0	55,3	55,3	54,2	46,9	39,7	38,9	57,6	58,0	61,1	57,6	51,1	46,6	44,7	52,7	56,9	41,6	45,8	40,8	44,3	33,6	33,6	27,1	26,0	16,4	27,5	19,8	19,1	20,6	23,3	26,7	13,4	19,8	14,9	13,7	17,6	15,3	16,0	4,2
Group/Time (min)	1470	1500	1530	1560	1590	1620	1650	1680	1710	1740	1770	1800	1830	1860	1890	1920	1950	1980	2010	2040	2070	2100	2130	2160	2190	2220	2250	2280	2310	2340	2370	2400	2430	2460	2490	2520	2550	2580	2610	2640	2670	2700	2730	2760	2790	2820	2850	2880
aqp-1; sir-2.1 20mM	14	21	30	23	29	38	20	43	16	15	7	9	18	9	11	7	5	10	3	1	1	1	11	3	3	1	13	4	4	1	3	1	11	2	2	0	0	2	3	0	3	0	1	2	1	4	1	5
Locomotor activities%	5,3	8,0	11,5	8,8	11,1	14,5	7,6	16,4	6,1	5,7	2,7	3,4	6,9	3,4	4,2	2,7	1,9	3,8	1,1	0,4	0,4	0,4	4,2	1,1	1,1	0,4	5,0	1,5	1,5	0,4	1,1	0,4	4,2	0,8	0,8	0,0	0,0	0,8	1,1	0,0	1,1	0,0	0,4	0,8	0,4	1,5	0,4	1,9

IR assay raw data

	0Gy			70Gy		
	L1	L4	L4%	L1	L4	L4%
N2	46	46	100,0	55	21	38,2
aqp-1	54	54	100,0	94	16	17,0
sir-2.1	32	32	100,0	22	1	4,5
atm-1	41	36	87,8	28	3	10,7
aqp-1;atm-1	43	40	93,0	53	6	11,3
aqp-1;sir-2.1	83	81	97,6	54	6	11,1

IR egg assay raw data

	0Gy					70Gy				
	Broods	L1	L1%	L4	L4%	Broods	L1	L1%	L4	L4%
N2	94	94	100,0	93	98,9	101	4	4,3	0	0,0
aqp-1	106	106	100,0	106	100,0	90	4	3,8	0	0,0
sir-2.1	63	63	100,0	56	88,9	33	19	33,9	1	3,0
atm-1	60	58	96,7	49	81,7	70	43	87,8	8	11,4
aqp-1;atm-1	87	87	100,0	87	100,0	86	21	24,1	0	0,0
aqp-1;sir-2.1	113	113	100,0	110	97,3	92	8	7,3	0	0,0

7.4 Supplementary Figure

Supplementary figure S1

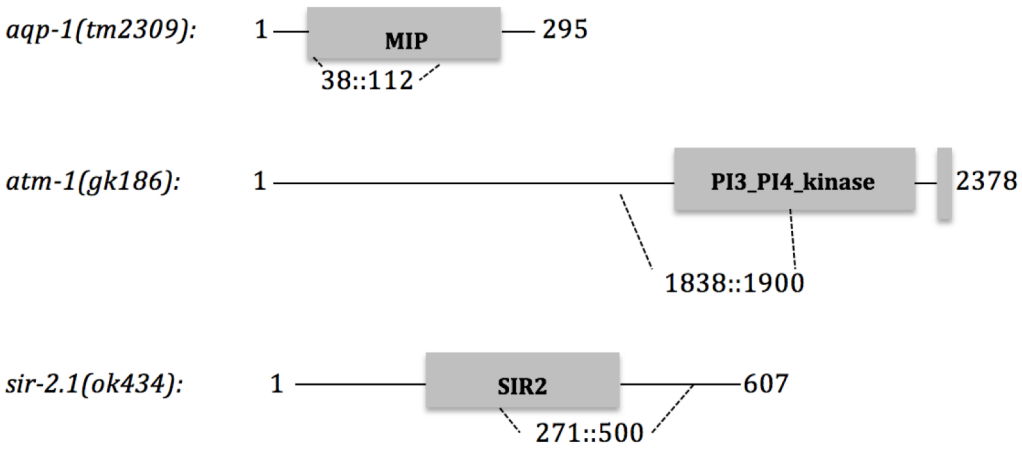

Supplementary Figure S1: Mutants. Cartoons showing the architecture of the indicated DNA repair or stress response proteins with conserved pfam domains important for DNA binding or activity as given in Wormbase (http://www.wormbase.org/). The deletions expected from the mutant alleles used in this study are indicated with amino acid numbers. All deletion mutations are expected to be loss-of-function alleles.

Supplementary Figure S2

Recommendations and Guidelines:

- PCR is a powerful technique capable of amplifying trace amounts of DNA; take all appropriate precautions to avoid cross-contamination.
- For multiple reactions, you can prepare a master mix of AccuPrime™ *Pfx* SuperMix and the component(s) common to all reactions.
- The optimal annealing temperature should be 5–10°C lower than the T_m of the primers used; if necessary, gradually increase the annealing temperature by 2–3°C for higher specificity.
- If the PCR efficiency is not optimal, repeat the reaction with different primer concentrations from 100 to 500 nM, in 100 nM increments.

PCR Protocol

1. Add the following components in any order to each reaction tube:
   - 22.5 µl AccuPrime™ *Pfx* SuperMix
   - Forward and reverse primers (200 nM final concentration of each is recommended)*
   - Template DNA solution (10 pg–200 ng)*

   *A standard 25-µl PCR reaction includes a combined primer and template volume of 2.5 µl; we have observed no decrease in product yield if the amount of primer and template solution is between 0.5 µl and 7.5 µl.
2. Mix contents of the tubes and overlay with mineral or silicone oil, if necessary.
3. Cap the tubes and load in the thermal cycler.
4. Use the following PCR program as a starting point for your template and primers:

   95°C for 5 minutes

   35 cycles of:

   95°C for 15 seconds

   55–65°C for 30 seconds

   68°C for 1 minute per kb
5. Maintain reaction at 4°C after cycling. Samples can be stored at -20°C.

Supplementary S2: Accuprime™ *Pfx* SuperMix guidelines and PCR protocol.